การสังเคราะห์และการหาลักษณะเฉพาะของพอลิอะมิโดแอมีนเดนไดรเมอร์นาโนพอลิเมอร์

นายไพรัตน์ ปุญญาเจริญนนท์

วิทยานิพนธ์นี้เป็นส่วนหนึ่งของการศึกษาตามหลักสูตรปริญญาวิทยาศาสตรดุษฎีบัณฑิต
สาขาวิชาวัสดุศาสตร์ ภาควิชาวัสดุศาสตร์
คณะวิทยาศาสตร์ จุฬาลงกรณ์มหาวิทยาลัย
ปีการศึกษา 2551

SYNTHESIS AND CHARACTERIZATION OF POLYAMIDOAMINE DENDRIMER NANOPOLYMERS

Mr. Phairat Punyacharoennon

A Dissertation Submitted in Partial Fulfillment of the Requirements
for the Degree of Doctor of Philosophy Program in Materials Science
Department of Materials Science
Faculty of Science
Chulalongkorn University
Academic year 2008

Thesis Title	SYNTHESIS AND CHARACTERIZATION OF POLYAMIDOAMINE DENDRIMER NANOPOLYMERS
By	Mr. Phairat Punyacharoennon
Field of Study	Materials Science
Thesis Advisor	Associate Professor Kawee Srikulkit, Ph.D.
Thesis Co-advisor	Assistant Professor Sireerat Charuchinda, Ph.D.

Accepted by the Faculty of Science, Chulalongkorn University in Partial Fulfillment of the Requirements for the Doctoral Degree

S. Hannongbua ....Dean of the Faculty of Science
(Professor Supot Hannongbua, Dr.rer.nat.)

THESIS COMMITTEE

.... Chairman
(Assistant Professor Sirithan Jiemsirilers, Ph.D.)

Srikulkit .... Thesis Advisor
(Associate Professor Kawee Srikulkit, Ph.D.)

Sireerat Charuchinda .... Thesis Co-advisor
(Assistant Professor Sireerat Charuchinda, Ph.D.)

............Vimolvan...Pimpan............ Examiner
(Associate Professor Vimolvan Pimpan, Ph.D.)

...Suwabun Chirachanchai Examiner
(Associate Professor Suwabun Chirachanchai, Ph.D.)

......Monthon......Nakpathom.. External Examiner
(Monthon Nakpathom, Ph.D.)

ไพรัตน์ ปุญญาเจริญนนท์ : การสังเคราะห์และการหาลักษณะเฉพาะของพอลิอะมิโดแอมีน
เดนไดรเมอร์นาโนพอลิเมอร์. (SYNTHESIS AND CHARACTERIZATION OF
POLYAMIDOAMINE DENDRIMER NANOPOLYMERS) อ.ที่ปรึกษาวิทยานิพนธ์หลัก :
รศ. ดร.กาวี ศรีกูลกิจ, อ.ที่ปรึกษาวิทยานิพนธ์ร่วม : ผศ. ดร.สิรีรัตน์ จารุจินดา, 111 หน้า.

พอลิอะมิโดแอมีนเดนไดรเมอร์สามารถสังเคราะห์ได้จาก 2 ปฏิกิริยาต่อเนื่องแบบซ้ำ คือ ปฏิกิริยาการรวมตัวแบบไมเคิลและปฏิกิริยาอะมิเดชัน เพื่อผลิตผลิตภัณฑ์ที่มีหมู่ปลายเป็นแอมีน ผลที่สังเคราะห์ได้ สามารถยืนยันด้วยเทคนิคการวิเคราะห์แบบฟูเรียร์ทรานสฟอร์มอินฟราเรดสเปกโทรสโกปี โปรตอนและคาร์บอน-13 นิวเคลียร์แมกเนติกเรโซแนนซ์สเปกโทรสโกปี การกราฟต์ไฮเปอร์บรานช์พอลิอะมิโดแอมีนลงบนผิวของซิลิกาชนิดความละเอียดสูง ตามด้วยการเปลี่ยนหมู่ฟังก์ชันที่ปลายสายโซ่โมเลกุลให้เป็นหมู่กรดฟอสฟอนิก ในขั้นตอนแรกเพิ่มหมู่เริ่มต้นที่ผิวของซิลิกาด้วยการทำปฏิกิริยาของหมู่ซิลานอลของซิลิกากับ 3-อะมิโนพรอพิลไตรเอทอกซีไซเลน เพื่อให้เกิดเป็นซิลิกาที่มีหมู่ฟังก์ชันแอมีน ปริมาณของหมู่แอมีนจะขึ้นกับสัดส่วนการผสมของเมทานอลกับน้ำในขั้นตอนของการไฮโดรไลซิสของปฏิกิริยาซิลาไนเซชัน การกราฟต์ไฮเปอร์บรานช์พอลิอะมิโดแอมีนทำได้โดยการเกิดปฏิกิริยารวมตัวแบบไมเคิลของหมู่แอมีนของซิลิกากับเมทิลอะคริเลต และการเกิดปฏิกิริยาอะมิเดชันของหมู่เมทิลเอสเทอร์ที่ปลายกับเอทิลีนไดแอมีน ความสมบูรณ์ของปฏิกิริยาการกราฟต์ในแต่ละขั้นตอน สามารถยืนยันได้ด้วยการวิเคราะห์แบบฟูเรียร์ทรานสฟอร์มอินฟราเรดสเปกโทรสโกปี แต่อย่างไรก็ตาม ปริมาณหมู่อะมิโนในแต่ละขั้นตอนพบว่ามีปริมาณน้อยกว่าค่าที่ได้ตามทฤษฎีอย่างมีนัยสำคัญ ซึ่งสาเหตุอาจเนื่องจากการเกิดปฏิกิริยาข้างเคียงและผลของการกีดขวางเนื่องจากขนาด เมื่อพอลิอะมิโดแอมีนเดนไดรเมอร์และไฮเปอร์บรานช์พอลิอะมิโดแอมีนกราฟต์ซิลิกา ผ่านการดัดแปรหมู่ฟังก์ชันโดยปฏิกิริยาแบบแมนนิช ได้เป็นฟอสฟอริเลตพอลิอะมิโดแอมีนเดนไดรเมอร์ และฟอสฟอริเลตไฮเปอร์บรานช์พอลิอะมิโดแอมีนกราฟต์ซิลิกา จากนั้นนำไปตกแต่งลงบนผ้าฝ้ายเพื่อผลิตผ้าหน่วงไฟ พบว่าสารที่สังเคราะห์ได้ทั้ง 2 ชนิดให้ผลการหน่วงไฟบนผ้าฝ้าย ภายหลังการซักพบว่า ฟอสฟอริเลตไฮเปอร์บรานช์พอลิอะมิโดแอมีนกราฟต์ซิลิกามีความคงทนต่อการซักดีกว่า นอกจากนั้นพบว่าความคงทนต่อแรงดันทะลุของผ้าที่ตกแต่งด้วยฟอสฟอริเลตพอลิอะมิโดแอมีนเดนไดรเมอร์มีค่าต่ำกว่า ซึ่งเป็นผลเนื่องมาจากมีปริมาณหมู่กรดฟอสฟอนิกมากกว่า ความเป็นกรดที่เพิ่มขึ้นช่วยเร่งการการสลายตัวเนื่องจากความร้อนของผ้าฝ้ายในระหว่างการอบผนึก

ภาควิชา วัสดุศาสตร์	ลายมือชื่อนิสิต
สาขาวิชา วัสดุศาสตร์	ลายมือชื่ออ.ที่ปรึกษาวิทยานิพนธ์หลัก
ปีการศึกษา 2551	ลายมือชื่ออ.ที่ปรึกษาวิทยานิพนธ์ร่วม

4773826923 : MAJOR MATERIALS SCIENCE
KEYWORDS : POLYAMIDOAMINE / GRAFTED SILICA / PHOSPHORYLATION / COTTON FINISHING / FLAME RETARDANCY

PHAIRAT PUNYACHAROENNON : SYNTHESIS AND CHARACTERIZATION OF POLYAMIDOAMINE DENDRIMER NANOPOLYMERS. THESIS ADVISOR : ASSOC. PROF. KAWEE SRIKULKIT, Ph.D., THESIS CO-ADVISOR : ASSIST. PROF. SIREERAT CHARUCHINDA, Ph.D., 111 pp.

The PAMAM dendrimers were synthesized by consecutively repeating two reactions; Michael addition and Amidation to produce amine terminated product. The FTIR, ^{1}H and ^{13}C-NMR analysis were employed to follow the synthesis reaction. In separate work, grafting of hyperbranched PAMAM polymers onto ultrafine silica followed by functionalization via the introduction of phosphonic acid groups into the branch ends was performed. First, an initiating site was incorporated into the silica surface by reacting the silica silanol group with 3-aminopropyltriethoxysilane, producing amino functionalized silica. The free amine group content was altered by varying the ratio of methanol to water in the hydrolysis step of the silanization reaction. Grafting of PAMAM was attained by three rounds of sequential Michael addition of silica amino groups to methyl acrylate and amidation of the resulting terminal methyl ester groups with ethylenediamine. Completion of the grafting reaction in each step was clearly confirmed using FTIR analysis. However, the amino group content determined in each step was found to be significantly lower than theoretically expected, perhaps indicative of side reactions and, in later stages, steric hindrance. The PAMAM dendrimers and hyperbranched PAMAM grafted silica were functionalized by a Mannich type reaction to phosphorylate the terminal amino groups, producing the phosphorylated PAMAM dendrimers and phosphorylated hyperbranched PAMAM grafted silica. Then they were applied on cotton fabric to produce flame-retardant cellulose. The two synthesized products showed flame retardancy effect on cotton fabric. After washing test, the phosphorylated hyperbranched PAMAM grafted silica showed better retention of fire retardancy than phosphorylated PAMAM dendrimers, indicating its wash-off resistancy performance. In addition, the bursting strength of phosphorylated PAMAM dendrimers finished cotton was worst than phosphorylated hyperbranched PAMAM grafted silica finished cotton. This might be due to the effect of more phosphonic acid groups content of phosphorylated PAMAM dendrimers. As a result, its higher acidicity accelerated the thermal degradation of cotton fabric during fixation of phosphorylated PAMAM dendrimers.

Department : Materials Science	Student's Signature P. Punyacharoennon
Field of Study : Materials Science	Thesis Advisor's Signature
Academic Year : 2008	Thesis Co-advisor's Signature

ACKNOWLEDGEMENTS

I would like to express my sincere gratitude and deepest appreciation to my principle advisor, Assoc. Prof. Dr. Kawee Srikulkit for his excellent guidance, invaluable advice and powerful encouragement throughout this research. He was never lacking in kindness and support. Without his guidance and persistent help this dissertation would not have been possible. I am grateful to Assist. Prof. Dr. Sireerat Charuchinda, my associate advisor for her construction comments and valuable advice. I would like to thank my committee members, Assist. Prof. Sirithan Jiemsirilers and Assoc. Prof. Dr Vimolvan Pimpan from Faculty of Science, Assoc. Prof. Dr. Suwabun Chirachanchai from The Petroleum and Petrochemical College, and Dr. Monthon Nakpathom from National Metal and Materials Technology Center for their kind comments and encouragement.

I am sincere grateful to the National Research Council of Thailand (NRCT), CU Graduate School Thesis Grant and Center of Excellent in Textile, Chulalongkorn University for a financial support. Furthermore, my sincere thanks go to my coworkers in Department of Textile Chemical Technology, Faculty of Industrial Textiles and Fashion Design, Rajamangala University of Technology Phra Nakhon for their helpfulness, consideration and encouragement throughout my study. I wish to thanks my friends in Doctorate program who made my life in this university more joyfulness than I expected.

Finally, I would like to express my deepest thanks to my beloved family for their helpfulness, care and endless encouragement. I always know that my successfulness based on them. In addition, I take this opportunity to think of my beloved grandmother who has not seen my successfulness.

CONTENTS

CHAPTER

CHAPTER **Page**

CHAPTER **Page**

LIST OF TABLES

LIST OF FIGURES

Figure **Page**

Figure **Page**

Figure **Page**

CHAPTER I

INTRODUCTION

Polyamidoamine (PAMAM) dendrimers, the starburst polymers with a plurality of terminal functional groups have attracted considerable interest due to their novel functionalities such as nanoscopic containers, delivery devices, ultrafine colloid stabilizers and nanocomposite materials [1-8]. Surface modifications of terminal groups with different functionalities such as acetamide, hydroxyl, carboxyl or quaternized PAMAM dendrimers further increase the versatile applicability of these materials [9-13]. Focused on nanoparticle fillers such as carbon black and silica, these materials are widely used for rubber and plastics. A good uniform dispersion of extremely fine particle size for most of their applications is important. However, these nanoparticles by nature are found in micron sized aggregate whose performance is inferior to those of the nanometer sized form. This problem of nanoparticles having a strong tendency to agglomerate is solved by surface modification [14-17]. The grafting of PAMAM dendrimer onto inorganic particle’s surface is one possibility [18-20]. The grafted dendrimer effectively prevents agglomerate formation, resulting in the stability of ultrafine nanoparticles in the colloidal state or dispersibility in the polymer matrix. Nanometer-sized fillers are expected to exhibit the attractive interaction with polymer matrix at very low filler content, resulting in an improved performance of nanocomposite materials. Another interesting effect is that the PAMAM attached on inorganic particles leads to hybrid materials with special characteristics particularly high performance chelating agents [21] and nanoreactors in which metal nanoparticles are stabilized [22]. Other interesting performance concerned with nanocomposites includes reduced gas permeability, increased solvent resistance and reduced flammability. In this study, this type of nanoparticle was specially designed to impart its flame retardancy performance on cotton cellulose. When considering flame retardants for cellulose and cellulose derivatives, phosphorus-based compounds have been a major interest because of their environmentally friendly products and their low toxicity, as well as, their low evolution of smoke in fire. These compounds were found to promote dehydration and char formation [23]. However, these flame retardants for cellulosic textile such as phosphoric acid are water soluble, causing the durability problem associated to wash treatment [24]. The immobilizations of these molecules in microcapsules could help improve the washing resistance [25-26]. It is interesting to propose that the attachment of these molecules to the nanoparticles could be an alternative method in decreasing water solubility of phosphorus-based flame retardants.

Scope of This Work

The PAMAM dendrimers are synthesized by the divergent method using ethylenediamine (EDA) as core, and allowed to undergo reiterative two step reaction sequences. These sequences consist of: (a) an exhaustive alkylation of primary amines (Michael addition) with methyl acrylate, and (b) amidation of amplified ester groups with a large excess of EDA to produce primary amine terminal groups. Iteration of Michael addition-amidation sequence produces the higher generations.

The PAMAM grafting onto silica nanoparticle surface will be also carried out. The hyperbranched PAMAM is grown from free amine groups attached on nanosized silica. The silica is first reacted with 3-aminopropyltriethoxysilane in order to introduce amino group onto silica surface. Grafting is carried out by repetitive reactions between Michael addition of amino group to methyl acrylate (MA) and amidation of the resulting terminal methyl ester group with ethylenediamine.

The second phase of this research is focused on the surface modification of the terminal amino groups of PAMAM hyperbranched polymers and hyperbranched PAMAM grafted silica in order to modify the nanoparticles with novel properties and apply in textile chemistry. Functionalization of terminal amino groups of PAMAM hyperbranched polymers and hyperbranched PAMAM grafted silica in order to incorporate phosphonic acid groups was carried out by Mannich type reaction.

CHAPTER II

LITERATURE REVIEW

2.1 Dendritic Polymers [1]

Dendritic polymers is the forth major class of macromolecular architecture. They are open, covalent assemblies of branch cells. Dendritic polymer consists of three dendritic subclasses; random hyperbranched polymers, dendrigraft polymers, dendron and dendrimer polymers (Figure 2.1).

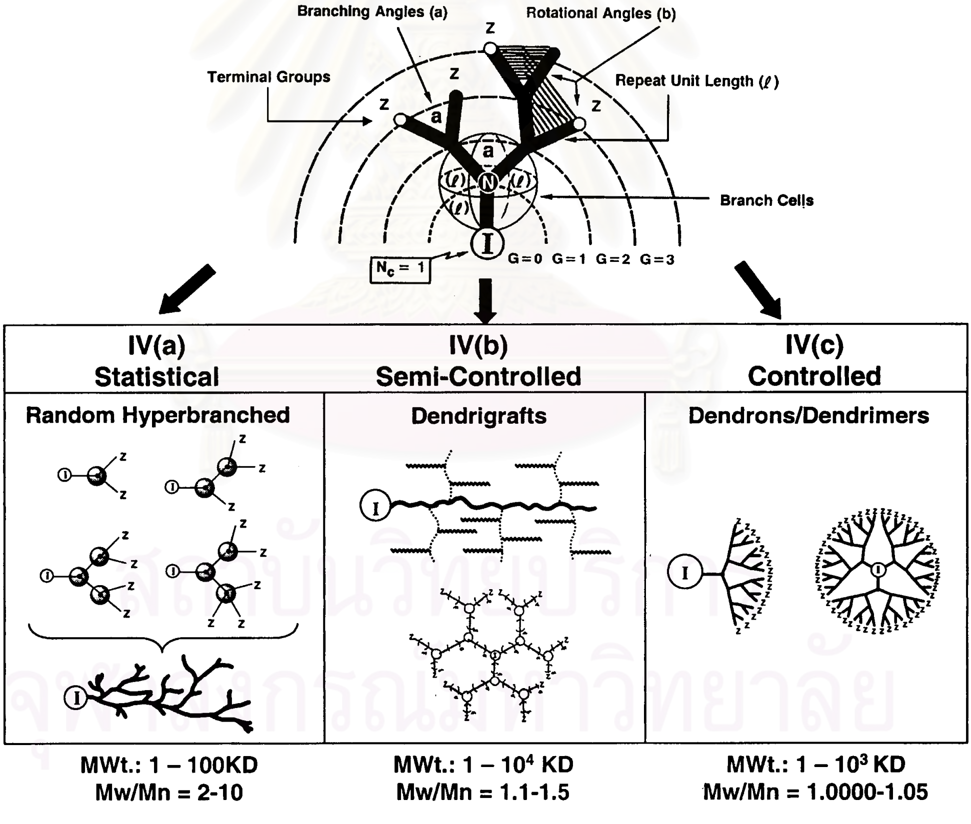

Figure 2.1 Branch cells tructural parameters (a) branching angles (b) rotation angles (l) repeat units lengths (Z) terminal groups and dendritic subclasses derived from branches (IVa) random hyperbranched (IVb) dendrigrafts and (IVc) dendrons/dendrimers [27].

2.1.1. Random hyperbranched polymers

Random hyperbranched polymers are generally prepared by polycondensation, ring opening or polyaddition polymerization of AB_x-type monomers, when x is 2 or more, polymerization of these monomers gives highly random branched polymers, as long as A reacts only with B from another molecules. They usually have broad and statistical molecular weight distributions. Some examples of random hyperbranched polymers include water soluble hyperbranched polyphenylene prepared by Kim and Webster [28] (Figure 2.2) and hyperbranched poly(siloxysilanes) prepared by Miravet and Fréchet [29].

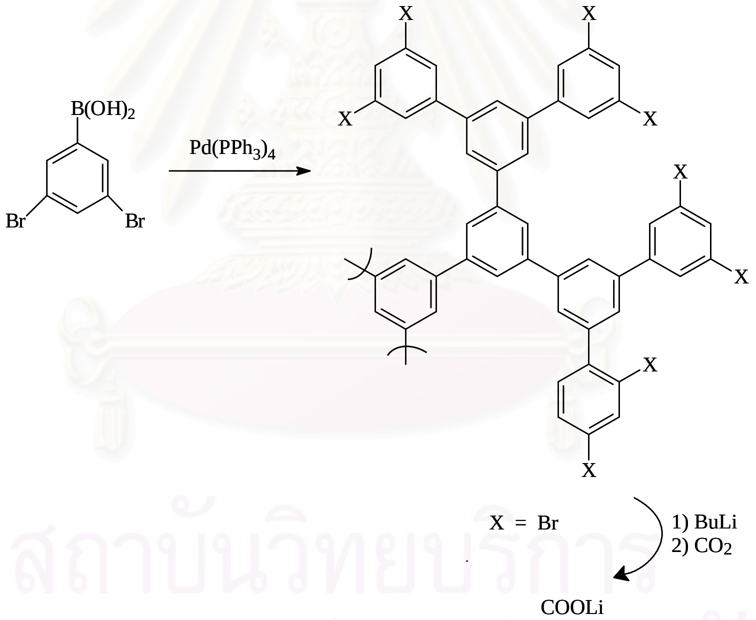

Figure 2.2 Synthesis of water-soluble hyperbranched polyphenylene [28].

2.1.2. Dendrigraft polymers [1, 30]

Dendrigraft polymers are generally larger structures than dendrimers, grow much faster and amplify surface groups more dramatically as a function of generational development. They are the most recently discovered and currently the least understood subset of dendritic polymers. Dendrigraft polymers obtained by ionic polymerization and grafting, combine features of dendrimers and hyperbranched polymers. The synthesis can be achieved by three different strategies, the ‘grafting onto’, ‘grafting from’ and ‘grafting through’ methods. The first reported dendrigrafted polymer in the literature is Comb-burst® (Figure 2.3) [31] and arborescent polymers [32].

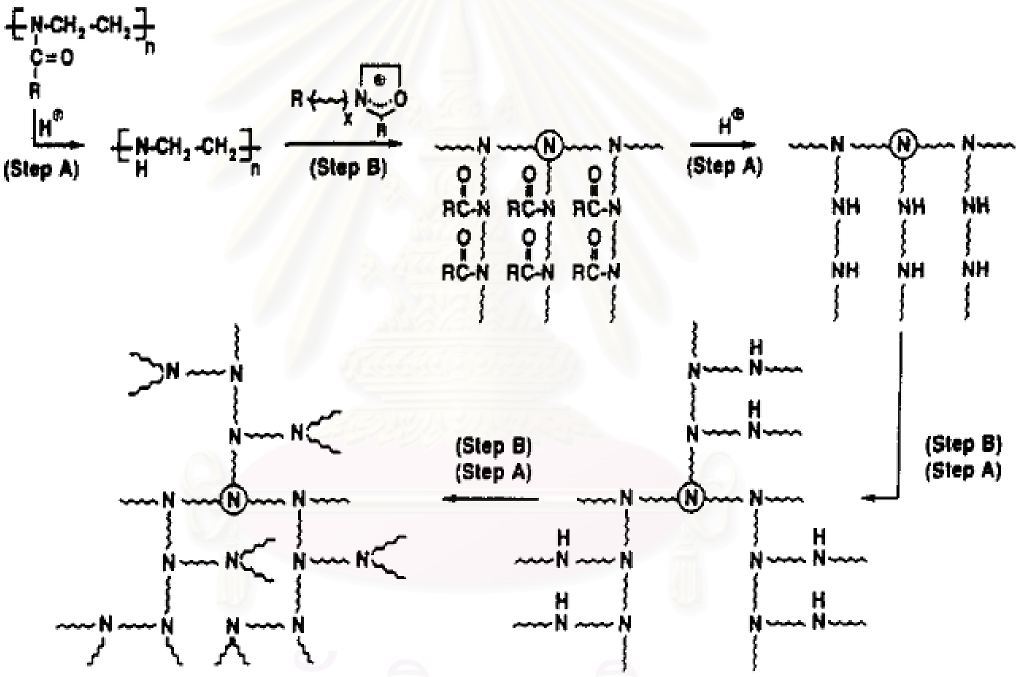

Figure 2.3 Synthetic iteration scheme leading to Comb-burst poly(ethyleneimines) [31]

2.1.3. Dendron and Dendrimers [1]

Dendron and dendrimers are the most intensely investigated subset of dendritic polymers. The word dendrimer is derived from Greek words that consist of dendri that means ‘tree branch-like’ and meros that means ‘part of’. The two most widely studied dendrimer families are the Fréchet-type polyether compositions (Figure 2.4) and the Tomalia-type PAMAM dendrimers.

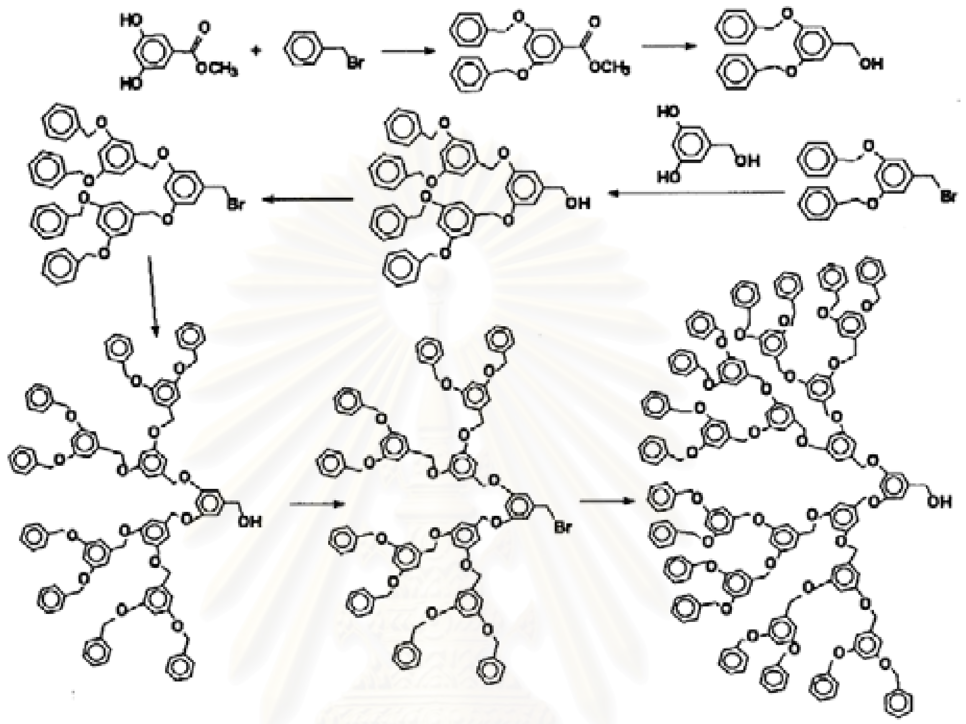

Figure 2.4 Preparation of Fréchet-type polyether to forth generation [27].

Due to the special structure of dendritic polymers, the physical and chemical properties of them are rather different from usual linear polymers. The comparison of their differences is shown in Table 2.1.

Table 2.1 Characteristics and properties of linear and dendritic polymers [27].

Linear polymer	**Dendritic polymer**
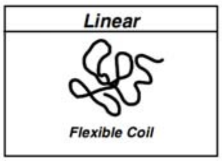	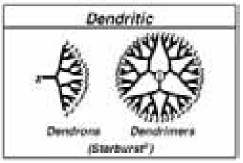
1. Random coil configuration	1. Predictable shape changes as a function of molecular weight and core - robust spheroids; breathing deformability
2. semicrystalline/crystalline material - higher glass temperature	2. Non-crystalline, amorphous materials - lower glass temperature
3. Lower solubility - decreases with molecular weight	3. Increased solubility - increases with molecular weight
4. Intrinsic viscosity follows logarithmic - increases with molecular weight	4. Exhibits viscosity maximum and minimum plateau with molecular weight - lower viscosity
5. Entanglement directed rheological properties - shear sensitivity	5. Newtonian-type rheology - no shear sensitivity, considerably lower viscosity
6. Mobility by reputation - segment and molecular mobility	6. Mobility involving whole dendrimer as the kinetic flow unit - virtually no reputation
7. Anisotropic electronic conductivity	7. Isotropic electronic conductivity

2.2 Dendronized Polymers [33]

Dendronized polymers originally termed ‘rod-shape dendrimers’, made their first appearance in a patent by Tomalia *et al.* at Dow chemical company in 1987. Dendronized polymers merge the concepts of dendrimers and polymers, their preparation is a combination of organic synthesis of the dendrons and polymer synthesis. The types of polymer backbones used in dendronized polymers are diverse and rather a reflection of the most common types of polymerization reactions applied. Polystyrene, polymethyacrylate and poly-*p*-phenylene backbones are often found. The synthetic strategy of dendronized polymers may be conceptually distinguished into three categories as shown in Figure 2.5.

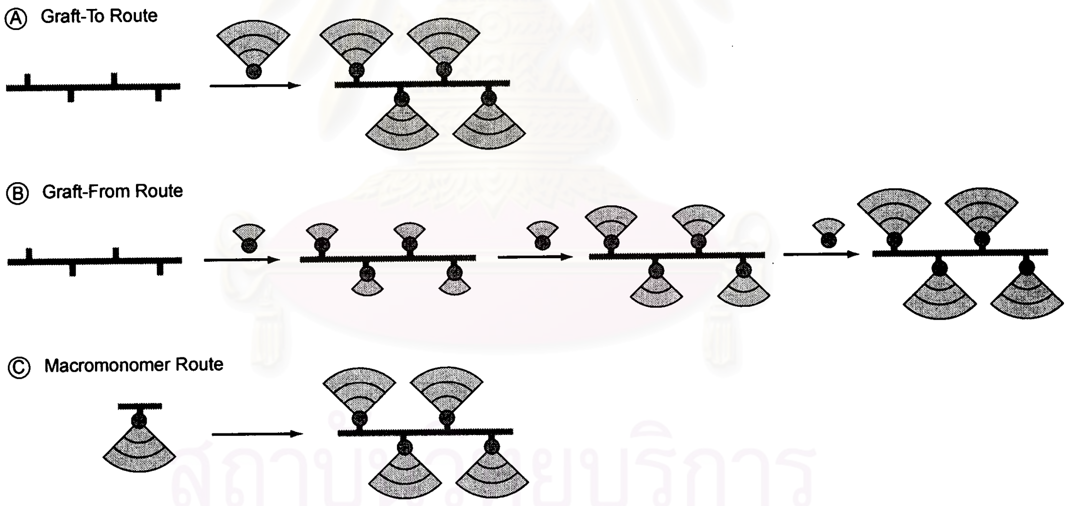

Figure 2.5 Schematic illustration of three different general synthetic strategies toward dendronized polymers [33].

1. Graft-to strategy. Preformed dendrons of desired generation are coupled to the performed polymer. This strategy is also referred to as the ‘convergent route’.

2. Graft-from strategy. G1 dendrons are attached to the preformed polymer, and higher generations are grown by successive attachment of G1 dendrons. This approach is also termed the ‘divergent route’.

3. Macromonomer strategy. Dendrons of the desired generation are equipped with a polymerizable group at their focal point and polymerized.

2.3 The Construction of Dendrimers [34]

Many dendrimer synthesis rely upon traditional reactions, such as the Michael reaction or the Williamson ether synthesis, whilst others involve the use of modern chemical techniques and practices, such as a solid-phase synthesis, organotransition-metal, organosilicon and organophosphorus chemistry, or other contemporary organic methodologies.

2.3.1. Divergent dendrimer growth

The divergent refers to the way in which the dendrimer is induced to grow outwards from the core, diverging into space. A schematic representation of divergent growth is shown in Figure 2.6. The divergent approach is successful for the production of large quantities of dendrimers since, in each generation-adding step, the molar mass of the dendrimer is double.

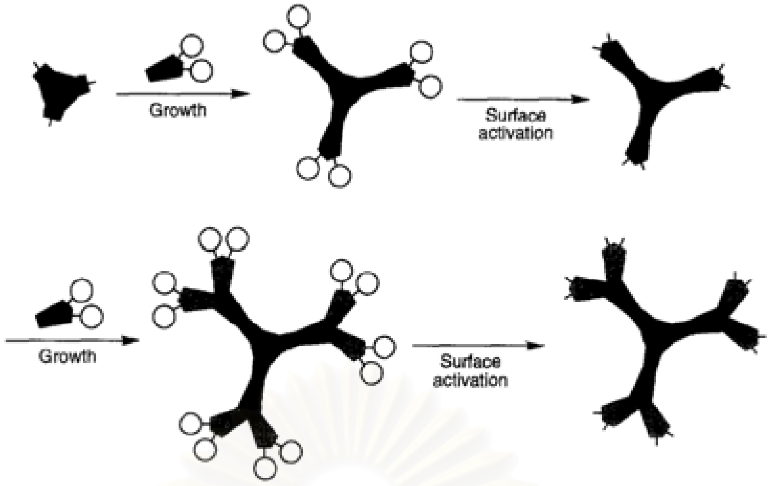

Figure 2.6 Schematic representation of divergent growth [34].

2.3.2. Convergent dendrimer growth

This method was developed several years after the divergent method. The convergent growth process begins at what ultimately becomes the surface of the dendrimer and works inwards by gradually linking surface units together with more monomers (Figure 2.7). The advantage of convergent over divergent growth stem from the fact that only two simultaneous reactions are required for any generation-adding step. Most importantly, the method makes the purification of perfect dendrimers relatively simple, as the side products and incomplete reaction products in a crude reaction mixture differ substantially from the desired dendrimer.

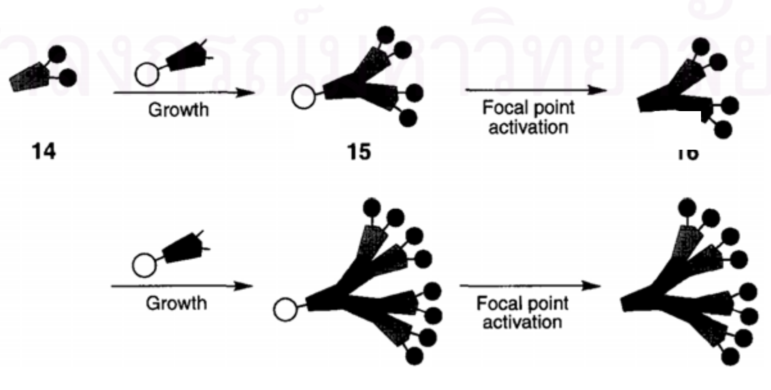

Figure 2.7 Schematic representation of convergent growth [34].

2.3.3. Hypercores and branched monomers

This method involves the pre-assembly of oligomeric species, which can be linked together to give dendrimers in fewer steps or higher yields, taking advantage of the best points of both the convergent and the divergents methods. The 'hypercores' and 'branched monomers' are pre-branched analogues of the cores and monomers that are used in traditional dendrimer synthesis. They can be synthesized by standard routes, and become powerful synthons for the production of dendrimers (Figure 2.8).

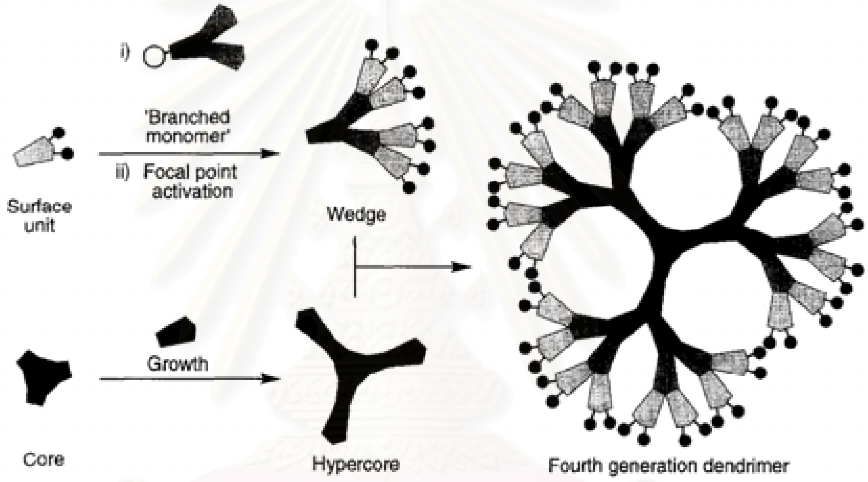

Figure 2.8 Schematic representation of hypercores and branched monomers [34].

2.3.4. Double exponential and mixed growth

The method employs an AB_2 monomer where the functional groups A and B are both protected. This fully protected monomer is deprotected selectively at the surface and at the focal point in separate reactions to give a convergent-type monomer and a divergent-type monomer. These two products are then reacted together to give an orthogonally protected trimer, which may be used to repeat the growth process again (Figure 2.9). The attributes of double exponential growth are more subtle than the ability to build large dendrimers in relatively few steps. The double exponential growth is so fast that it can be repeated only two or perhaps three times before further growth becomes impossible. Most importantly, this method provides a means whereby a dendritic fragment can be extended in either the convergent or the divergent direction as required.

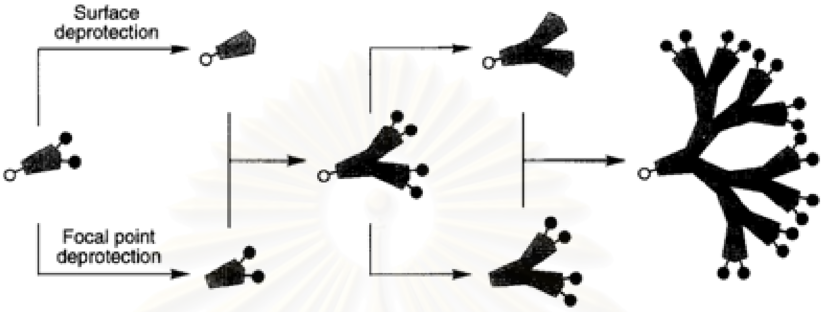

Figure 2.9 Schematic representation of double exponential and mixed growth [34].

Table 2.2 Some methodologies used for the synthesis of dendrimer [34].

Repeat unit	Synthetic methodology
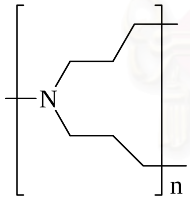	Viigtle and co-workers (1978) and later improved by de Brabander van den Berg and Meijer (1993), among others. Double Michael-type addition of acrylonitrile to a primary amine; reduction of a nitrile to an amine. This was the first reported dendrimer synthesis to be attempted, and has been completed up to g = 10.
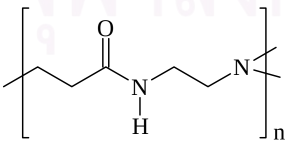	Tomalia *et al.* (1985). Double Michael addition to a primary amine; the reaction of an ester with an excess of amine to give an amide. These are the most studied dendrimers, and are commercially available. The high generation dendrimers (up to g = 10) have a small, unavoidable polydispersity.

Table 2.2 Some methodologies used for the synthesis of dendrimer. (Continued)

Repeat unit	**Synthetic methodology**
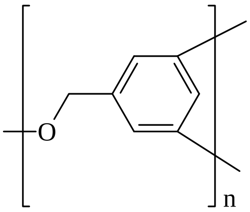	Hawker and Frechet (1990). Reaction of a phenol with a benzylic bromide; bromination of a benzylic alcohol with PPh$_3$ and CBr$_4$. The first "convergent" synthesis. These dendrimers have been studied thoroughly up to g = 6.
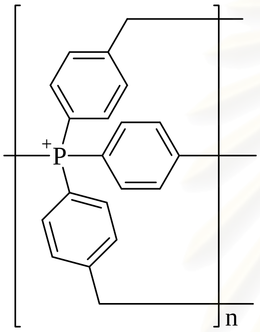	Rengan and Engel (1991). Cleavage of a benzyl methyl ether with Me$_3$Sil to give a benzyl iodide; displacement of iodide from the benzylic position by a triarylphosphine. The first example of an ionic dendrimer and of a phosphorus-containing dendrimer. The ^{13}P NMR spectra and solubility properties of the compounds were studied up to g = 3.
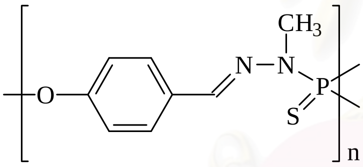	Majoral and co-workers (1995). Reaction of phenoxide with the phosphorus-chlorine bond: condensation of a hydrazine derivative with a primary amine. These dendrimers have been synthesized up to g = 4.
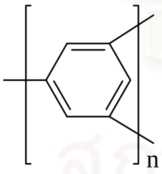	Miller, Neenan and co-workers (1992). Aryl Grignard reagents or Suzuki coupling for linking units; the transformation of an aryl trimethylsilane into an arylboronic acid with BBr$_3$. The first all-hydrocarbon dendrimers. These structures were synthesized up to g = 3.
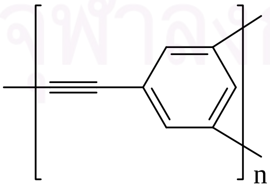	Moore (I 995). Palladium-catalysed cross-coupling of a terminal acetylene to an aryl halide; TMS protection of the terminal acetylene; 1-aryl-3,3-dialkyltriazene masking of the aryl iodide. The largest hydrocarbon dendrimers, synthesized up to g = 4.
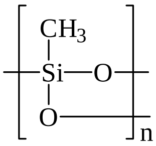	Zhdanov and co-workers (1990). Silylation of sodium bisethoxy methylsiloxide with methyltrichlorosilane; cleavage of the ethoxy silyl end-groups and chlorination with thionyl chloride. Synthesized up to g = 4.

Table 2.2 Some methodologies used for the synthesis of dendrimer. (Continued)

Repeat unit	Synthetic methodology
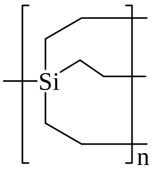	Seyferth *et al.* (1994). Platinum-catalysed addition of trichlorosilane to an alkene; nucleophilic substitution with vinylmagnesium bromide. Used to generate star polymers. Synthesized up to g = 3.
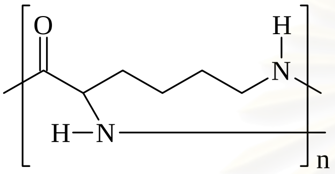	Denkewalter *et al.* (1978). Synthesis based on peptide methodology-BOC rotection/deprotection and DCC coupling of lysine. These dendrimers are unlike most others in that the lengths of the two branches are not equal. These dendrimers were not fully characterized.
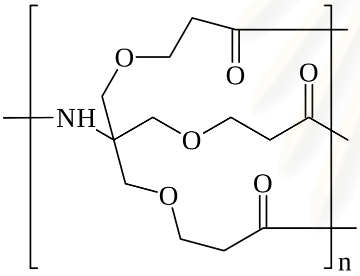	Newkome *et al.* (1985). Use of “tris” DCC/HOBT coupling; base-promoted hydrolysis of an ester in the presence of amide bonds. This and similar “tris” based branching have been used by many researchers.
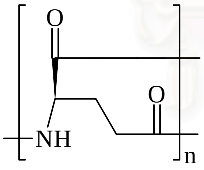	Mitchell and co-workers (1994, 66). Coupling of an amine with a succinate-activated ester; deprotection of a benzyloxycarbonyl-protected amine with Me$_3$SiI or H$_2$/Pd. These dendrimers, synthesized up to g = 4, were the first fully characterized dendrimers to be based on a chiral branching unit.
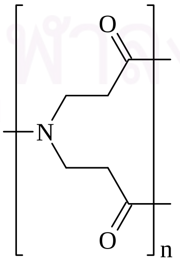	Uhrich and Fréchet (1992). DMAP-catalysed DCC coupling; BOC deprotection with TFA. Synthesized up to g = 4.

Table 2.2 Some methodologies used for the synthesis of dendrimer. (Continued)

Repeat unit	Synthetic methodology
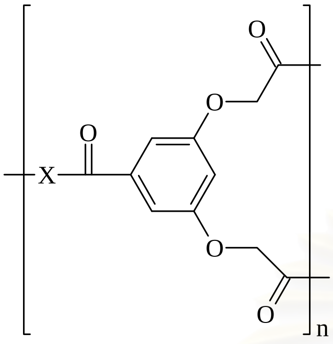	Shinkai *et al.* (1992). In the diagram, X is l,l0-diaza 18-crown-6, linked via its two nitrogen atoms. Amide bond formation from a secondary amine and a carboxylic acid using Me_3CCOCI; based-promoted ester hydrolysis; deprotection of CBZ protection with H_2/Pd. Dendrimers were synthesized up to g =4.
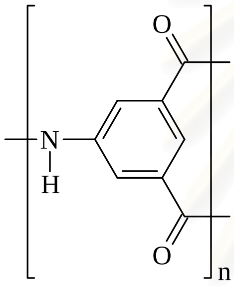	Miller *et al.* (1993). Reaction of an aniline with acyl chloride to give an amide; reduction of any aryl nitrate to an aniline with Hz/Pt. Also synthesized by Feast *et al.* (1994) up to g = 2. These dendrimers have a problematic synthesis as a consequence of the low reactivity of anilines and the high degree of steric hindrance.
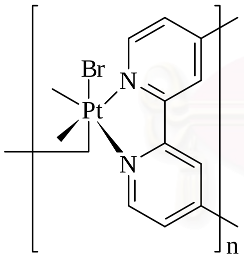	Achar and Puddephatt (1994). Oxidative addition of a benzylic bromide to a square planar dimethylplatinum species; coordination of a dimethylplatinum (II) to a 2,2'-bipyridine. These dendrimers were synthesized up to g = 2, with a four- directional core.
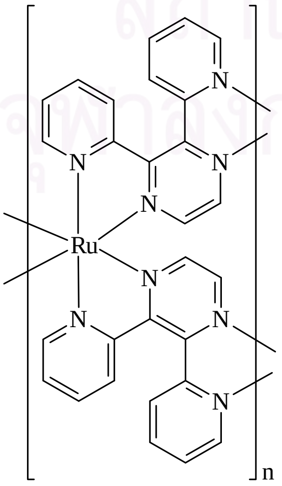	Balzani (1995). Protection of a pyridine by methylation with trimethyloxonium tetrafluoroborate or methyl triflate; deprotection of the methylated pyridine with 1,4-diaza-bicyclo[2.2.2]octane; displacement of chloride ligands by bipyridyl ligands. Dendrimers up to g = 3 were synthesized, and they were studied for their electrochemical and luminescence properties. Further structures using other (and mixed) metal centers were investigated.

2.4 Polyamidoamine (PAMAM) Dendrimers

Polyamidoamine dendrimer is the one of the most popular dendrimers that was first reported in Tomalia and coworker's paper in 1985 [3]. They refer to as 'Starburst polymers'. The polyamidoamine dendrimers are synthesized by the divergent method [35] which involves the *in situ* branch cell construction in stepwise, iterative stages around a desired core to produce mathematically defined core-shell structure (Figure 2.10 and 2.11).

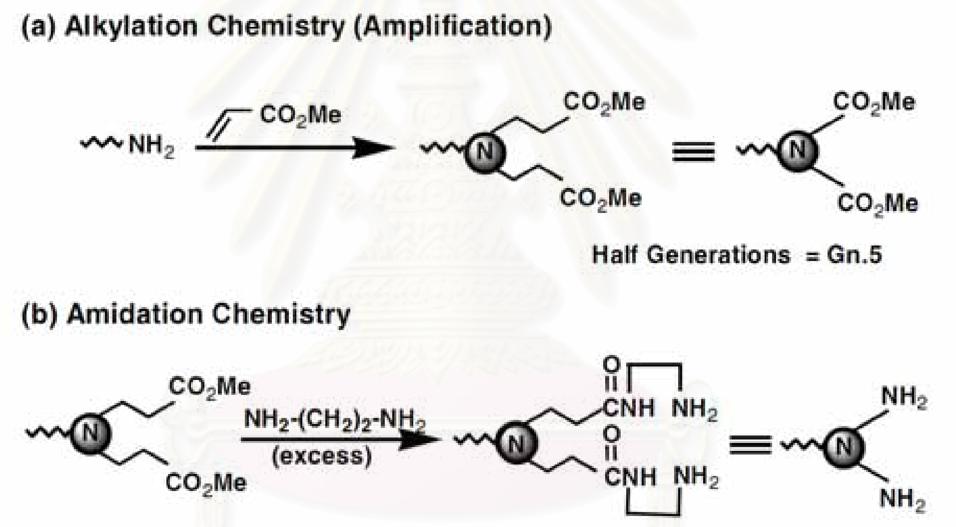

Figure 2.10 In situ branch cell method to synthesize PAMAM dendrimer [35].

The *in situ* method is a two-step iterative process that involves

a) Alkylation step produces ester terminated products that are referred to 'half generation'.

b) Amidation of the ester terminated products with large excess of ethylenediamine to produce amine terminated products that are referred to a 'full generation'.

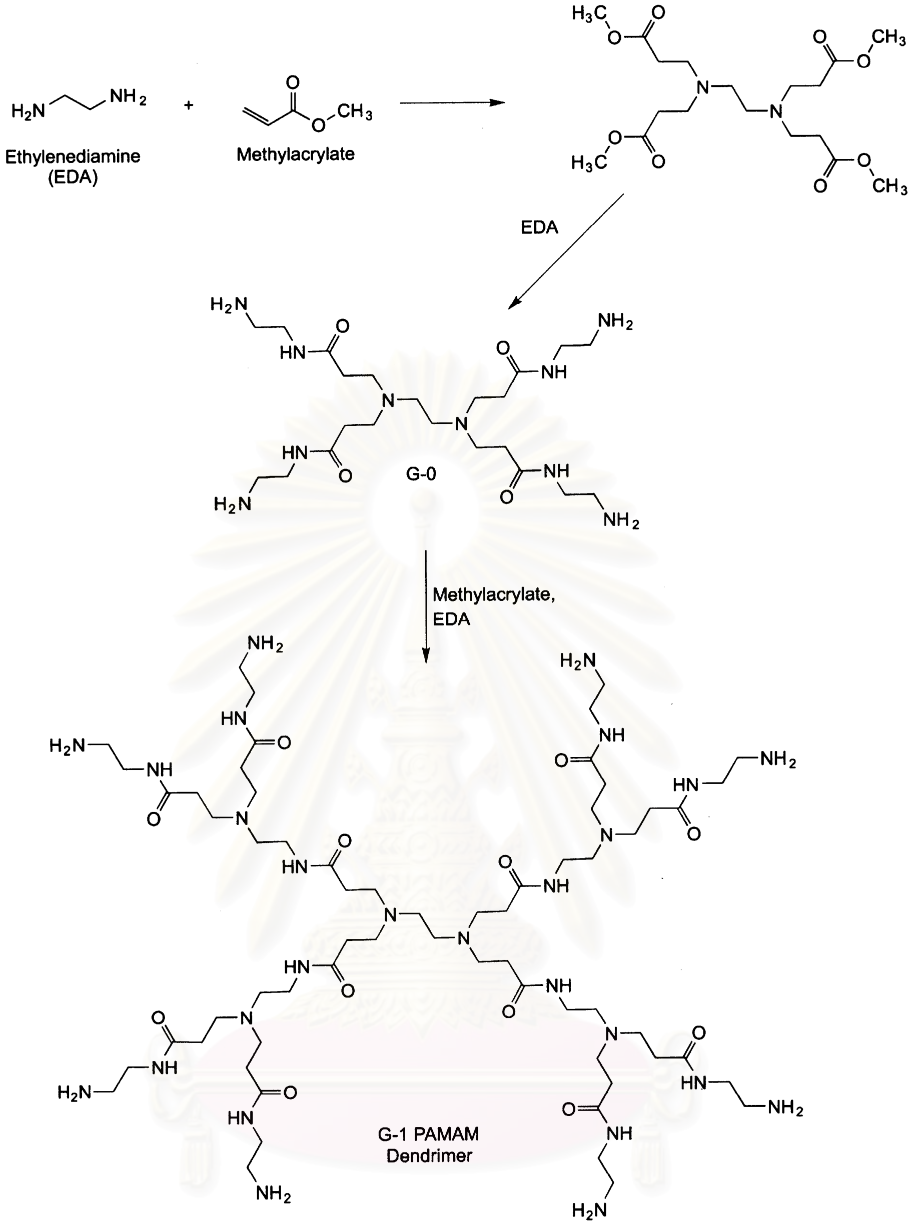

Figure 2.11 Synthesis of a PAMAM-type dendrimer proceeds from ethylenediamine core [36].

The structure of PAMAM dendrimers consists of three parts; the core, the interior and the surface functional groups (Figure 2.12). The core is as the molecular information center from which size, shape, directionality and multiplicity are expressed via the covalent connectivity to the outer shells. Within the interior, one finds the branch cell amplification region, which defines the type and amount of interior void space that may be enclosed by the terminal groups as the dendrimer is grown. Branch cell multiplication (N_b) determines the density and degree of amplification as an exponential function of generation (G). The core multiplication (N_c) and branch cell multiplication determine the precise number of terminal groups (Z) and mass amplification as a function of generation. The mathematical equation to determine the number of surface groups, number of branch cells and molecular weight of dendrimers was shown in Figure 2.13. And the theoretical values of surface functional groups and molecular weight of EDA-core PAMAM dendrimers shows in the Table 2.3.

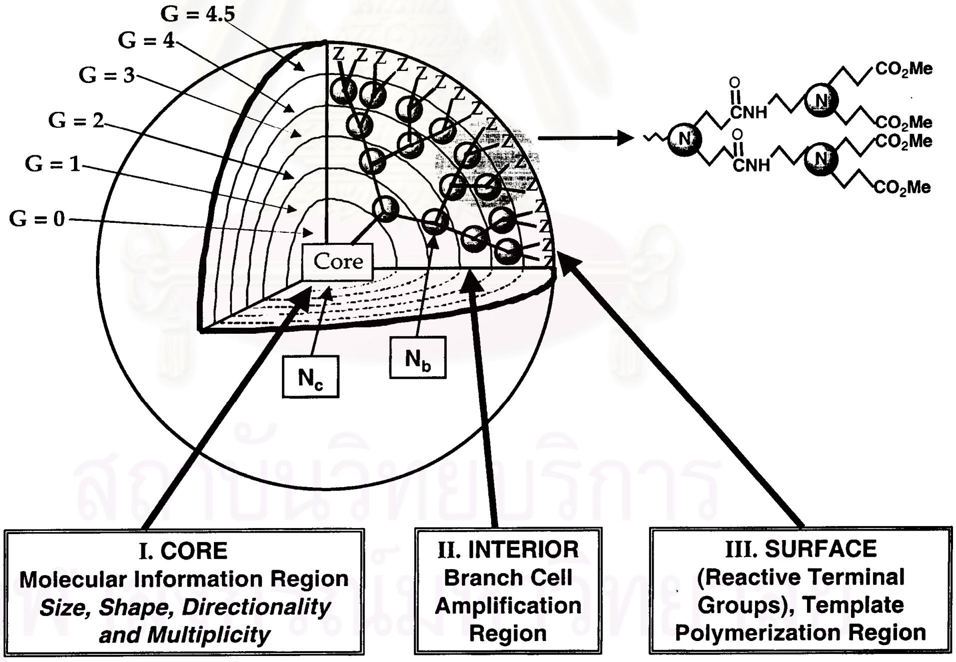

Figure 2.12 Three dimensional projection of dendrimer core-shell architecture for G = 4.5 poly(amidoamine) (PAMAM) dendrimer with principal architectural components (I) core, (II) interior and (III) surface [27].

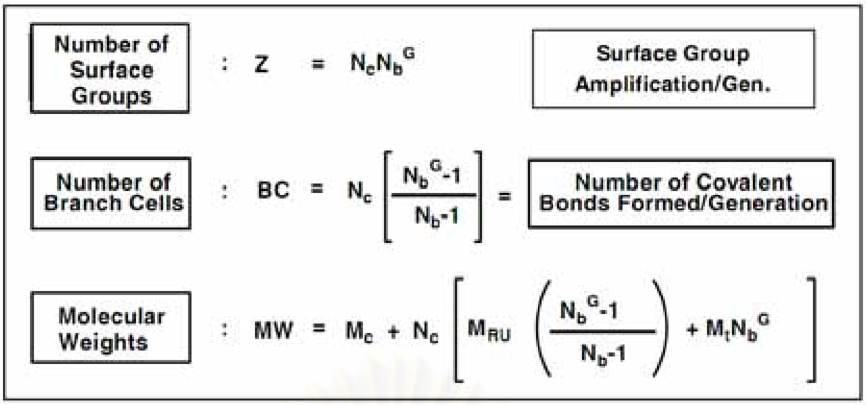

Figure 2.13 Mathematical relation between branch cell, core and generation [27]

Table 2.3 Mathematically defined values for surface groups, molecular formulae and molecular weight as a function of generation for the (EDA core), PAMAM dendrimer family [35].

Generation	Surface Groups	Molecular Formula	MW	Diameter (nm)
0	4	$C_{11}H_{48}N_{10}O_4$	517	1.4
1	8	$C_{62}H_{126}N_{26}O_{12}$	1,430	1.9
2	16	$C_{142}H_{288}N_{58}O_{28}$	3,256	2.6
3	32	$C_{302}H_{608}N_{122}O_{60}$	6,909	3.6
4	64	$C_{622}H_{1248}N_{250}O_{124}$	14,215	4.4
5	128	$C_{1262}H_{2528}N_{506}O_{252}$	28,826	5.7
6	256	$C_{2542}H_{5088}N_{1018}O_{508}$	58,048	7.2
7	512	$C_{5102}H_{10208}N_{2042}O_{1020}$	116,493	8.8
8	1,024	$C_{10222}H_{20448}N_{4090}O_{2044}$	233,383	9.8
9	2,048	$C_{20462}H_{40928}N_{8186}O_{4092}$	467,162	11.4
10	4,096	$C_{40942}H_{81888}N_{16378}O_{8188}$	934,720	~13.0

2.5 Unique Properties of PAMAM Dendrimers [37]

2.5.1 Nanoscale monodispersity

The PAMAM dendrimers show nanoscale monodispersity properties. The level of monodispersity is determined by the skill of the synthetic chemist, as well as the isolation and purification method utilized. In general, convergent methods produce the most nearly monodisperse dendrimers. The dispersity of some generation shows in the Figure 2.14.

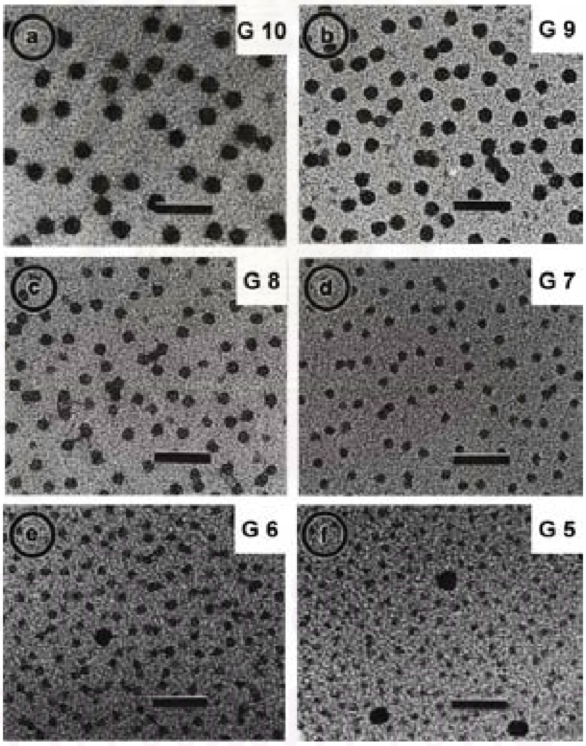

Figure 2.14 Transmission electron micrographs (TEMs) of Gen5–10 PAMAM dendrimers. Sample (f) contains three molecules of Gen10 dendrimer for comparison. Bar length = 50nm [1].

2.5.2 Nanoscale container and scaffolding properties

Unimolecular container and scaffolding behavior appears to be a periodic property that is specific to each dendrimer family. These properties are determined by the size, shape and multiplicity of the construction components that are used for the core, interior and surface of the dendrimer (Figure 2.15). Within the PAMAM dendrimer, they show flexible scaffolding in the lower generation (G=0-3), semiflexible scaffolding (container properties) in G = 4-6 and rigid surface scaffolding in the higher generation (G > 7).

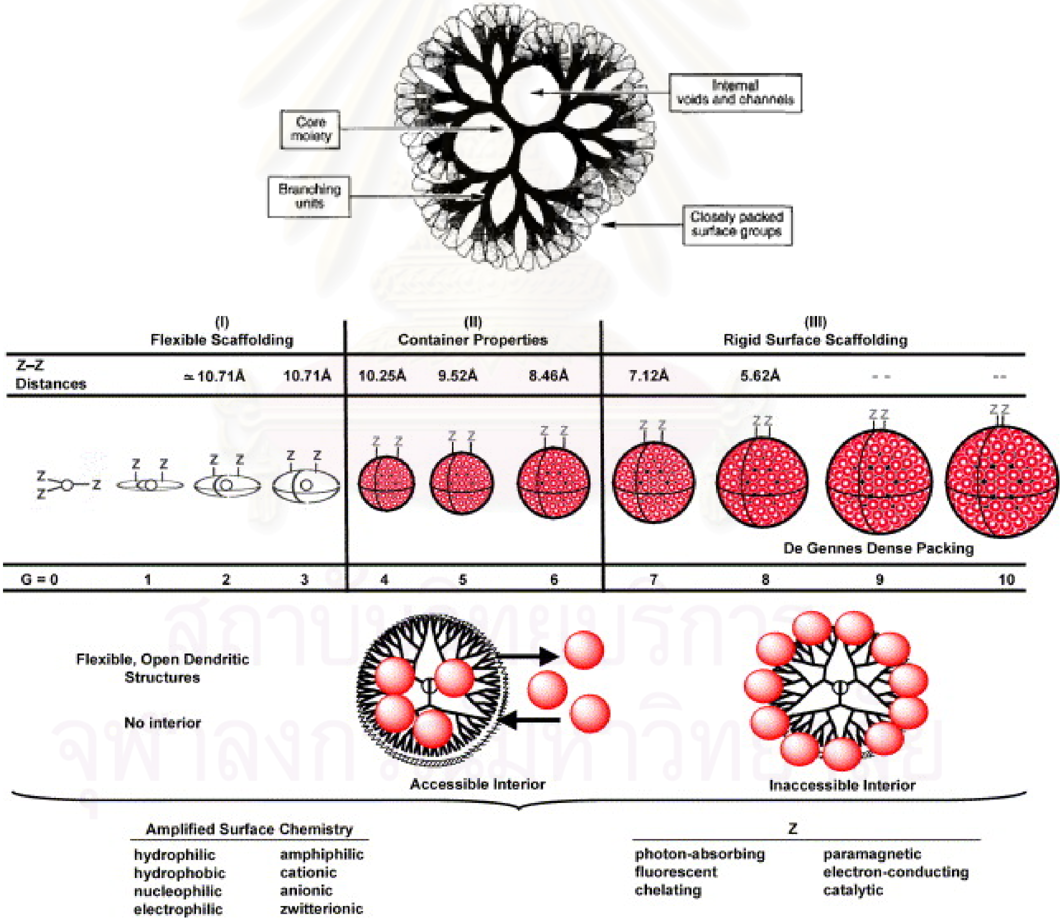

Figure 2.15 Periodic properties of PAMAM dendrimers as a function of generation [1, 34].

2.5.3 Amplification and functionalization of dendrimer surface groups

The various surface presentation of PAMAM dendrimers become congested and rigid as a function of increasing generation level. The number of surface groups of dendrimer can calculate from equation Z = $N_c N_b^G$. Dendrimer can be viewed as versatile, nanosized objects that can be surface functionalized with a lot of chemicals and application features as shown in Figure 2.16.

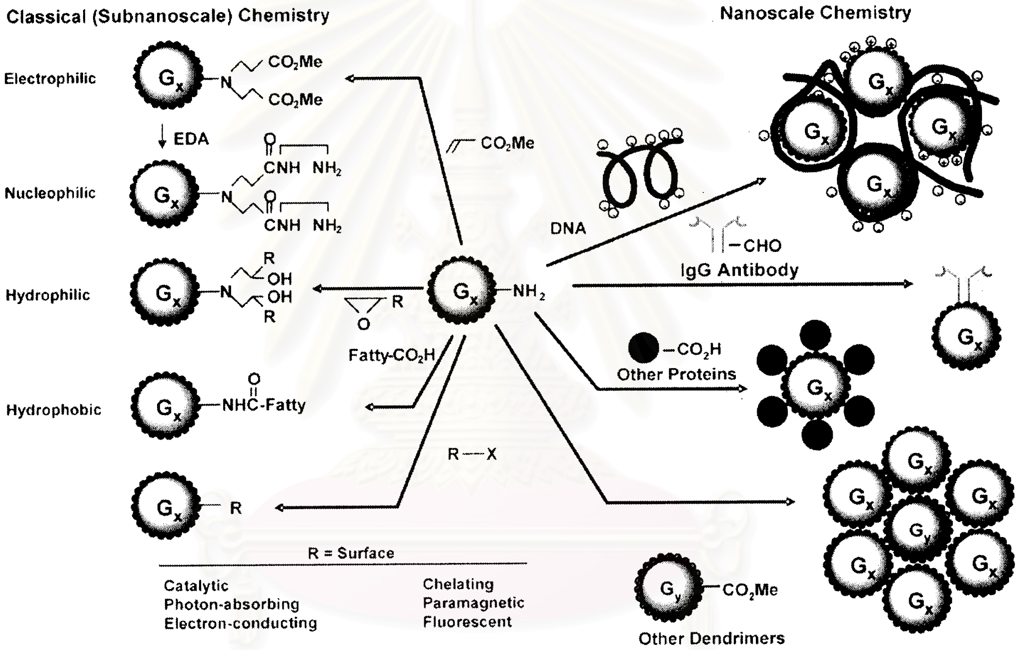

Figure 2.16 Options for modifying amine-terminated dendrimers by utilizing classical subnanoscale and nanoscale reagents [1].

2.5.4. Nanoscale dimensions and shape that mimic protein

Dendritic nanopolymers, especially dendrimers, fulfill many applications in the biological technology. From the nanoscale dimension of dendrimers, they are extensive interested in their use as globular protein mimic as shown in Figure 2.17.

Base on their systematic, size-scaling properties and electroretic and hydrodynamic behavior, PAMAM dendrimers are referred to as artificial protein. They are used for site-isolation mimicry of protein, enzyme-like catalyst, as well as other biomimetic applications, drug delivery, surface engineering and light harvesting.

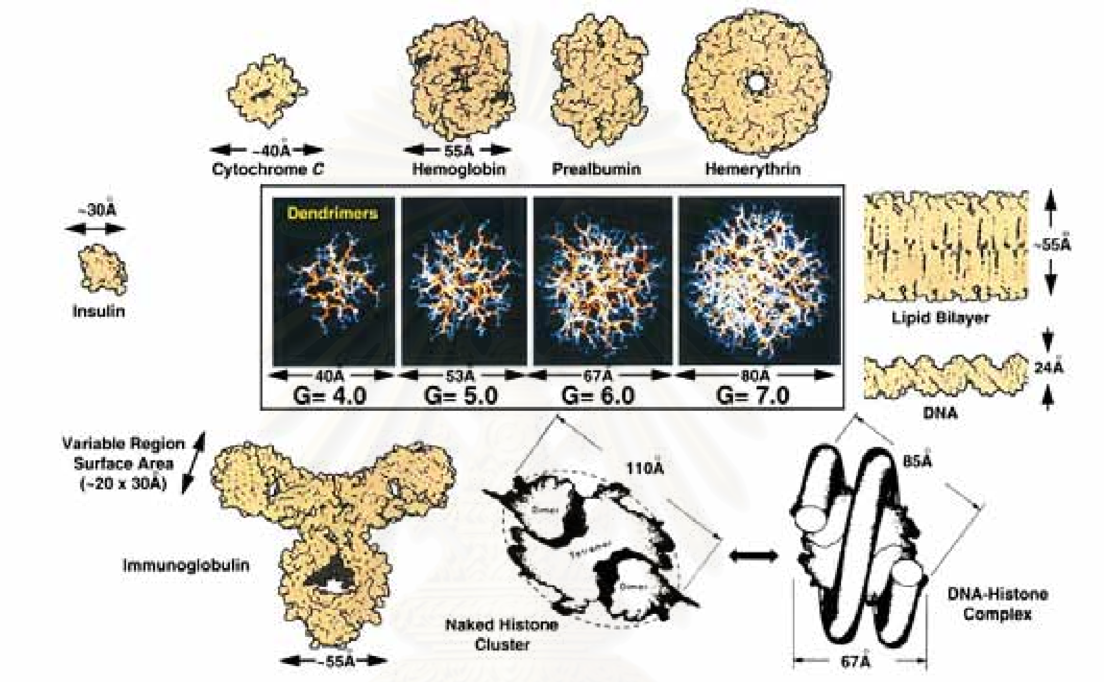

Figure 2.17 Dimensionally scaled comparison of a series of PAMAM dendrimers (NH_3 core; G 4–7) with a variety of proteins, a typical lipid-bilayer membrane and DNA, indicating the closely matched size and contours of important proteins and bioassemblies.[38]

2.6 Hyperbranched Polyamidoamine Polymers

Hyperbranched polymers are highly branched macromolecules that are prepared by a one-step self-polymerization of AB_x type multi-functional monomer (Figure 2.18). Hyperbranched polymers are potentially promising materials due to their relative ease of preparation compared to dendrimers. It has been shown that most of the hyperbranched polymer possess some of the unique properties exhibit dendritic macromolecules, such as low viscosity, good solubility and multi-functionality [39]. However, unlike dendrimer, hyperbranched polymers exhibit polydispersity and irregularity in term of branching and structure.

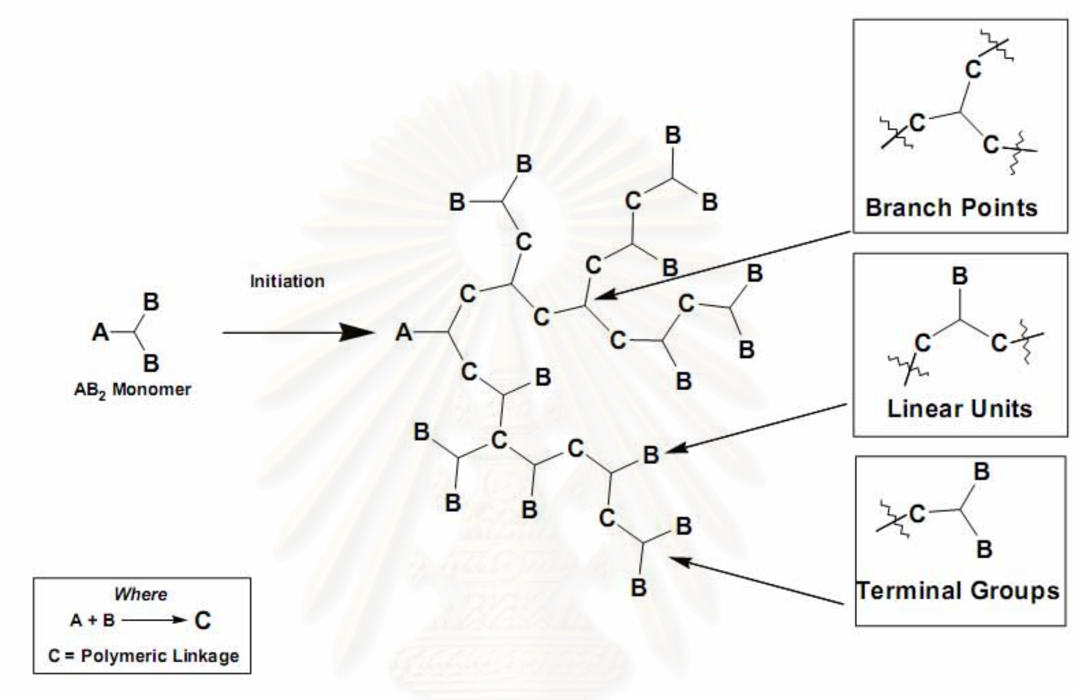

Figure 2.18 Schematic representation of a hyperbranched polymer constructed by the homopolymerisation of AB_2 type monomers [40].

Hyperbranched polyamidoamine have been reported by Hobson L.J. and Feast W.J. [41]. They prepared hyperbranched PAMAM by addition polymerization in the melt from a series of AB_2 aminoacrylate hydrochloride monomers using Michael addition chemistry, where A represents a Michael acceptor and B_2 a primary aliphatic amine. This step-growth polymerization process has led to the synthesis of PAMAM hyperbranched materials (Figure 2.19).

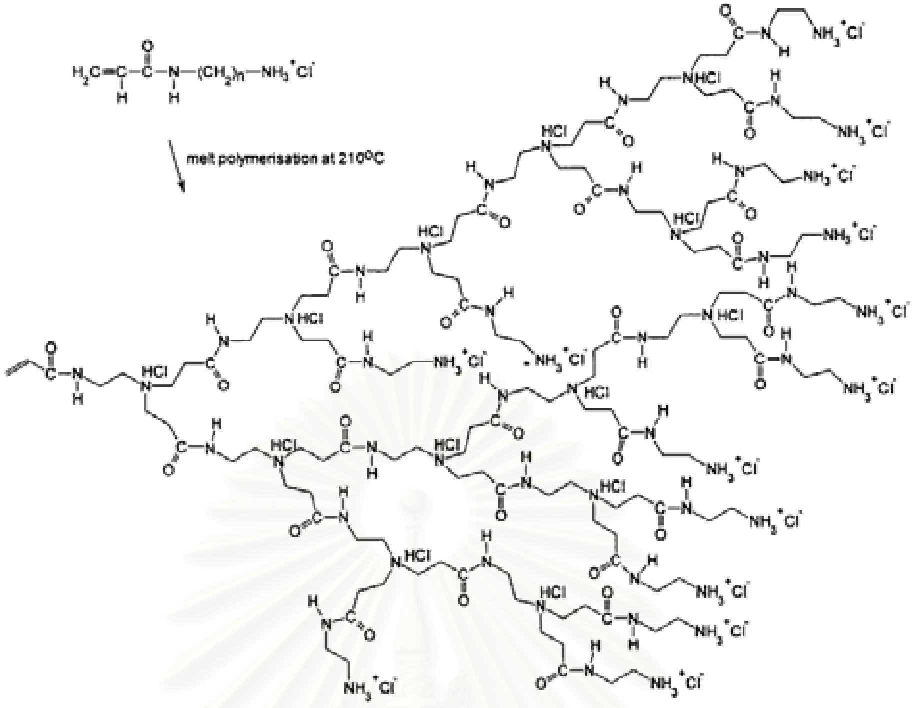

Figure 2.19 Proposed structure of an AB_2 polymer hydrochloride salt [41].

Twyman *et al.* [42] synthesized aromatic hyperbranched PAMAM polymers by polymerization of aromatic AB_2 bis-amino acid monomer at 165^0C under vacuum (Figure 2.20).

Twyman and Martin [43] patented the preparation of hyperbranched PAMAM and used it in biological field. The synthesis of monomer for polymerization in initiated from a β-alanine core (Figure 2.21). Growth of the PAMAM units is performed by standard PAMAM synthesis described in Tomalia’s work.

Martello *et al*. [44] prepared hyperbranched PAMAM by hydrogen –transfer polyaddition of *N,N’*-bisacryloylcystamine with ethylenediamine and of *N,N’*-bisacryloylpiperazine with cystamine. They used hyperbranched PAMAM containing disulfide linkages in the main chaun for DNA transfection.

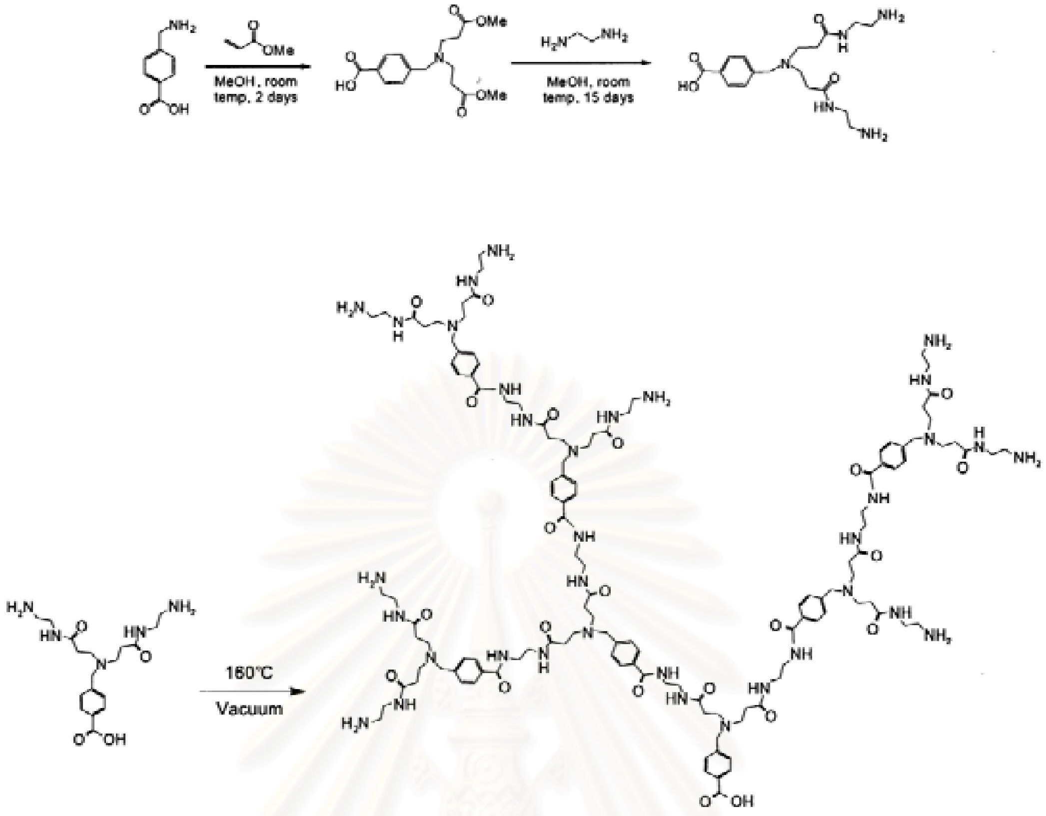

Figure 2.20 Synthesis of aromatic hyperbranched PAMAM polymers [42].

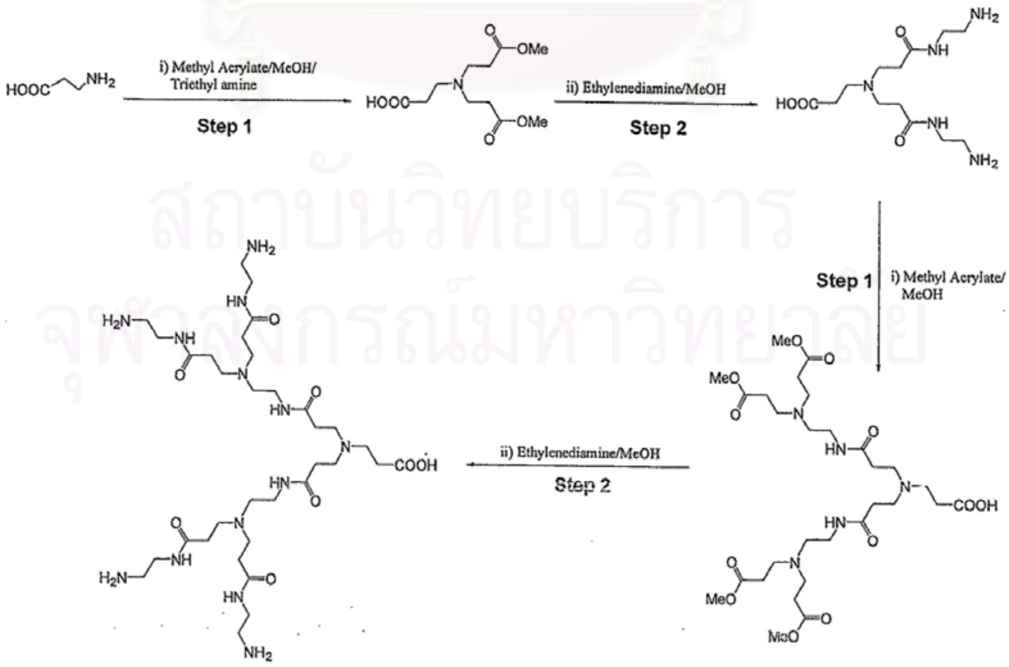

Figure 2.21 Synthesis of hyperbranched polyamidoamine (PAMAM) [43].

Cao *et al.* [45] synthesized hyperbranched PAMAM from different feed ratio of diethylene triamine and methyl acrylate. The synthesized products showed fluorescence properties that were influenced by pH, solvent, concentration and terminal groups.

Sun *et al.* [46] prepared hyperbranched PAMAM by reaction between *N,N'*-methylenebis-acrylamine and *N*-aminoethylpiperazine. The products in each step were precipitated into cold acetone. The final product used to synthesize Ag nanoparticles.

Dodiuk-Kenig *et al.* [47] studied a novel adhesion promoters based on hyperbranched PAMAM. Hyperbranched PAMAM was synthesized base on epoxy-amine reaction. The process is based on two quantitative steps: diethoxy-amine addition and polyamide-epoxy addition. The effect on properties of hyperbranched PAMAM was studied in epoxy and polyurethane systems.

The surface modification of some materials with polymers may be endowed with special function, such as photosensitivity, bioactivity, crosslinking ability and amphiphilic properties. Tsubokawa *et al.* [18] modified ultrafine silica surface by grafting of hyperbranched PAMAM. Before the grafting, the silica was introduced amino groups as an initiator site on the silica surface by treatment of silica with γ-aminopropyltriethoxysilane. And then hyperbranched PAMAM was propagated from silica surface by repeating two processes: Michael addition and amidation (figure 2.22). The hyperbranched PAMAM grafted ultrafine silica gave a stable dispersion in solvent.

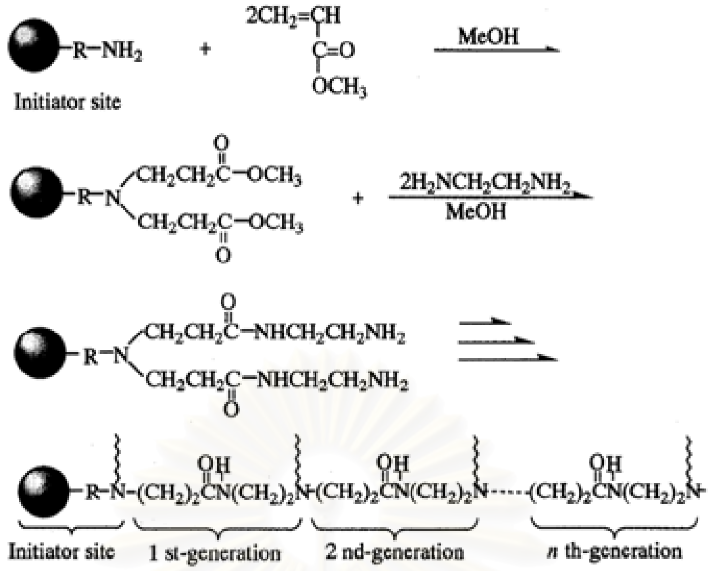

Figure 2.22 Theoretical scheme of synthesis of ‘dendrimer-like’ grafted ultrafine silica [18].

Another works that related to surface grafting of hyperbranched PAMAM onto the silica surface; Kaneko *et al.* [48] grafted hyperbranched PAMAM onto a colloidal silica surface in a solvent-free dry system and in a methanol solvent system. They found that the terminal amino groups of hyperbranched PAMAM grafted silica to be effective in curing epoxy resin.

Yoshikawa *et al*. [49] studied post-grafting of polymer with controlled molecular weight onto silica surface by termination of living polymer cation with terminal amino groups of hyperbranched PAMAM grafted ultrafine silica.

Qu *et al.* [50] functionalized silica-gel with ester- and amino-terminated hyperbranched PAMAM polymer. And then studied the adsorption and desorption behaviors of Pd(II) on functionalized silica gel. Qu *et al.* [51] also surface functionalized chitosan with ester- and amino-terminated hyperbranched PAMAM polymers. The results showed that the functionalized products exhibited better adsorption capabilities for Au^{3+} and Hg^{2+}.

Tsubokawa and Takayama [52] modified the surface of chitosan powder by grafting of hyperbranched PAMAM onto the surface. It was found that the average particle size of hyperbranched PAMAM grafted chitosan powder was decreased by grafting of hyperbranched PAMAM polymers.

Yoza *et al.* [53, 54] modified baterial and artificial magnetic particles using hyperbranched PAMAM. The modified products were used to extract DNA from blood.

Most of the application of hyperbranched polymers is based on the absence of chain entanglements, the globular shape, and the nature and the large number of functional groups within a molecule. Modification of the number and type of functional groups on hyperbranched polymers is essential to control their solubility, compatibility, reactivity, adhesion to various surfaces, self-assembly, chemical recognition, and electrochemical and luminescence properties. The large number of functional groups allows for the tailoring of their thermal, rheological and solution properties and thus provides a powerful tool to design hyperbranched polymers for a wide variety of application (Figure 2.23). Some companies already produce commercially available hyperbranched polymer on a large scale (Figure 2.24) [55].

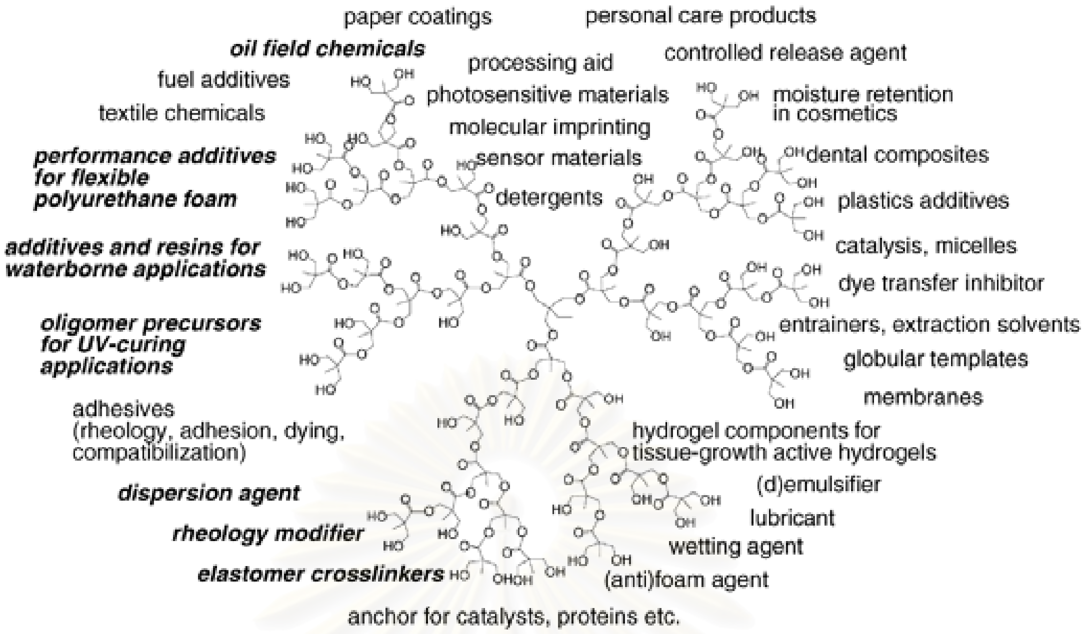

Figure 2.23 Applications of hyperbranched polymers discussed in literature. Bold italic: commercial applications of hyperbranched polymers [55].

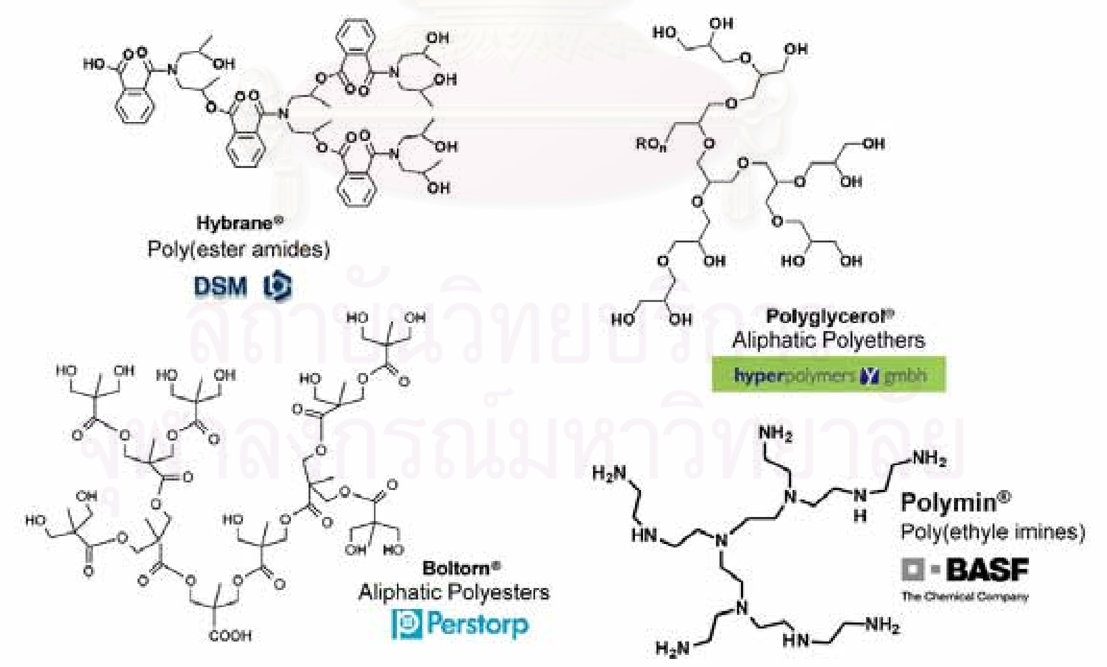

Figure 2.24 Commercially available hyperbranched polymers [55].

2.7 Application of Dendritic Polymers in Related Textiles

Dendrimers have attracted much interest for their symmetry, high degree of branching and high density of terminal functional groups. Many of the dendrimer's chemical and physical properties, such as aggregation, reactivity, stability and solubility, are closely related to the nature of the end groups. So that it is possible to tailor the properties of dendrimers by appropriate chemical modification of the end groups. One of the features of dendrimers is the regular and highly branched structure. The highly branched molecules should be able to act as a host for the entrapment of guest molecules [56-59].

Baars *et al.* [60] modified the poly(propylene imine) dendrimers with apolar end groups, such as linear alkyl chains and adamantine, to extract the anionic dyes from the water to solvents. The extraction model of this research shows in Figure 2.25.

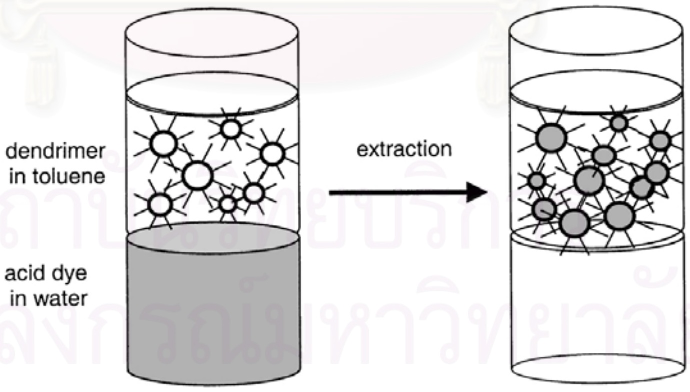

Figure 2.25 Extraction of an anionic dyes from aqueous solution by an alkyl modified poly(propylene imine) dendrimer in toluene [61].

Yiyun and Jiepin [62] studied the effect of PAMAM dendrimers in decolorizing of triarylmethane dye in wastewater. PAMAM dendrimer acted as flocculant due to it contains high density of amino groups. The PAMAM dendrimers could be used several times and still maintain high decolorization activity. It is possible to decolorize high concentration of dyes with low concentrations of PAMAM dendrimers.

Ahmed *et al.* [9] prepared a chromophore-bearing dendrimer by reaction of 2nd generation of PAMAM dendrimer with 4-acetamidobenzene sulphonyl chloride. The synthetic scheme shows in Figure 2.26. The product was an orange color in the solid state and exhibited good solubility in water at alkaline pH, giving deep red solution.

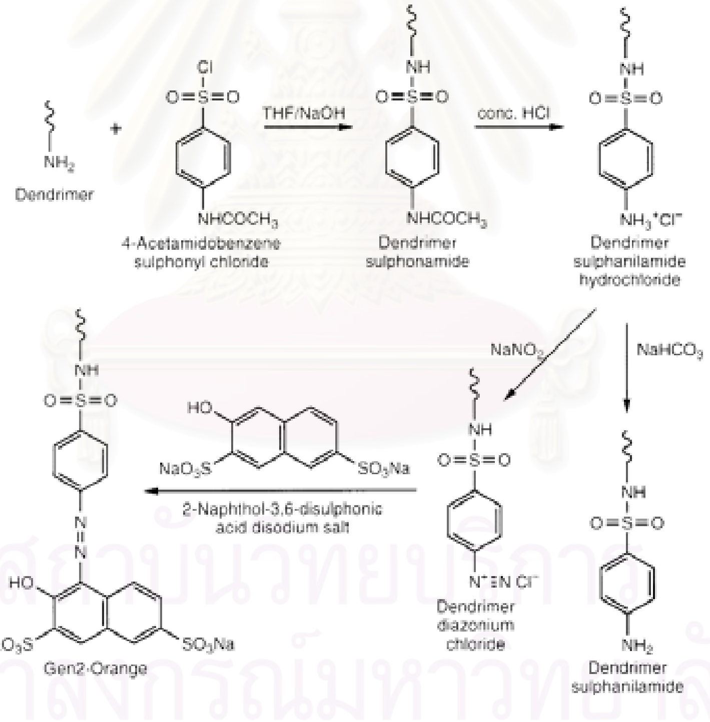

Figure 2.26 Synthetic scheme for preparation of Gen2-Orange [9].

The other chromophore bearing dendrimer was introduced by Stephan *et al.* [63]. They synthesized Methyl orange bearing poly(propyleneamine) dendrimers. It showed an unique phase-transfer behavior with respect to pH changes and offer a new approach for controlled inclusion and release of anionic substrates. Hyperbranched polymers were also applied in dyeing of hydrophobic fiber, such as poly(propylene) which cannot be dyed in the conventional dyeing methods. Burkinshaw *et al.* [64] incorporated hyperbranched polymers into poly(propylene) prior to fiber spinning markedly enhanced the dyeability of polypropylene fiber with disperse dye. It showed very good washing fastness. The model of this dyeing mechanism shows in Figure 2.27.

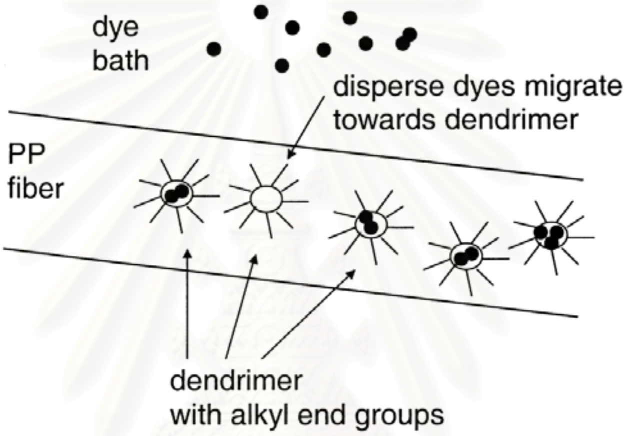

Figure 2.27 Dyeing of poly(propylene) fibers. The fiber contains alkyl modified dendrimers or hyperbranched polymers, which extract the dyes out of the dye bath [61].

Zhang *et al*. [65] synthesized amino-terminated hyperbranched polymers and applied in reactive dyeing on cotton fabric as a salt-free dyeing auxiliary. A water-soluble amino-terminated hyperbranched polymers was synthesized from methyl acrylate and diethylene triamine by melt condensation. The cotton fabric treated with an aqueous solution of the amino-terminated hyperbranched polymers in the presence of citric acid and sodium hypophosphite. It exhibited high color strength, good washing and rubbing fastnesses and good leveling properties.

Burkinshaw *et al.* [66] treated dendrimer (derivative of $Am_{16}decanamide_8$) on the cotton fabric to modify the dyeing behavior of reactive on cotton. The reactive dyeing had been carried out in the absence of electrolyte and alkaline. It displayed markedly enhanced color strength.

CHAPTER III

EXPERIMENTAL

3.1 Materials and Chemicals

Table 3.1 Chemicals used in this study

Chemicals	**Grade**	**Suppliers**
Fumed silica (AEROSIL 200)	Commercial	JJ Degussa (Thailand)
Methyl acrylate (MA)	Analytical	Fluka
Ethylene diamine (EDA)	Analytical	Fluka
3-Aminopropyltriethoxysiliane (APTES)	Analytical	Fluka
Dicyandiamide	Commercial	JJ Degussa (Thailand)
Phosphorus acid	Analytical	Aldrich
Formaldehyde	Analytical	BDH
Hydrochloric acid	Laboratory	J.T.Baker
Urea	Laboratory	Unilab
Toluene	Commercial	TSL Chemical (Thailand)
Methanol	Commercial	TSL Chemical (Thailand)
Standard soap	Laboratory	AATCC

Table 3.2 Materials used in this study

Materials	Suppliers
Dyed single jersey knitted cotton fabric, weight of fabric = 258 g/m^2	Nanyang Textile Co., LTD
Dialysis membrane	Membrane Filtration Products, Inc.

3.2 Equipments

1. Fourier transform infrared spectrophotometer (FTIR): Nicolet Impact 400D

2. Thermal gravimetric analyzer (TGA): Mettler Toledo STARe System DCS822e Module

3. Scanning electron microscope (SEM): JEOL Model JSM-5410LV, Japan.

4. Stenter oven (Rapid): Labortex Co.,Ltd. Taiwan

5. Padding machine (Labtec): Newave Lab Equipments Co.,Ltd. Taiwan.

6. Automatic flammability tester : Shirley M233B, England.

7 .Proton nuclear magnetic resonance spectrometer. (^{1}H NMR): Bruker DPX-300, Germany

8. Particle size analyzer: Mastersizer 2000, Malvern Instruments, United Kingdom.

9. Washing tester (Gyrowash): James H Heal Co.,Ltd. England

10. Bursting strength tester: SDL 229B, P1000 Bursting strength tester, Shirley, England.

3.3 Synthesis of Hyperbranched PAMAM Dendrimers

The synthesis of hyperbranched PAMAM was carried out by divergent method which involved in situ branch-cell construction in stepwise. The method consists of two step reactions: a) Michael addition of primary amine with MA and b) amidation of amplified ester groups with EDA. Hyperbranched PAMAM were synthesized as follows;

PAMAM G-0.5

A solution of EDA (50 g, 0.83 mole) in methanol (200 ml) was added dropwise to a stirred solution of MA (350 g, 4.08 mole) in methanol (200 ml) at 0^0C over a period of 2 hours. The mixture temperature was allowed to rise to room temperature and the mixture was continuously stirred for 48 hours. The solvent was removed using a rotary evaporator under reduced pressure at 50^0C.

PAMAM G0.0

A solution of G-0.5 PAMAM (50 g) in methanol (100 ml) was carefully added to a vigorously stirred solution of EDA (418 ml) in methanol (300 ml) at 0^0C. The rate of addition was carefully controlled to assure that the temperature did not rise over the room temperature. After completion of addition, the mixture was stirred for 72 hours at room temperature. The solvent and unreacted EDA were removed under reduced pressure at the temperature not higher than 50^0C. The excess EDA was removed at azeotropic temperature using toluene to methanol mixture (9:1).

PAMAM G0.5

A solution of G0.0 PAMAM (50 g) in methanol (150 ml) was added to a stirred solution of MA (90 g) in methanol (100 ml) at 0^0C. The mixture was stirred at room temperature for 48 hours. The solvent and unreacted MA were removed in similar manner to previous procedure.

PAMAM G1.0

A solution of G0.5 PAMAM (120 g) in methanol (100 ml) was added to a vigorously stirred solution of EDA (642 ml) in methanol (200 ml) at 0^0C. The mixture was stirred for 96 hours at room temperature. After the reaction, the solvent and unreacted EDA were removed in similar manner to previous procedure.

PAMAM G1.5

A solution of G1.0 PAMAM (200 g) in methanol (200 ml) was added to a stirred solution of MA (217 g) in methanol (200 ml) at 0^0C. The mixture was stirred at room temperature for 48 hours. And then, the solvent and unreacted MA were removed in similar manner to previous procedure.

PAMAM G2.0

A solution of G1.5 PAMAM (200 g) in methanol (200 ml) was added to a vigorously stirred solution of EDA (1192 ml) in methanol (500 ml) at 0^0C. The mixture was stirred for 96 hours at room temperature. After the reaction, the solvent and unreacted EDA were removed.

PAMAM G2.5

A solution of G2.0 PAMAM (230 g) in methanol (200 ml) was added to a stirred solution of MA (260 g) in methanol (500 ml) at 0^0C. The mixture was stirred at room temperature for 48 hours. And then, the solvent and unreacted MA were removed.

PAMAM G3.0

A solution of G2.5 PAMAM (4400 g) in methanol (300 ml) was added to a vigorously stirred solution of EDA (2000 ml) in methanol (300 ml) at 0^0C. The mixture was stirred for 96 hours at room temperature. After the reaction, the solvent and unreacted EDA were removed.

3.4 Incorporation of Amino Groups onto Ultrafine Silica Particle

The attachment of amino groups onto the silica surface was performed by the condensation reaction between surface silanol groups and 3-aminopropyl-triethoxysilane. Into a 600 ml flash, 15.0 g of silica and 500 ml of 10% v/v toluene solution of 3-aminopropyltriethoxysilane were charged, and the mixture was stirred for 30 minutes with a magnetic stirrer. Then 50 ml of methanol:water (2:1 volume ratio) was added to the mixture and stirred for 72 hours. After the reaction, the mixture was filtrated and extracted with toluene for 24 hours using Soxhlet extractor. The APTES treated silica was dried in oven at 60^0C for 24 hours and stored in autodehumidity desiccator.

3.5 Grafting of Polyamidoamine Hyperbranched Polymer from Silica Surface

Michael addition was carried out as follows; Into a 1,000 ml flask that containing 20.0 g APTES treated silica and 600 ml of methanol, then methyl acrylate (10 times of amino content) in methanol was dropwise added. The mixture was stirred at room temperature for 48 hours. The methanol and unreacted methyl acrylate were evaporated by reduced pressure evaporator.

The amidation of terminal ester groups from Michael addition step was carried out as follows: Into 1000 ml round bottom flask that containing ester terminated silica from Michael addition step, and 500 ml of methanol. A solution of 45 ml of EDA in 100 ml of methanol was carefully added to a vigorously stirred solution of ester terminated silica in methanol. The mixture was stirred at room temperature for 72 hours. The solvent and unreacted EDA were removed under reduced pressure maintaining the temperature no higher than 40^0C.

The propagation for second and third generation was carried out by the repeating of two step reactions, Michael addition and amidation. The second generation was as follows: the product obtained from the above reactions was reacted with MA (2 times of MA used from the above reaction) in 100 ml of methanol. The mixture was stirred at room temperature for 48 hours, and then evaporated the solvent and unreacted MA. After that, the resulting silica was reacted with EDA (2 times of EDA used from the above reaction) in 100 ml of methanol. After 72 hours, the solvent and unreacted EDA were removed. The third generation was followed the second generation preparation. It was carried out by using 2 times of MA and EDA employed in second generation.

3.6 Determination of Amino Group Content on PAMAM Grafted Silica

The amino group content of PAMAM grafted silica were determined by titration technique. Into 125 ml flask, 0.1000 g of treated silica and 25 ml of 0.01 M hydrochloric acid aqueous solution were charged. The mixture was stirred at room temperature for 2 hours. And then, the mixture was filtrated and titrated with standardized aqueous solution of sodium hydroxide by using phenolphthalein as an indicator.

3.7 Determination of Percent Grafting

The weight of PAMAM grafted onto the silica surface was determined by weight loss measurement. PAMAM grafted silica was burnt out at 800^0C using TGA (Mettler Toledo STARe System DCS822e Module). The percentage of grafting was calculated from the difference between percentage of determined original weight of PAMAM grafted silica sample and the percent residual silica.

3.8 Phosphorylation of PAMAM and PAMAM Grafted Silica

PAMAM or PAMAM grafted silica (0.2 mole) and crystalline phosphorous acid (0.4 mole) were dissolved in 200 ml of water and concentrated hydrochloric acid (0.6 mole). The mixture was heated to reflux in a three-necked flask fitted with thermometer, condenser and dropping funnel. In the course of ca 1 hour, 40% aqueous formaldehyde solution (0.8 mole) was added dropwise, and the reaction was kept at the reflux temperature for an additional hour. The water was evaporated at low temperature using the rotary evaporator. The concentrated solution was neutralized with concentrated ammonium solution. And then, the concentrated solution was precipitated in methanol. The general mechanism of this reaction (Mannich type reaction) is given in Figure 3.1.

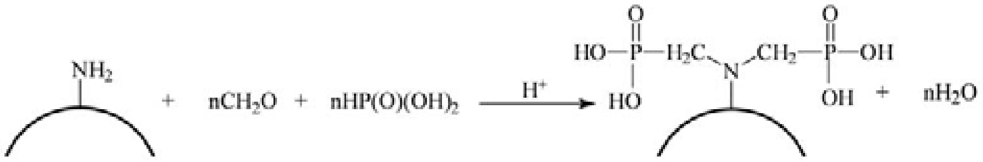

Figure 3.1 The general mechanism of Mannich type reaction.

3.9 Fixation of Phosphorylated Hyperbranched PAMAM Grafted Silica on Knitted Cotton Fabric

Knitted cotton fabrics were treated with a solution containing 30 % (w/w) phosphorylated hyperbranched PAMAM grafted silica and 20 g/l dicyandiamide as a activating agent and 300 g/l of urea**.** The application was performed using a pad mangle set a pressure nip at 80 percent wet pick up. The padded fabric was dried at 100 ºC for 5 min and cured at 170 ºC for 3 min to allow the covalent reaction, leading to phosphonated cellulose produced. The treated fabric was washed-off according to ISO105 C01 for 1 cycle to remove unfixed agents.

3.10 Bursting Strength Test [67,68]

The strength of knitted cotton fabric was determined by P1000 Bursting strength tester, SDL 229B. The preconditioning of the sample fabric must take place before testing. The testing was conducted according to ASTM D3786 - 01 Standard Test Method for Bursting Strength of Textile Fabrics - Diaphragm Bursting Strength Tester Method. The conditioned specimen was clamped in the position and the pressure was applied. Immediately after the fabric burst occurred, the burst pressure as recorded. In the rapid succession, the clamping pressure was released and the fabric was removed. The machine button on the main control panel was then pressed in order to record the Diaphragm correction factor. The corrected mean bursting pressure was calculated using the following equation.

Bursting pressure = Mean bursting pressure – Diaphragm correction factor

3.11 Flammability Test [69]

The flammability test of cotton fabric was investigated according to BS EN ISO 6940:1995 (Textile fabrics-Burning behaviour-Determination of ease of ignition of vertically oriented specimens). The specimens were cut to be 200 mm x 80 mm and placed on the template. For the surface ignition, the position of the burner was perpendicular to the surface of the specimen. And then, the flame was applied to the specimen for 5 seconds and the burning behaviour was observed.

3.12 Characterizations

3.12.1 FTIR Spectroscopy

The functional groups of the samples were characterized by Nicolet FTIR spectrophotometer (Nicolet Impact 400D). PAMAM dendrimers, hyperbranched PAMAM grafted silica and their surface functionalized products were coated on KBr disc. The spectra were taken at 32 scans, resolution of 4 cm^{-1} and in frequency range of 4000-400 cm^{-1}. In the case of virgin silica and silane functionalized silica, they were mixed with KBr powder and compressed into KBr pellet before characterization.

3.12.2 ^{1}H and ^{13}C NMR Spectroscopy

The samples were dissolved in deuterated chloroform containing 1% tetramethylsilane (TMS), which was used as an internal reference. The ^{1}H and ^{13}C NMR spectra of the samples were recorded on Bruker DPX-300 spectrometer.

3.12.3 Scanning Electron Microscopy

Morphology of hyperbranched PAMAM grafted silica was determined by scanning electron microscope (SEM; Model JSM-5410LV, JEOL). It was operated at 15 kV to image the samples. The surface of sample was sputter-coated with a thin layer of gold before scanning.

3.12.4 Thermogravimetric Analysis

Thermogravimetric analysis (TGA) was performed using Mettler Toledo STARe System DCS822e Module. The samples were heated from 40^{0}C to 800^{0}C under oxygen atmosphere at a heating rate of 10^{0}C/min. Before the experiment, the samples were dried in an oven at 60^{0}C for at least 12 hours.

3.12.5 Particles Size Analysis

The particle size distribution was measured on Mastersizer 2000 using laser light scattering technique. The samples were dispersed in methanol for 24 hours before measurement. They were added dropwise to the sample area containing distilled water as dispersant. The particle size distribution was analyzed by particle sizing program.

CHAPTER IV

RESULTS AND DISCUSSION

4.1 Synthesis of Polyamidoamine (PAMAM) Dendrimers

The synthesis route of PAMAM dendrimer was carried out based on the previous report [35]. It consists of consecutively repeating two reactions; Michael addition to produce ester terminated products and amidation of the ester terminal group with large excess of ethylenediamine to produce amine terminated PAMAM. The theoretical reaction of this synthesis is shown in the Figure 4.1.

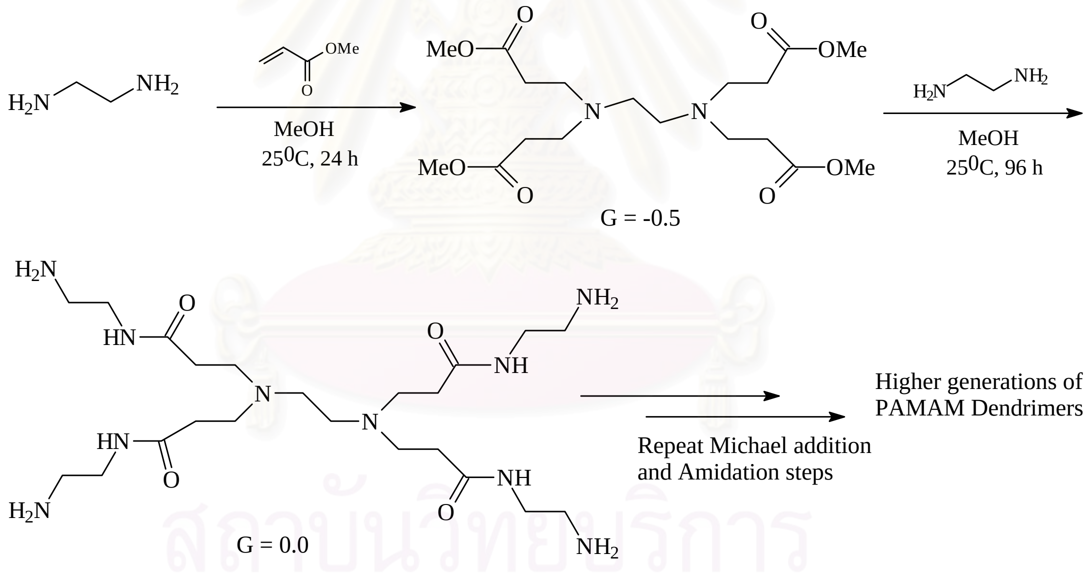

Figure 4.1 Theoretical synthesis of PAMAM dendrimers

The synthesized products of each generation were characterized by FTIR, ^{1}H-NMR and ^{13}C-NMR analysis. The FTIR spectra of each generation are shown in Figure 4.2. In Michael addition steps, (product G-0.5, G0.5, G1.5 and G2.5) the strong absorption band around 1740 cm^{-1} is observed which indicates the methyl ester groups. From the spectra of G0.0, G1.0, G2.0 and G3.0 PAMAM dendrimers obtained from amidation steps, the peak representing methyl ester band disappears. New absorption band around 3290-3370 cm^{-1} shows up strongly, particularly in generation G3.0. This peak is assigned to the NH band. The other peaks at 1639 cm^{-1} and 1558 cm^{-1} are noticed, indicating the characteristics of C=O stretching and N-H bending, respectively. In addition, the absorption bands at 3293 cm^{-1} and 3364 cm^{-1} are N-H antisymmetric stretching and symmetric stretching of N-H primary amine.

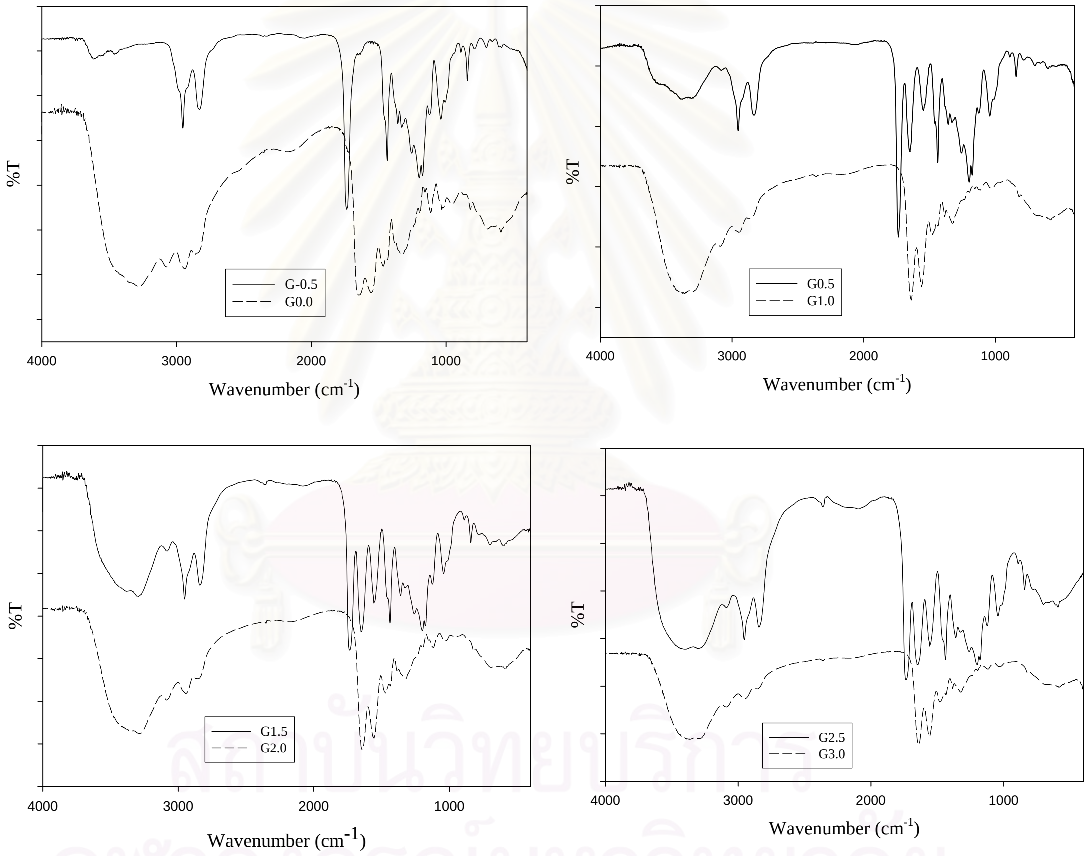

Figure 4.2 FTIR spectra of polyamidoamine dendrimers

The ^{1}H-NMR spectrum of ester terminated PAMAM dendrimer is shown in Figure 4.2. The chemical shift of methyl ester terminated group (CH_3-O-) is found at ~3.54 ppm. The methylene proton (-CH_2CH_2-) appears at the region of 2.22-2.42 ppm and the methylene proton of methylene groups linked to nitrogen atom (-CH_2-N-) appears at around 2.61-2.78 ppm. The proton of amide groups (-CO-NH-) exhibits the signals around 7.46-7.75 ppm [35].

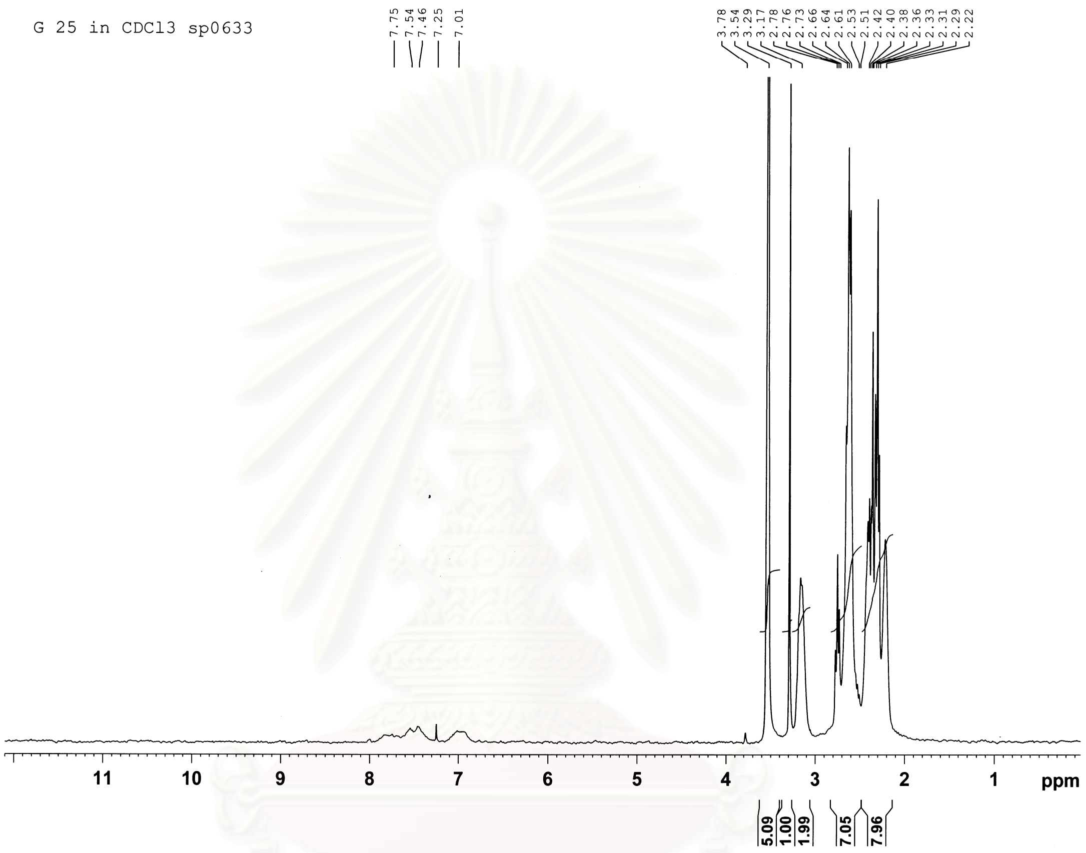

Figure 4.3 ^{1}H-NMR spectrum of G2.5 PAMAM dendrimer.

The ^{13}C-NMR spectrum of G2.5 PAMAM dendrimers shows in Figure 4.4, the carbon of carbonyl ester and amide groups appear at 172-173 ppm.

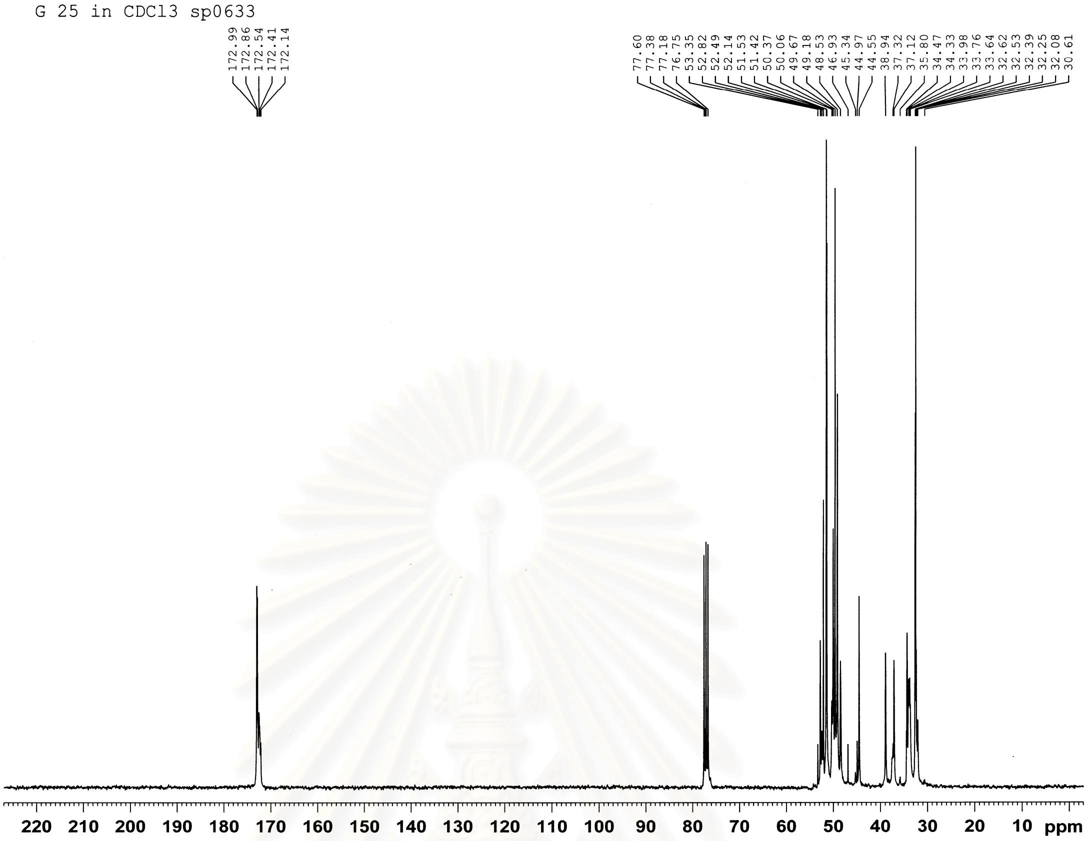

Figure 4.4 ^{13}C-NMR spectrum of G2.5 PAMAM dendrimers.

The ^{1}H-NMR spectrum of amine terminated PAMAM dendrimers is shown in Figure 4.5. The signals indicating the presence of amide groups (-CO-NH-), the methylene groups adjacent to amide group (-CO-NH-CH_2-), amine groups (-NH_2) and methylene groups adjacent to amine group (-CH_2-NH_2) are found at 7.7-7.8 ppm, 3.10 ppm, 2.47 ppm, and 2.26 ppm, respectively. The ^{13}C-NMR spectrum shown in Figure 4.6 illustrates the chemical shift of carbon atom of amide (-CO-NH-) at 172-173 ppm, carbon atom of methylene adjacent to amide group (-CONH-CH_2-) at 49-52 ppm and carbon atom of methylene adjacent to amine (-CH_2CH_2-N-CH_2CH_2-) at the region of 33-46 ppm [35].

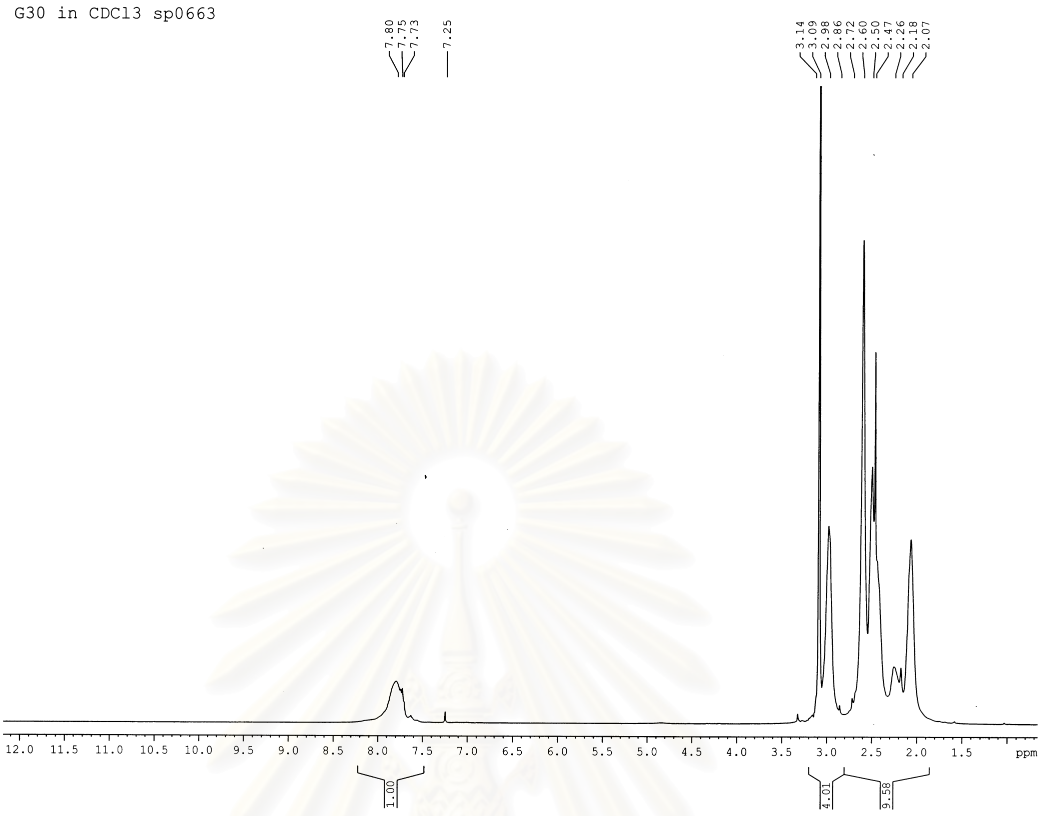

Figure 4.5 ^{1}H-NMR spectrum of G3.0 PAMAM dendrimers.

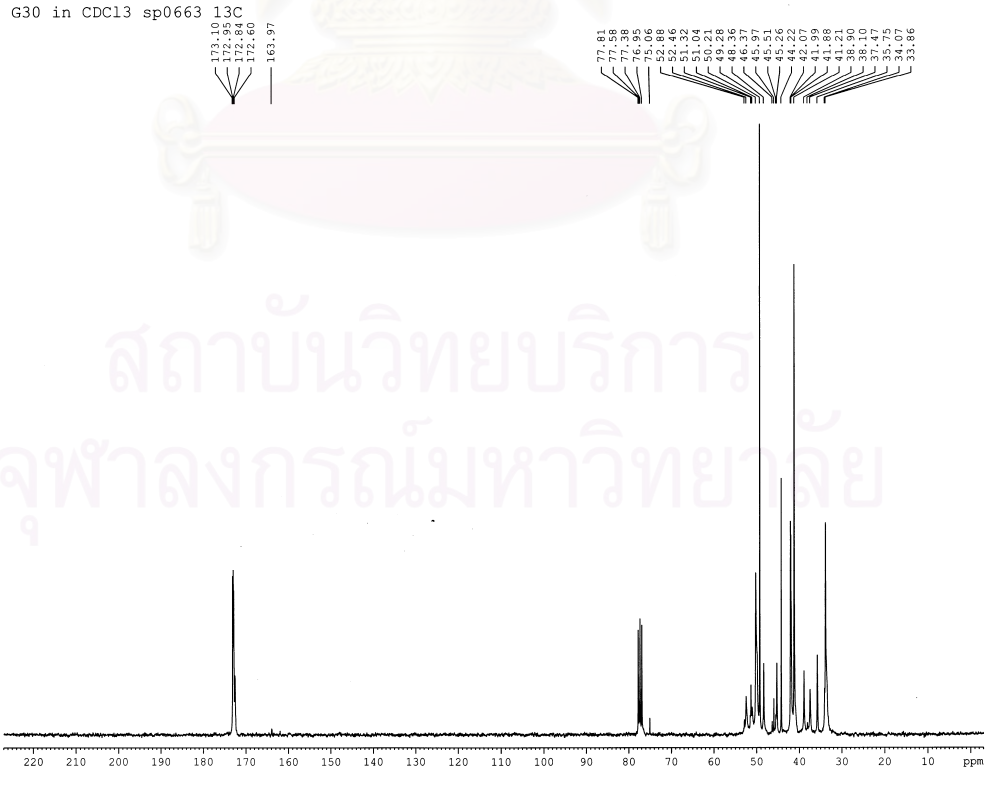

Figure 4.6 ^{13}C-NMR spectrum of G3.0 PAMAM dendrimers.

4.2 Introduction of Amino Groups onto the Silica Surface

The surface functionalization of silica particles was carried out by the condensation reaction of silica silanol group with 3-aminopropyltriethoxysilane (APTES), resulting in silica particle containing amino groups on the surface which acted as the initiator sites for PAMAM grafting. There are several treatment methods concerning APTES grafting onto silica surface including graftings in acid-aqueous solution and in anhydrous solution. In this study, the condensation reaction was base-catalyzed and APTES amine groups were self-catalyzed component. The mechanism involved the hydrolysis of APTES triethoxy groups by water, generating silanol groups. Then condensation reaction between APTES silanol group and silica silanol group took place on silica surface as shown in Figure 4.7. Self condensation of APTES also occurred, resulting in undesirable products. The amount of water present in the system significantly influenced the hydrolysis reaction of triethoxy groups which then determined the condensation reaction on silica surface [70].

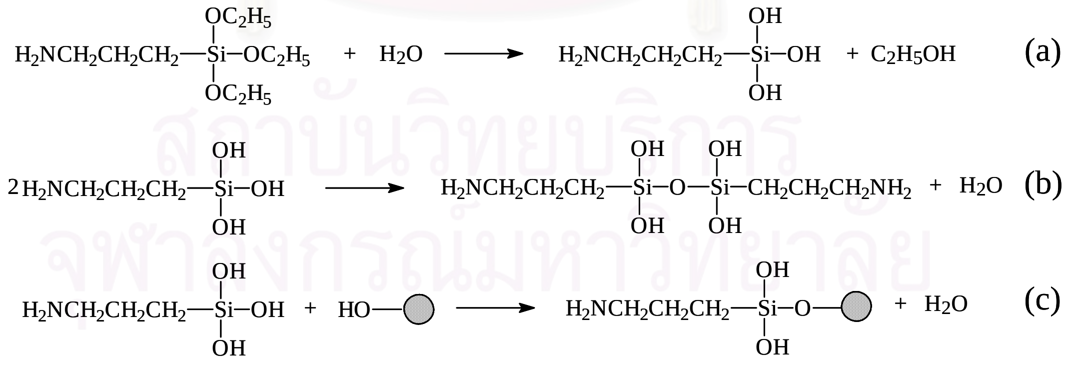

$$H_2NCH_2CH_2CH_2-Si(OC_2H_5)_3 + H_2O \longrightarrow H_2NCH_2CH_2CH_2-Si(OH)_3 + C_2H_5OH \quad \text{(a)}$$

$$2\,H_2NCH_2CH_2CH_2-Si(OH)_3 \longrightarrow H_2NCH_2CH_2CH_2-Si(OH)_2-O-Si(OH)_2-CH_2CH_2CH_2NH_2 + H_2O \quad \text{(b)}$$

$$H_2NCH_2CH_2CH_2-Si(OH)_3 + HO-\bigcirc \longrightarrow H_2NCH_2CH_2CH_2-Si(OH)_2-O-\bigcirc + H_2O \quad \text{(c)}$$

Figure 4.7 Chemical equation of hydrolysis reaction from alkoxysilane (a) and self condensation reaction (b) or (c) condensation reaction between APTES and silica.

The rate of hydrolysis and condensation reaction was controlled by using a mixture of water and methanol. In this study, the methanol to water volume ratios of 4: 1 and 2: 1 were used. The measured amino contents on silica plotted against reaction times are shown in Figure 4.8. As can be seen, the amino group content increases with an increase in the amount of water and reaction time. Water was consumed to convert APTES triethoxy groups to silanol groups (hydrolysis reaction). The amount of water, hence, determined the rate of hydrolysis. Consequently, the more silanol groups produced the higher the rate of subsequent silanol condensation reaction. In this work, amino-functionalized silica for PAMAM grafting was prepared as follows: a 2:1 ratio of methanol to water was used and the surface functionalization of silica particles was allowed to occur for three days.

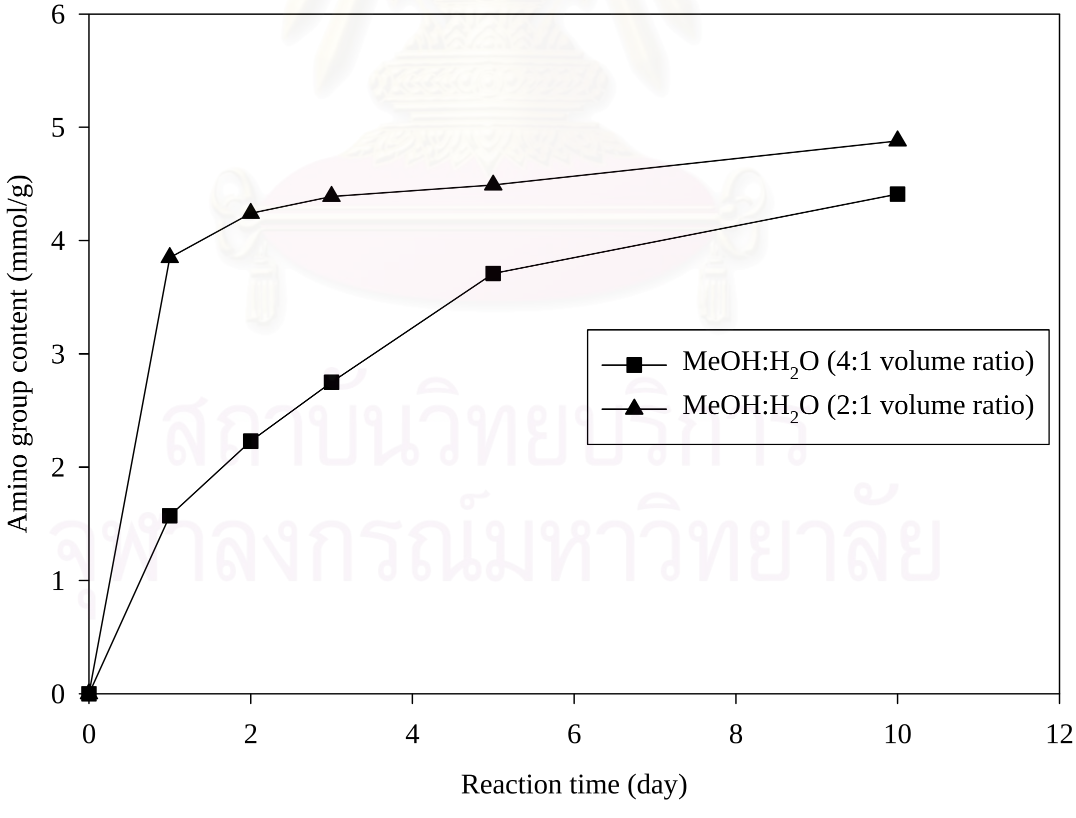

Figure 4.8 Amino group content measured on APTES treated silica versus reaction time

As a result of silanization reaction, the amino functionalized silica was produced. An FTIR analysis was further employed to provide the evidence of the attachment of APTES on silica.

Figure 4.9 FTIR spectra of silica, APTES and APTES grafted silica

Figure 4.9 compares FTIR spectra between APTES grafted silica, virgin silica and APTES. Silica which is an inorganic substance in nature exhibits the strong absorption band of siloxane (Si-O-Si) bonding at ~1,200 cm^{-1} and the silanol OH band in the range of 3,200 ~3,400 cm^{-1}. When considering the APTES silica, organo-functionalized silica, its spectrum exhibits new absorption frequencies at 2932 cm^{-1} and 1640 cm^{-1}. These bands are associated to C-H stretching and primary amine ($-NH_2$) stretching absorptions, respectively. Also, these bands are found corresponding with the absorption characteristics of APTES spectrum. These results indicate that APTES is incorporated into silica particles. The silica surface modification is further confirmed by change observed in spectrum pattern in the region of silanol OH band (3200 – 3400 cm^{-1}) due to new inter-hydrogen bonding interaction among amino silica particles.

4.3 Grafting of Hyperbranched PAMAM from Silica Surface

After the introduction of primary amine functional groups was successful and yielded amino initiating sites, grafting of hyperbranched PAMAM onto the surface of amino-functionalized silica was carried out by repeating two reactions, Michael addition and amidation which were used in the same manner as in the synthesis of PAMAM dendrimers. A removal of excessive MA and EDA in each reaction step was necessarily performed during grafting reaction. In Michael addition step, excessive amount of MA was easily removed from the reaction product by reduced pressure evaporator due to its low boiling temperature. On the other hand, excessive amount of EDA left in the amidation step was hardly removed by a typical rotary evaporator. In this work, EDA was therefore separated from the reaction product using dialysis membrane. The purified products were analyzed by FTIR analysis which is a useful tool for monitoring Michael addition and amidation reaction. FTIR results are shown in Figure 4.10. In Michael addition step, the terminal methyl ester group of G0.5, G1.5 and G2.5 products shows a strong and distinguishable band at 1740 cm^{-1}. This peak completely disappears from the spectra of G1.0 and G2.0 as a result of the amidation reaction. In this step, the terminal amine group was obtained which corresponds to the appearance of the strong absorption intensity of the N-H band in the region of 3000 - 3350 cm^{-1}. Its absorption intensity remarkably increases with an increase in PAMAM generation, reflecting that the number of terminal amine groups also significantly increases. When considering G3.0 hyperbranched PAMAM grafted silica, the absorption peaks at 1649 cm^{-1} and 1568 cm^{-1} are found, indicating the characteristics of C=O stretching and N-H bending. In addition, the absorption peaks at 3281 cm^{-1} and 3086 cm^{-1} are correspondent to N-H antisymmetric stretching and N-H symmetric stretching of primary amine, respectively. In accordance, the C-H band at 2900 cm^{-1} which shows up strongly in the spectra of G0.5 and G1.5 becomes less dominant due to suppressing influence by the surrounding N-H band. The theoretical reaction scheme is shown in Figure 4.11.

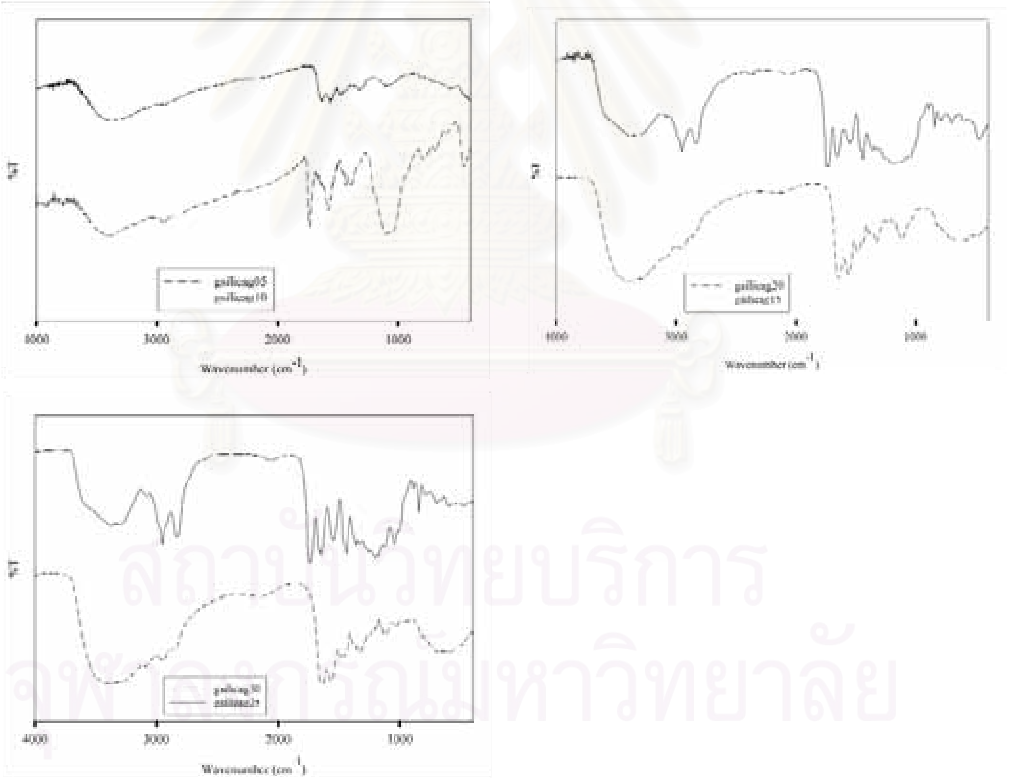

Figure 4.10 FTIR spectra of G0.5 – G 3.0 PAMAM grafted silicas

Proton NMR analysis was also performed. The ^{1}H NMR spectrum of ester terminated PAMAM grafted silica is shown in Figure 4.12. The signal which indicates the presence of terminal methyl ester group (CH_3-O-) appears at ~3.8 ppm. When comparing with the ^{1}H NMR spectrum of free amine terminated PAMAM grafted silica shown in Figure 4.13 it is seen that the signal of methyl proton completely disappears due to the amidation reaction. Again, the signal peak at ~3.8 ppm shows up strongly in the NMR spectrum of G2.5 hyperbranched PAMAM grafted silica (not present). The results obtained from FT-IR and ^{1}H NMR lead to a conclusion that grafting of PAMAM polymer onto silica particle was successful.

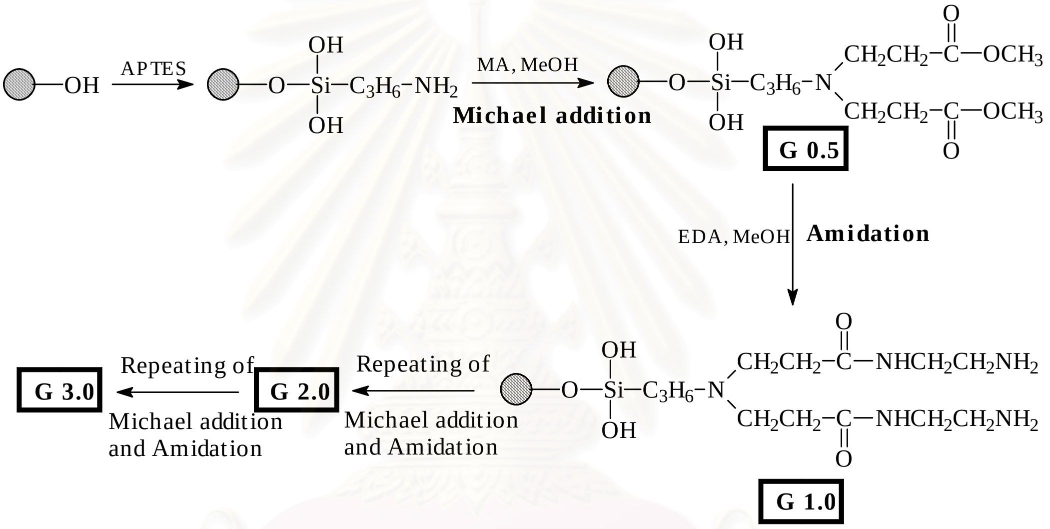

Figure 4.11 Theoretical synthesis of PAMAM grafted silica

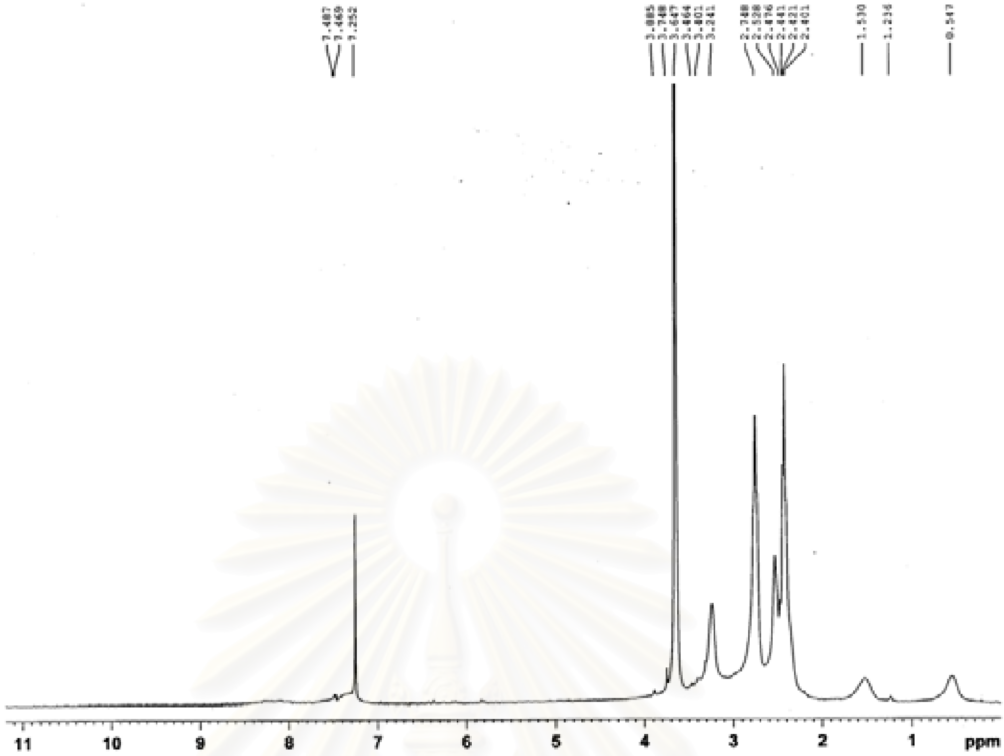

Figure 4.12 ^{1}H NMR spectrum of G1.5 hyperbranched PAMAM grafted silicas.

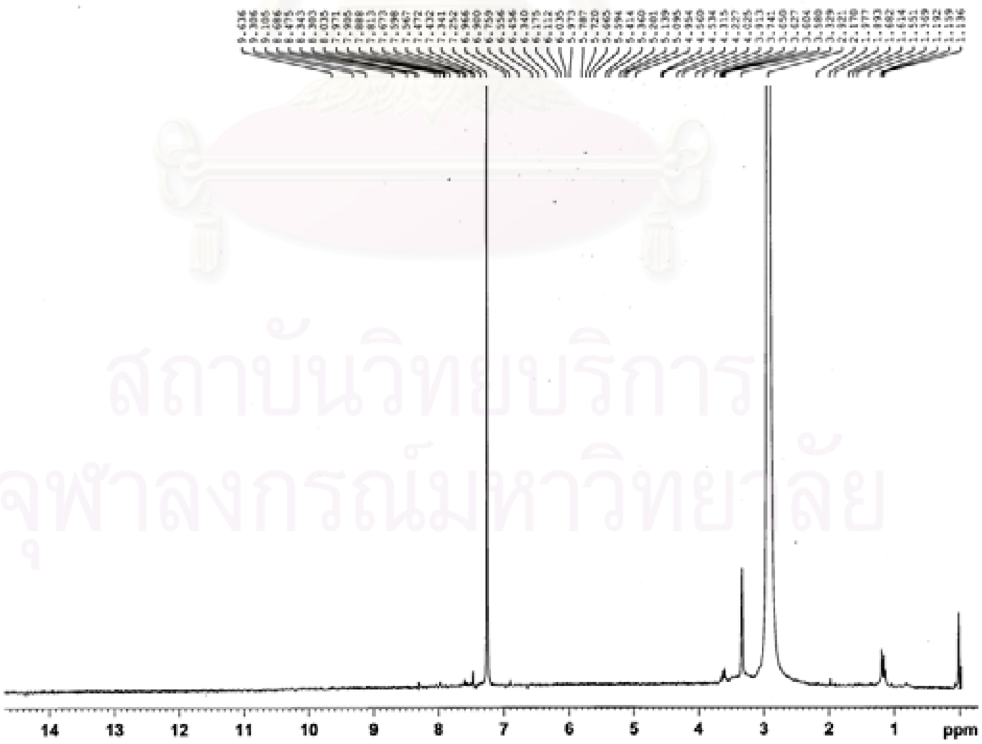

Figure 4.13 ^{1}H NMR spectrum of G2.0 hyperbranched PAMAM grafted silicas.

TGA thermograms of hyperbranched PAMAM grafted silicas from G0.5 to G3.0 are shown in Figure 4.14.

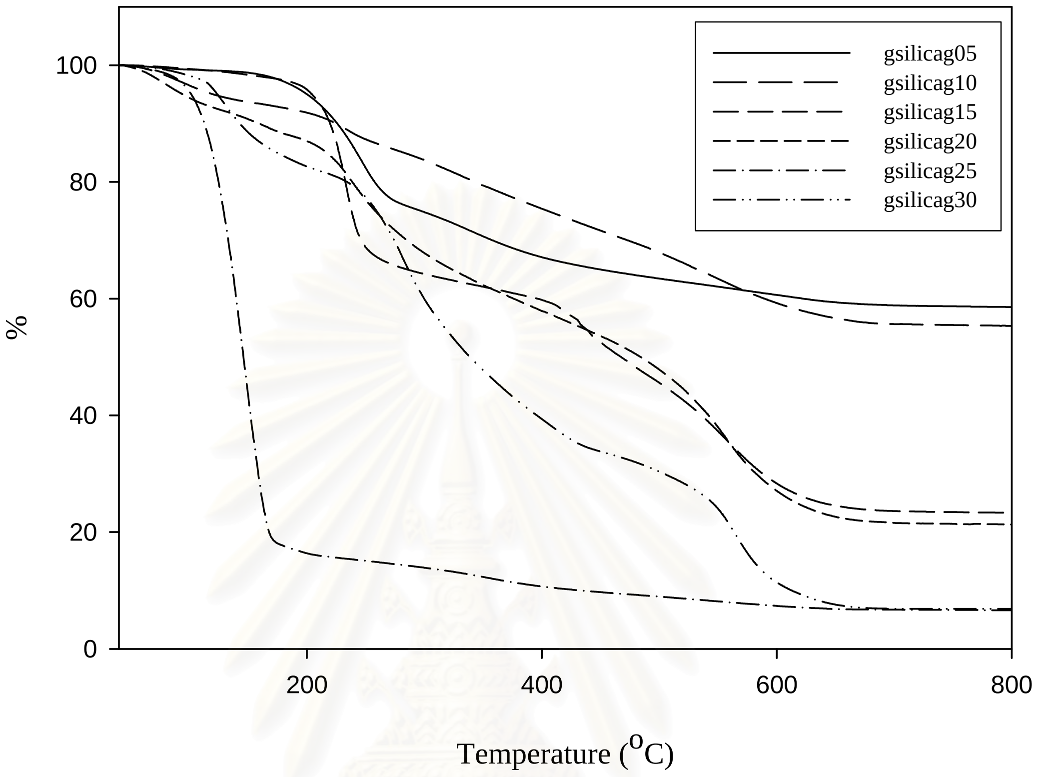

Figure 4.14 TGA thermograms of G0.5 – G3.0 hyperbranched PAMAM grafted silicas.

From the thermogram curves, percent graftings were calculated and their results are also given in Figure 4.15. As seen, percent grafting increases when PAMAM generation grows as a result of PAMAM propagation from the silica surface amine groups. For example, percent grafting obtained from G1.0, G2.0, and G3.0 are 41.20%, 76.05%, and 91.33%, respectively. As observed, percent grafting trend exponentially increases due to the characteristics of PAMAM synthesis. The amino group contents were expected to increase in a similar manner to percent grafting. Also from Figure 4.15, the amino group contents of G1.0, G2.0, and G3.0 are 14.62, 23.26, and 60.21 mmol/g of silica, respectively. However, the measured amounts are much lower than the theoretical value (Table 4.1). Based on the reaction chemistry, there were two main reasons why the theoretical value was hardly to achieve. One was the effect of steric hindrance arising from congestion of end groups; the higher the reaction step the more the congestion effect. As a result, the propagation of PAMAM branches was blocked. The second drawback suppressing an increase in amino content occurred in the amidation step; the side reaction of one EDA with two molecule ester groups to form intra- and inter-group crosslink products as shown in Figure 4.16, decreased the amount of ester groups available for the next step reaction [17].

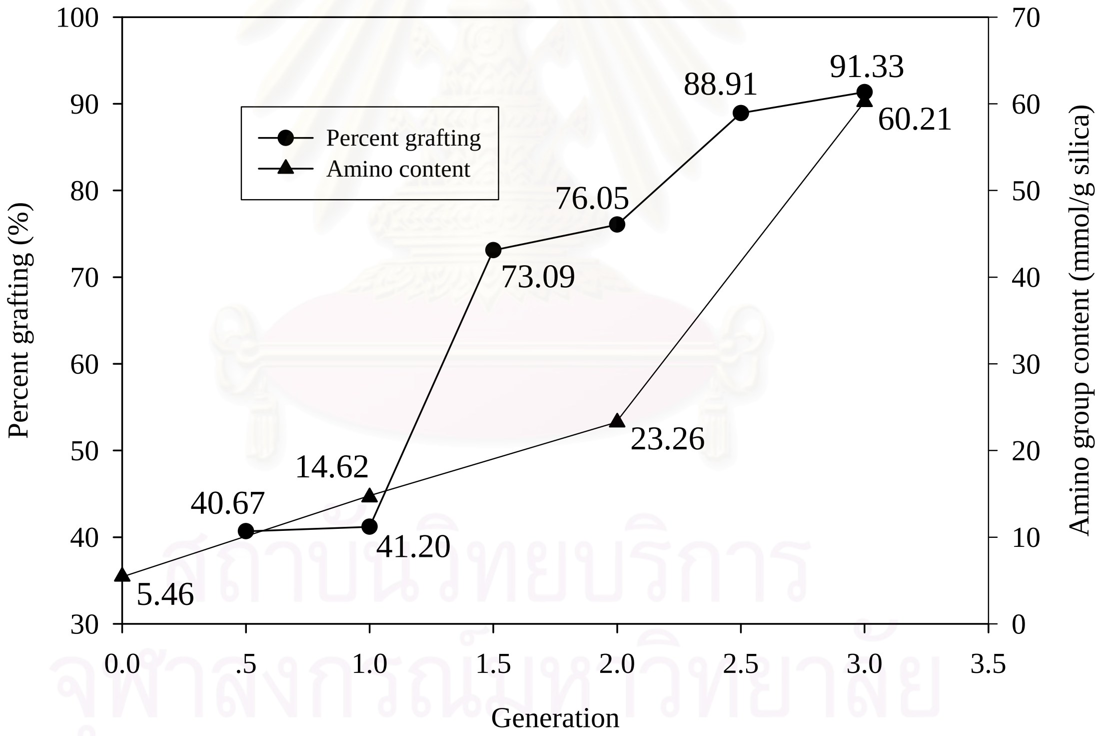

Figure 4.15 Percent grafting of PAMAM on silica surface and amino group content

Table 4.1 Amino groups content on silica particles

Generation	Amino group content (mmol/g of silica)	
	Found	**Theoretical**
0.0	5.46	-
1.0	14.62	30.55
2.0	23.26	53.35
3.0	60.21	416.00

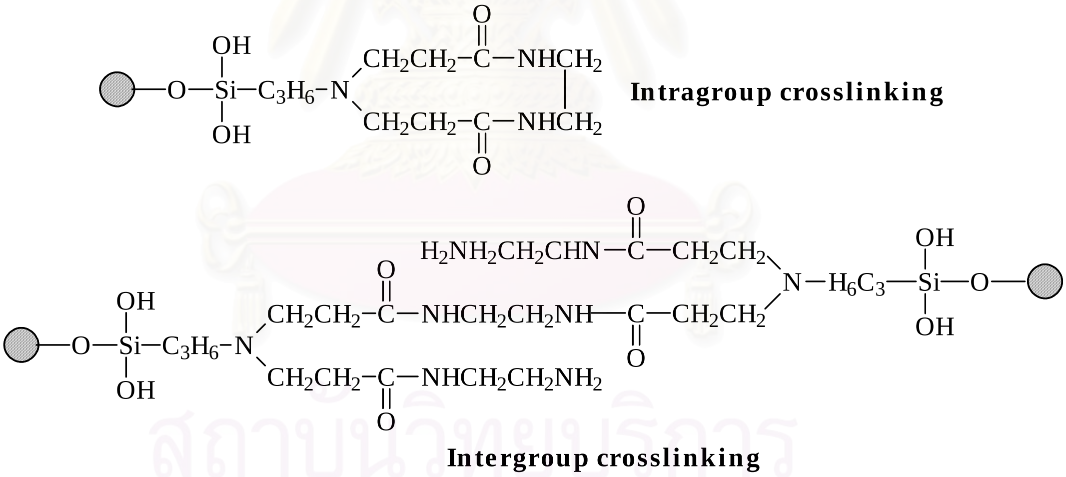

Figure 4.16 Intra- and inter group reaction of terminal amine group and terminal ester group of hyperbranched PAMAM grafted silica.

4.4 SEM Analysis and Particle Size Analysis

By nature, the as-received fumed silica nanoparticles powder aggregated and formed micron-sized nanoclusters. Typically, physical interaction among nanoparticles is too strong to separate them by mechanical agitation means into individual particles due to its large surface area characteristic. In this study, the effect of hyperbranched PAMAM dendrimer grafted onto silica surface on particle disaggregation and its stability was examined using SEM and particle size analysis. SEM images are shown in Figure 4.17. As found in SEM, as-received fumed silica particles are tightly packed and adhered together in agglomerate form. It is understandable that physical force such as hydrogen bonding is solely responsible for particle aggregation. After grafting, changes in particle distribution behavior as well as the agglomerate size were observed and the results are also shown in Figure 4.18. The results indicate that hyperbranched PAMAM grafting onto silica has been proven to be successful in dispersing particle agglomeration. This achievement was due to the steric role of grafted hyperbranched PAMAM. In addition, as observed in SEM images, the grafted hyperbranched PAMAM resulted in reducing the agglomerate size. The particle size of sample was further measured with laser light scattering. Figure 4.18 shows the particle size distribution comparison between as-received fumed silica, G0.5, G1.5 and G2.5 hyperbranched PAMAM graft silicas. In this experiment, G1.0, G2.0 and G3.0 hyperbranched PAMAM graft silicas were excluded due to the fact that the attractive force among agglomerates is pH dependent. In case of free amino terminated silicas, pH value was higher than pH 10. Therefore, the silica silanol groups started becoming deprotonated and repulsive force took effect on particle size measurement. In case of ester terminated PAMAM grafted silicas, their pH values were mildly basic (pH <9). As can be seen, the particle sizes before treatment are in an average size of ~100 microns. The average size of G0.5 PAMAM silica particles decreases to ~10 microns and then after PAMAM propagation reaching G2.5 the particle sizes decrease to ~100 nanometers.

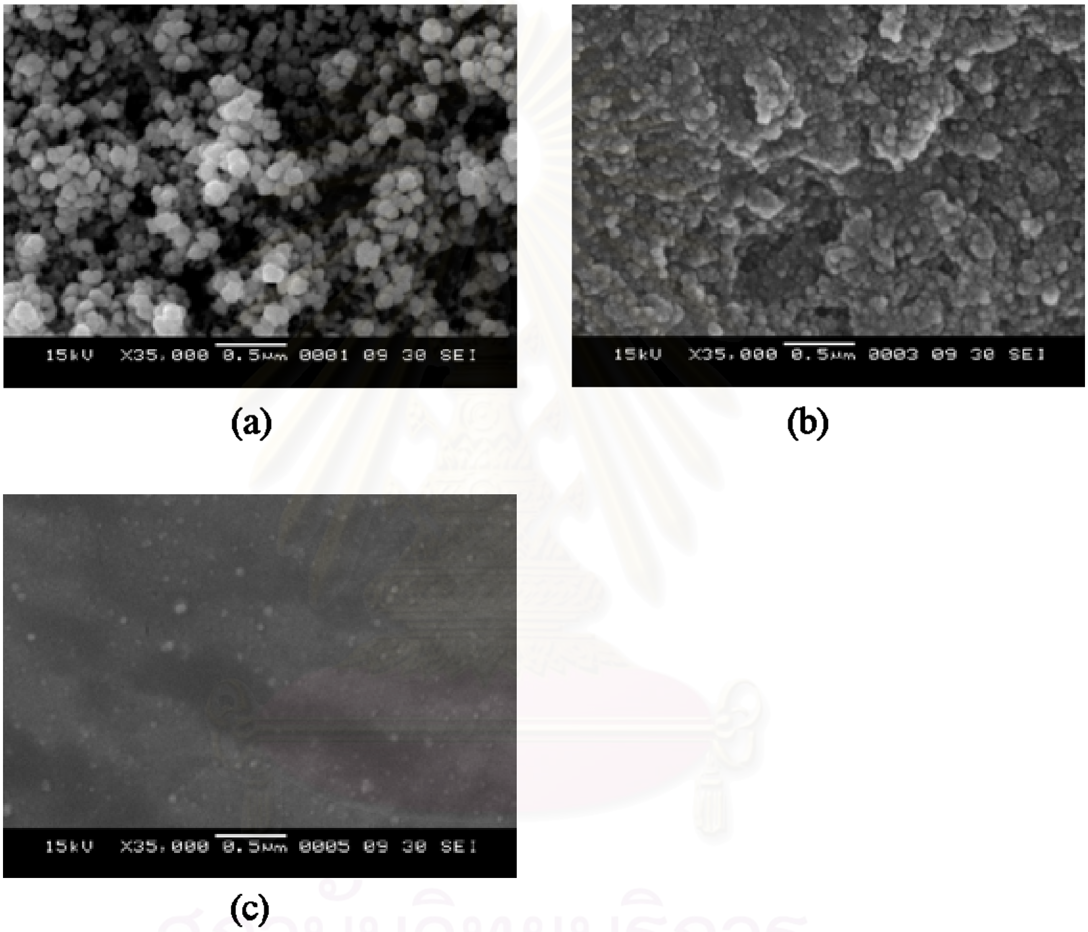

(a)

(b)

(c)

Figure 4.17 SEM images of (a) silica, (b) G0.5 PAMAM grafted silica and (c) G1.0 PAMAM grafted silica.

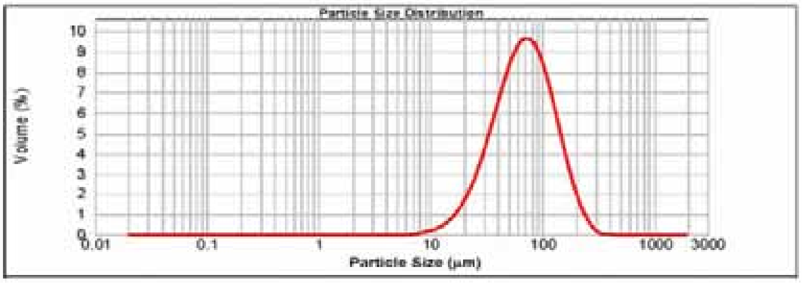

(a) Virgin silica

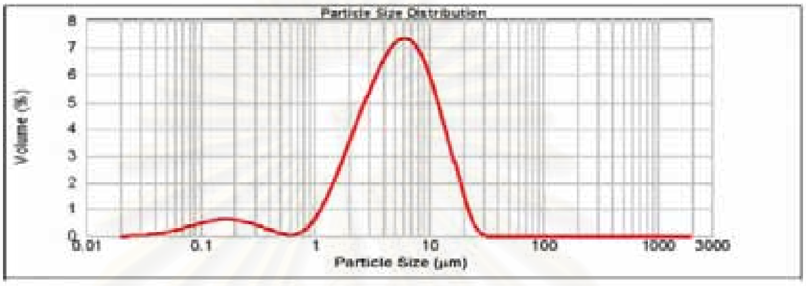

(b) gsilicag0.5

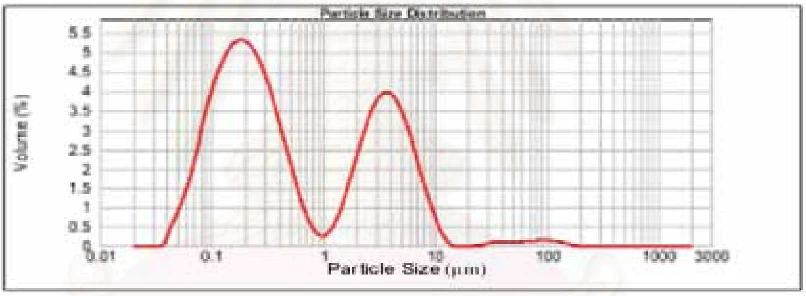

(c) gsilicag1.5

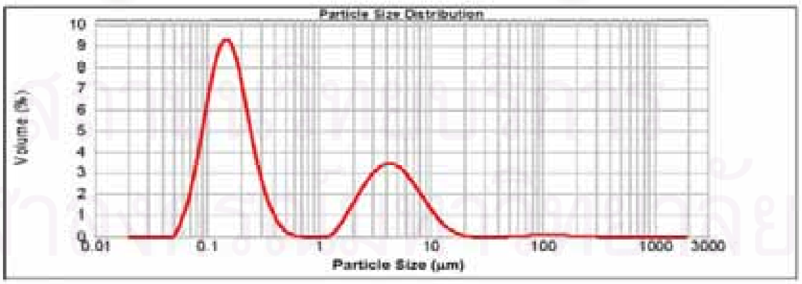

(d) gsilicag2.5

Figure 4.18 Particle size distribution of (a) virgin silica, (b) G0.5grafted silica, (c) G1.5 PAMAM grafted silica and (d) G2.5 PAMAM grafted silica.

4.5 Phosphorylation of Hyperbranched PAMAM Grafted Silica and G3.0 PAMAM Dendrimers

Functionalization of terminal amine groups was carried out in order to introduce special properties into hyperbranched PAMAM grafted silica. In this study, terminal amine groups were functionalized into phosphonic groups which are known to play powerful chelating performance and flame retardancy. Incorporation of phosphonic acid groups into PAMAM branch ends was easily achieved. The straightforward method is the Mannich type reaction of phosphorous acid with formaldehyde and primary amine compounds. The reaction proceeds well at low pH, such as in the presence of ca. 2-3 moles of concentrated hydrochloric acid per mole of an amine. The general mechanism of Mannich type reaction of an amine, formaldehyde and phosphorous acid is given in Figure 4.19.

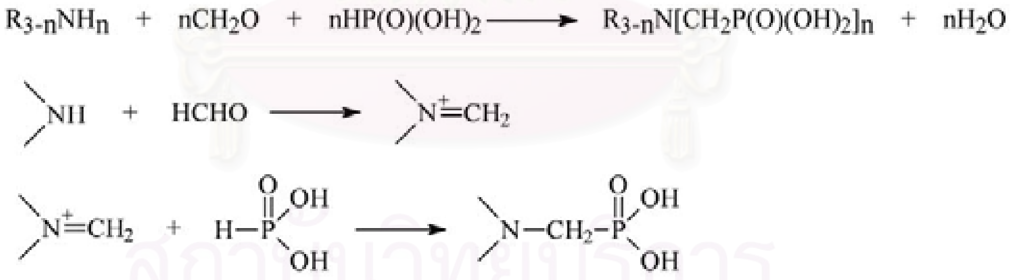

Figure 4.19 Mannich reaction involving an amine, formaldehyde and phosphorous acid.

In this experiment, the introduction of phosphonic acid groups into hyperbranched PAMAM grafted silica and G3.0 PAMAM dendrimers was carried out. The theoretical structure of phosphonic acids functionalized PAMAM grafted silica is proposed in Figure 4.20. The reaction products were characterized using FTIR analysis and FTIR spectra are shown in Figure 4.21 and Figure 4.22. When considering the spectrum of the phosphonic acid functionalized PAMAM grafted silica and G3.0 PAMAM dendrimers, new peaks are observed, indicating change occurring in the structure of hyperbranched PAPAM grafted silica and G3.0 PAMAM dendrimers. The presence of phosphonic acid moiety of phosphorylated hyperbranched PAMAM grafted silica is correspondent to the absorption bands at 1182 cm^{-1} , 1078 cm^{-1} , 923 cm^{-1} which are the characteristic peaks of (P=O), (P-OH) and (P-O) groups, respectively [71-74]. And the presence of phosphonic acid groups of phosphorylated G3.0 PAMAM dendrimers is shown in Figure 4.22 that shows the absorption bands at 1159 cm^{-1} (P=O), 1058 cm^{-1} (P-OH) and 924 cm^{-1} (P-O). The absorption band at 1401 cm^{-1} confirms the phosphorylation of $–NH_2$ groups [75]. A very broad band extending from 3,600 cm^{-1} to as low as 2,500 cm^{-1} is also observed, attributing to the absorption characteristic of the phosphonic acid hydroxyl group (OH). It is noticed that N-H stretching band at 3500 cm^{-1} in hyperbranched PAMAM grafted silica markedly decreases, reflecting its consumption by Mannich reaction. Proton NMR analysis was also performed. In the ^1H NMR spectrum of phosphonic acids functionalized PAMAM grafted silica in Figure 4.23, signals indicate the presence of C(1)-H_2 and C(2)-H_2 groups and a methylene group adjacent to phosphorous nucleus are found at 3.6 and 3.7 ppm, respectively. FTIR and ^1H NMR results provide convincing evidence that phosphonic acid groups successfully replaced hyperbranched PAMAM grafted silica amine groups, leading to hyperbranched dendrimer grafted silica with new functionalities.

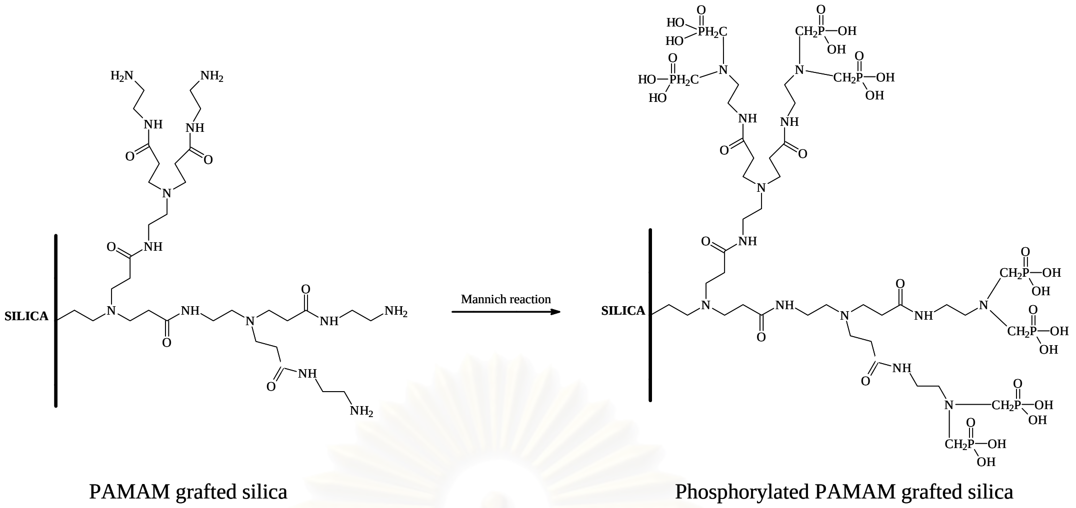

Figure 4.20 Theoretical structure of phosphonic acid functionalized PAMAM grafted silicas.

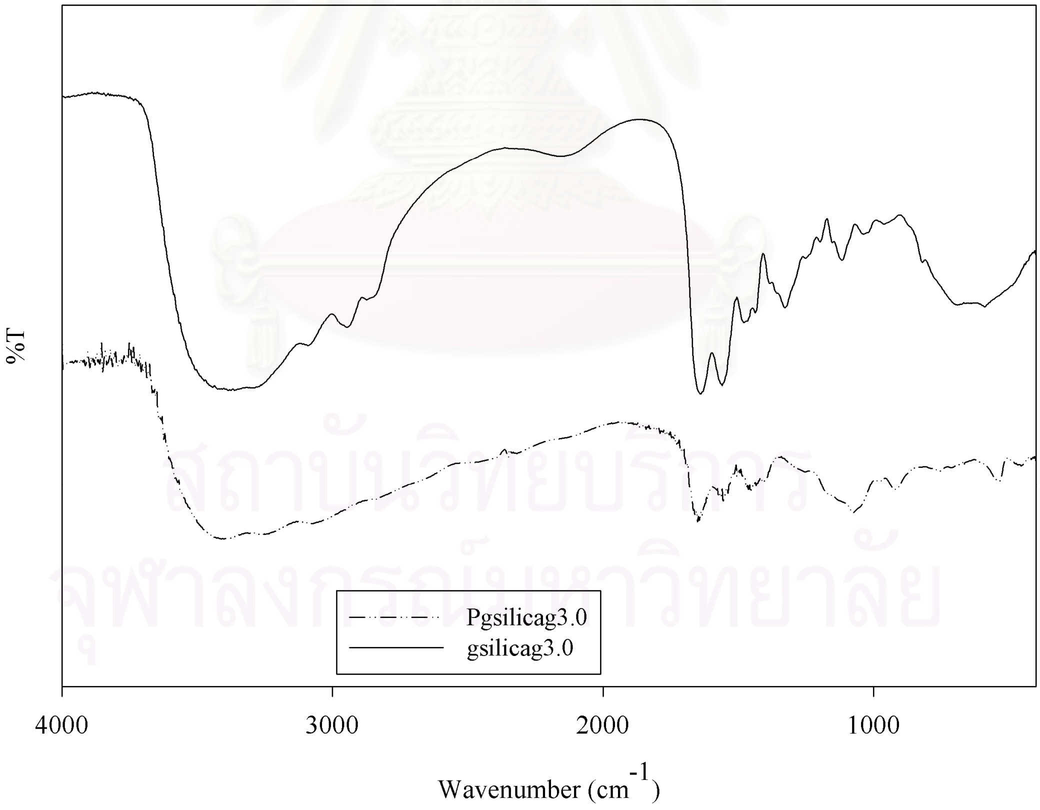

Figure 4.21 FTIR spectra of hyperbranched PAMAM grafted silica (gsilica 3.0) and phosphorylated hyperbranched PAMAM grafted silica (Pgsilica 3.0).

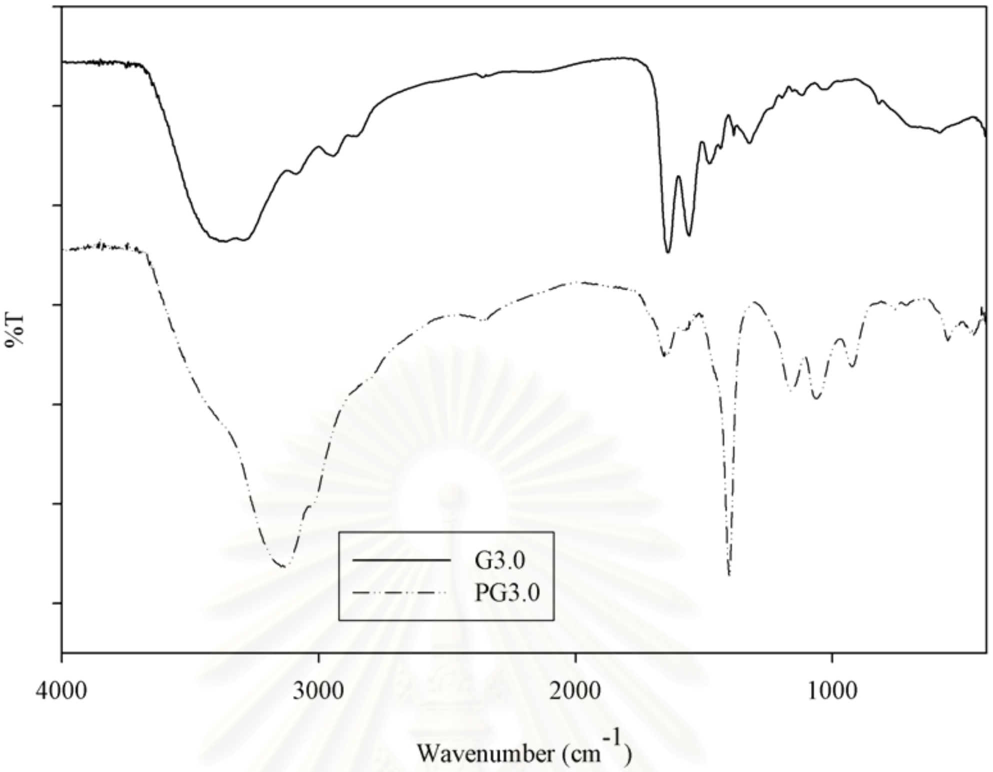

Figure 4.22 FTIR spectra of G3.0 PAMAM dendrimers (G3.0) and phosphorylated G3.0 PAMAM dendrimers (PG3.0).

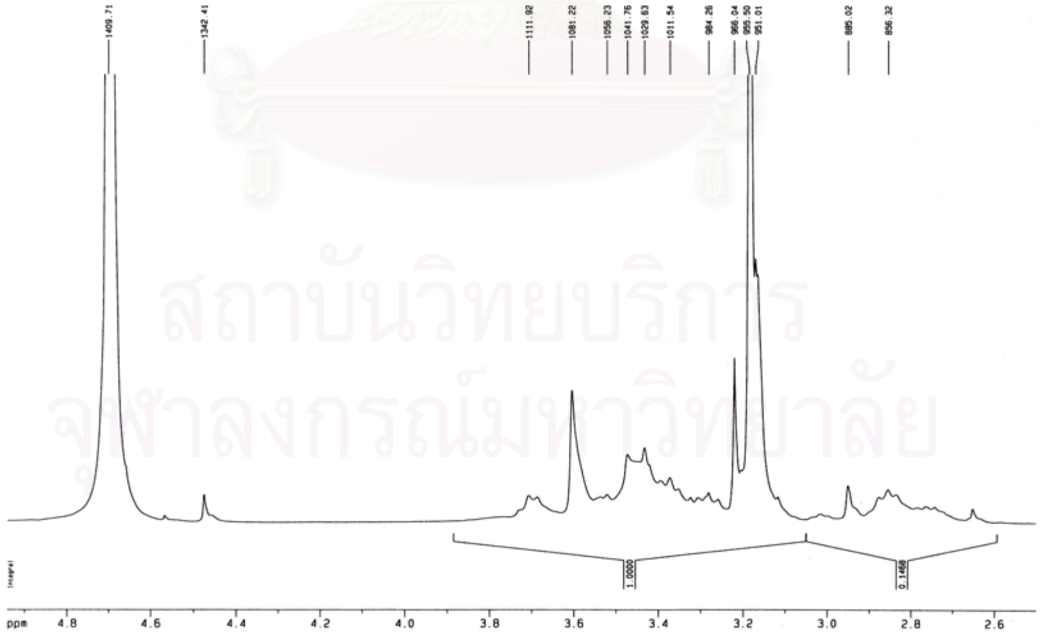

Figure 4.23 ^{1}H NMR spectrum of phosphorylated hyperbranched PAMAM grafted silica

4.6 Flame Retardancy Effect

Phosphorylated hyperbranched PAMAM grafted silica potentially offers both strong chelating powers and flame retardancy properties. The later was tentatively investigated in this study. Preliminary evaluation of flame retardancy effect on cotton fabric was undertaken. Cotton substrate was chosen due to its relatively high flammability characteristic as well as common usage. In a standard burning test, phosphorylated hyperbranched PAMAM grafted silica treated cotton exhibits a marked fire retardancy property as shown in Figure 4.24. The treated cotton fabric used in this preliminary test was treated with only phosphorylated hyperbranched PAMAM grafted silica at the concentration of 10%, 20% and 30% w/v. The effect of the amount of finishing agent (phosphorylated hyperbranched PAMAM grafted silica) on the flame retardancy of cotton fabric was evaluated. From the preliminarily results, above 20% (w/v) of finishing agent was found effective in causing the treated fabric unburnt. So that the formulation variation study begun with 20% w/v of phosphorylated hyperbranched PAMAM grafted silica and the amount of dicyandiamide was fixed at 20 g/l. The amount of urea (fiber degradation stabilizer) was varied from 10%, 20% and 30% (w/v). The flammability behavior of treated fabric after washing is shown in Figure 4.25. It is found that 20% of the finishing agent was partially washed off, resulting in ineffectiveness of flame retardancy. When the amount of finishing agent was increased to 30% w/v, the flame test showed the satisfactory result thank to the no ignition observed after washing as shown in Figure 4.26. Urea is important additive in order to improve the durability of fixed finishing agent, washing and the fabric’s physical properties (tensile and discoloration control);

the more the amount of urea the higher the thermal stability of treated fabric during fixation of phosphorylated hyperbranched PAMAM. The problem of cotton fabric degradation commonly occurred with acid treated fabric at high temperature, producing poor bursting strength as shown in Figure 4.27. With the addition of urea this problem is reduced.

Phosphorylated G3.0 PAMAM dendrimers was also applied onto cotton fabric and its flame retardancy effect was compared to phosphorylated hyperbranched PAMAM grafted silica. The 30% w/v of phosphorylated G3.0 PAMAM dendrimers was employed in the same manner to the phosphorylated hyperbranched PAMAM grafted silica. The flammability test is shown in Figure 4.28. In case of phosphorylated hyperbranched PAMAM, the treated fabric after washing showed the relatively poor wash fastness although the amount of finishing agent was up to 30% w/v. In addition, the bursting strength was reduced to almost 50 % when compared to the untreated fabric. This may be due to the effect of more phosphonic acid groups of phosphorylated G3.0 PAMAM dendrimers than phosphorylated hyperbranched PAMAM grafted silica. The higher acidicity accelerates the thermal degradation of cotton fabric during fixation of phosphorylated hyperbranched PAMAM.

Figure 4.24 Vertical flammability test of phosphorylated hyperbranched PAMAM grafted silica treated cotton fabric at various concentrations

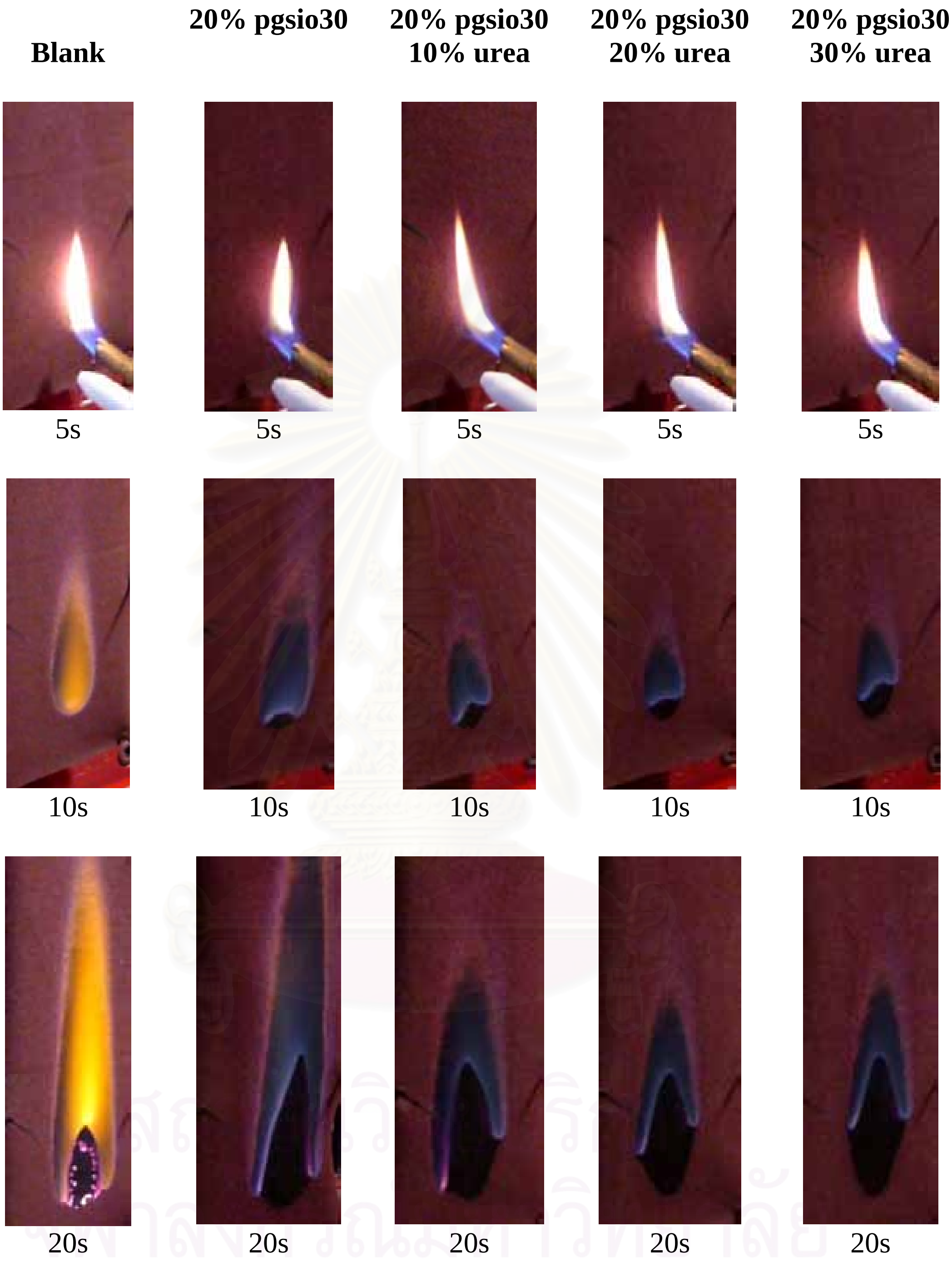

Figure 4.25 Vertical flammability test of 20 % phosphorylated hyperbranched PAMAM grafted silica treated cotton fabric at various concentrations of urea after washing.

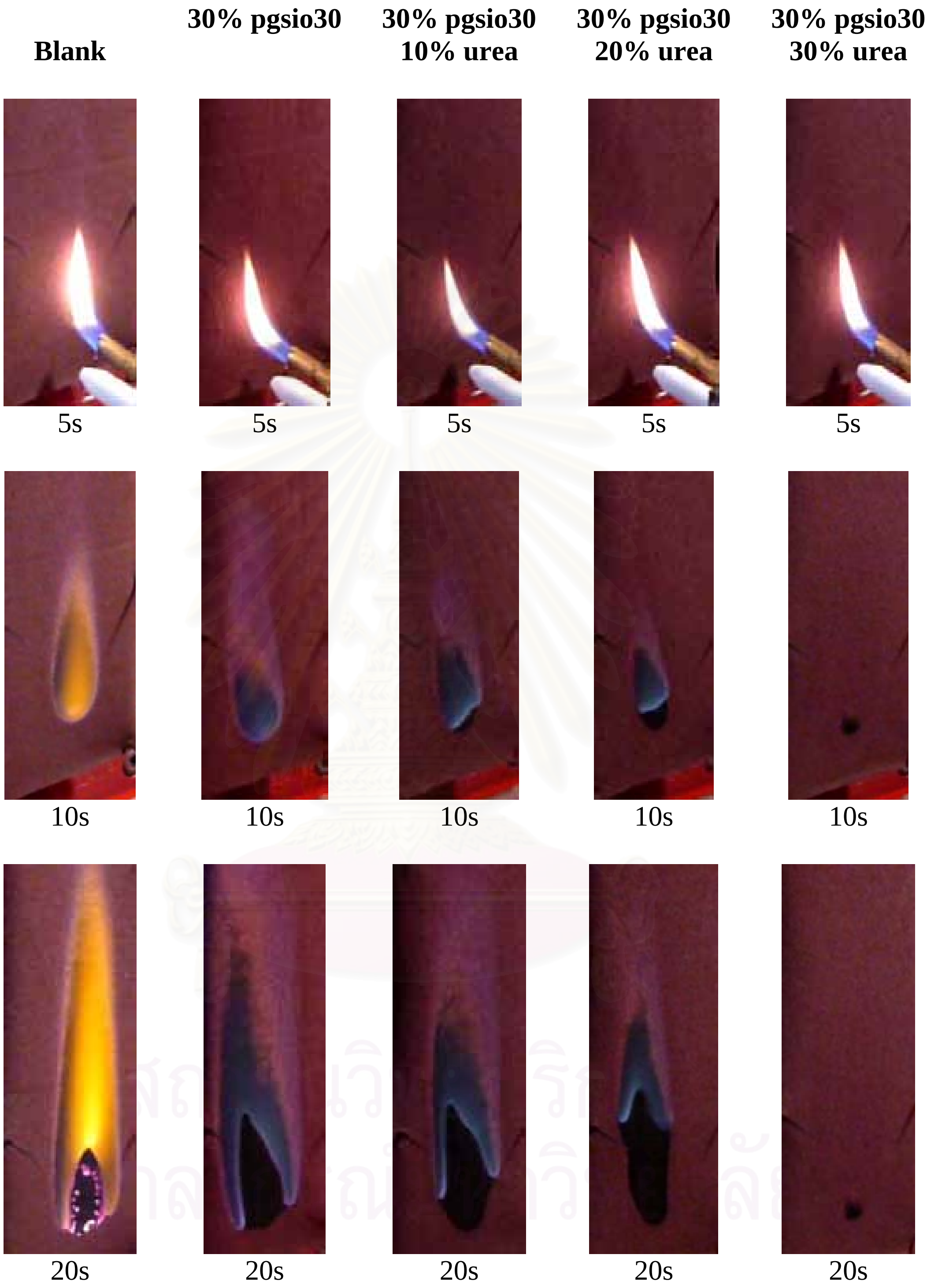

Figure 4.26 Vertical flammability test of 30 % phosphorylated hyperbranched PAMAM grafted silica treated cotton fabric at various concentrations of urea after washing.

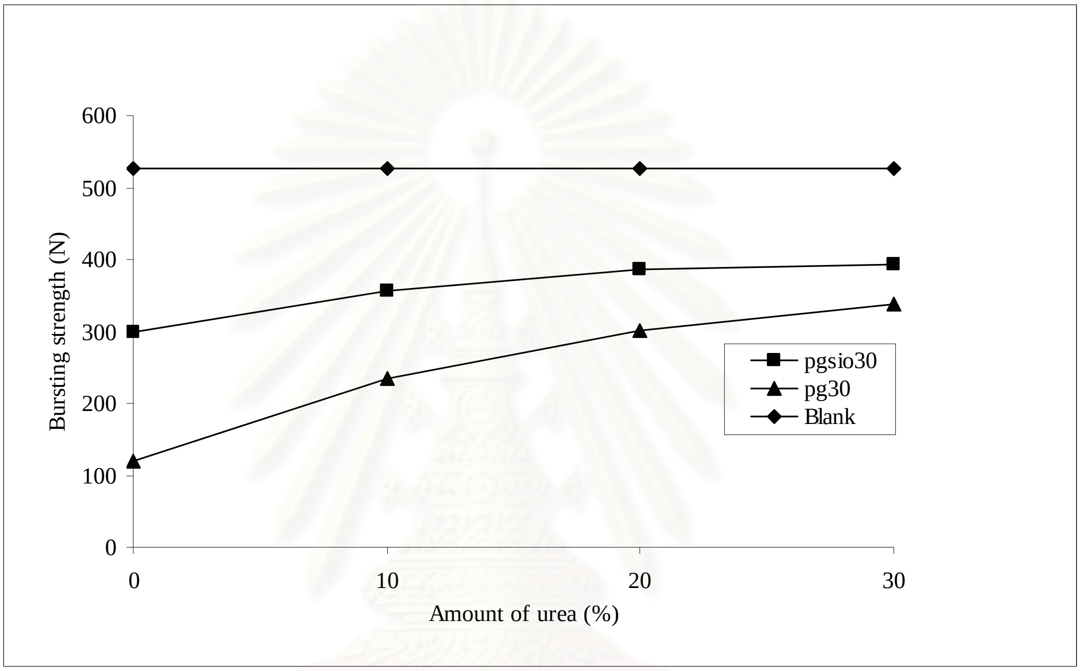

Figure 4.27 Bursting strength of after washing of phosphorylated G3.0 PAMAM dendrimer and phosphorylated hyperbranched PAMAM grafted silica treated cotton fabrics.

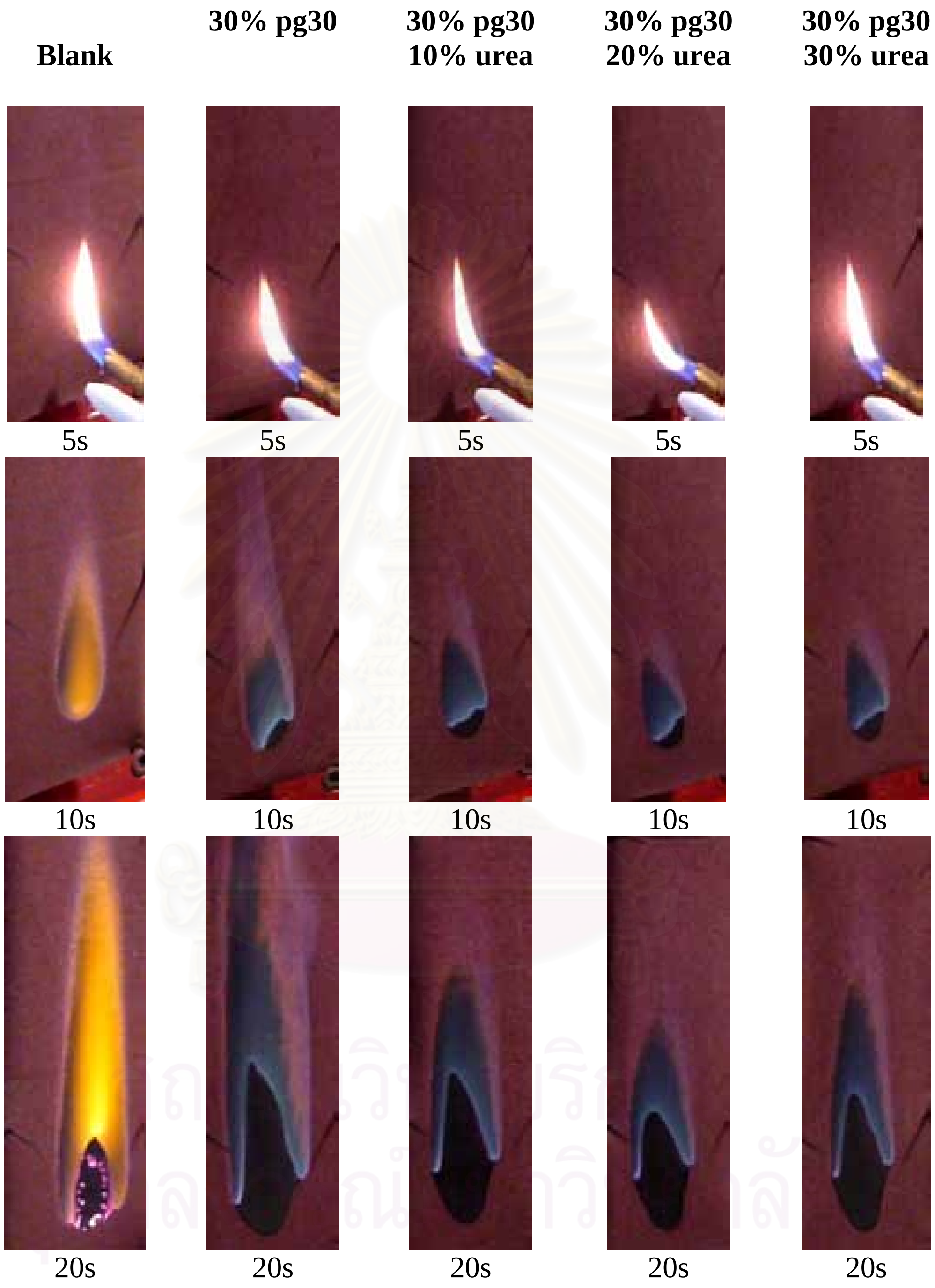

Figure 4.28 Vertical flammability test of 30 % phosphorylated G3.0 PAMAM treated cotton fabric at various concentrations of urea after washing.

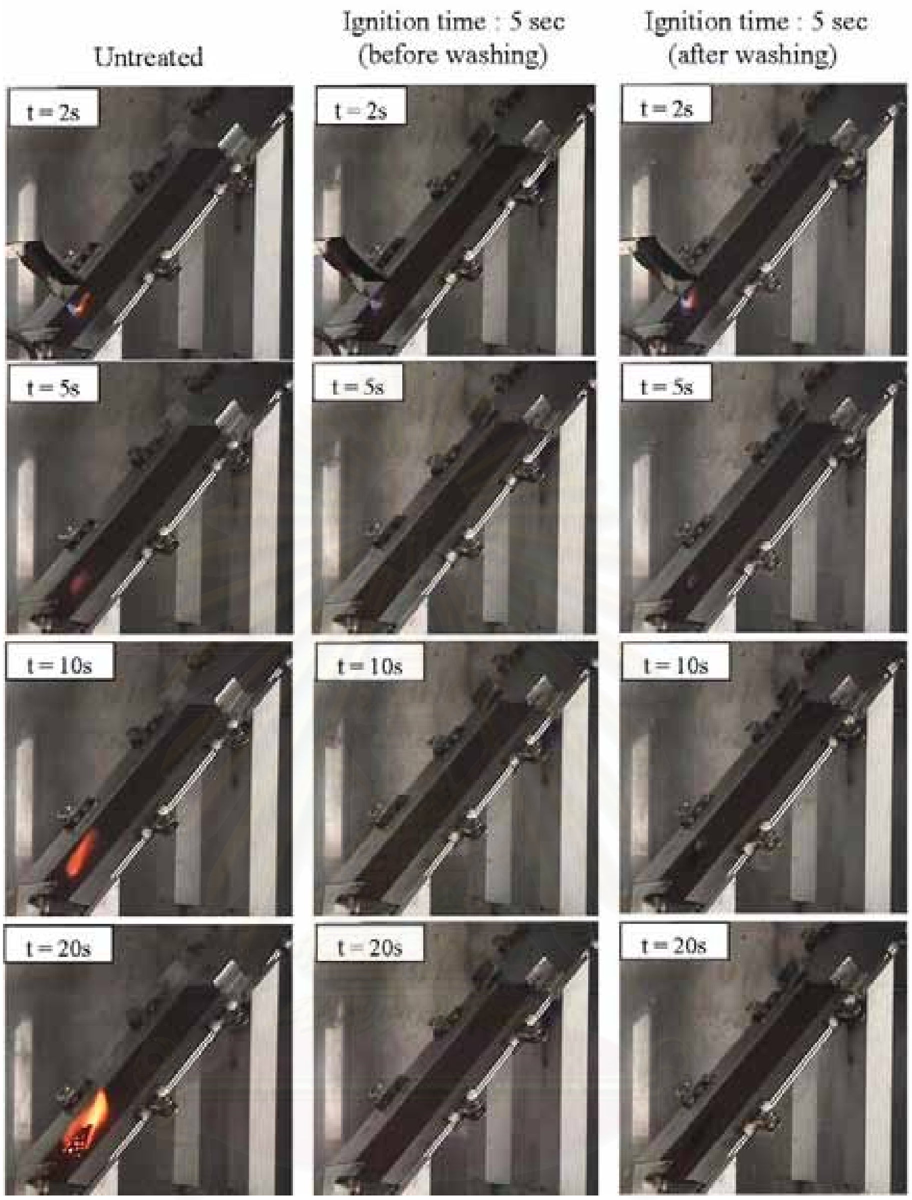

Figure 4.29 45^{o} Flammability test of phosphorylated hyperbranched PAMAM grafted silica

For the phosphorylated hyperbranched PAMAM grafted silica, it also was tested on the 45^{0} standard flammability tests to confirm the test as shown in Figure 4.29. From both burning test, in case of the untreated control, fabric is ignited easily and burned severely. The flame spreads very quickly and burns the entire fabric. After washing, the treated fabric is still able to exhibit satisfactory flame retardancy performance, indicating the durable property of phosphorylated hyperbranched PAMAM grafted silica. A large amount of char and molten viscous layer are formed on the fabric's surface, acting as an insulation layer, and then protecting fabric from flame and oxygen to further decompose the fabric.

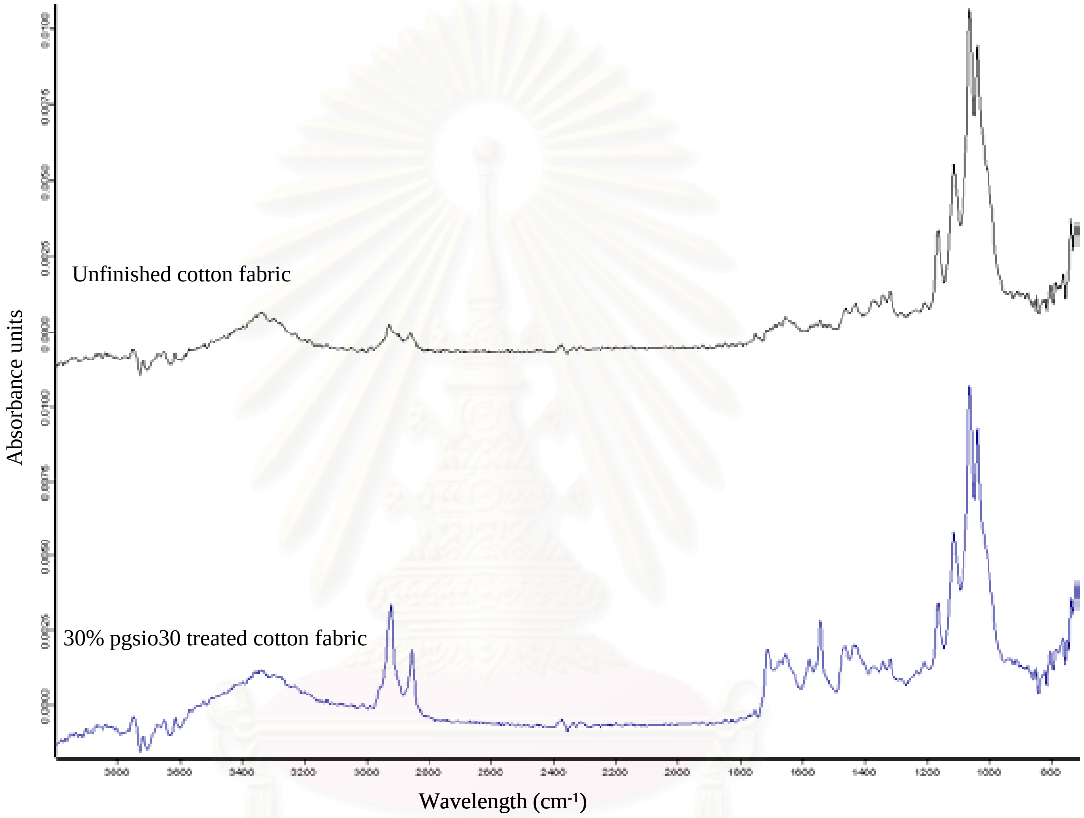

Figure 4.30 ATR-FTIR spectra of untreated and phosphorylated PAMAM grafted silica treated cotton fabrics.

The interaction between phosphorylated PAMAM grafted silica and cotton fabric was followed up using ATR-FTIR analysis. The results are shown in Figure 4.30. It is found that FTIR fingerprint of the phosphorylated PAMAM grafted silica treated cotton exhibits similar pattern to that of untreated fabric. However, the differences between the two spectra are noticeable, where the strong absorptions at

3000-2900 cm^{-1} and 1720-1500 cm^{-1} are shown in the spectrum of treated fabric. The peaks at 1650 and 1539 cm^{-1} could be correspondent to the PAMAM grafted silica characteristics of C=O stretching and N-H bending while the absorption band detectable at 1710 cm^{-1} could be assigned to carbonyl functionalities arising from the occurrence of oxycelluose (oxidation of cellulose unit during thermal treatment) [76]. The absorption band of P=O and P-O of phosphorylated cotton is difficult to be assigned due to its presence in the vicinity of 920-1200 cm^{-1} where the main absorption band of cellulose units also appears. The intensity of absorption bands at 2918 and 2851 cm^{-1} of treated cotton shows up strongly which indicate the CH_2 antisymmetric and symmetric stretching of PAMAM grafted silica. From these finding, it could be assured that the interaction between cotton cellulose and PAMAM grafted silica did occur, leading to the linkage formation of phosphorylated ester bonding between finishing agent and cotton cellulose.

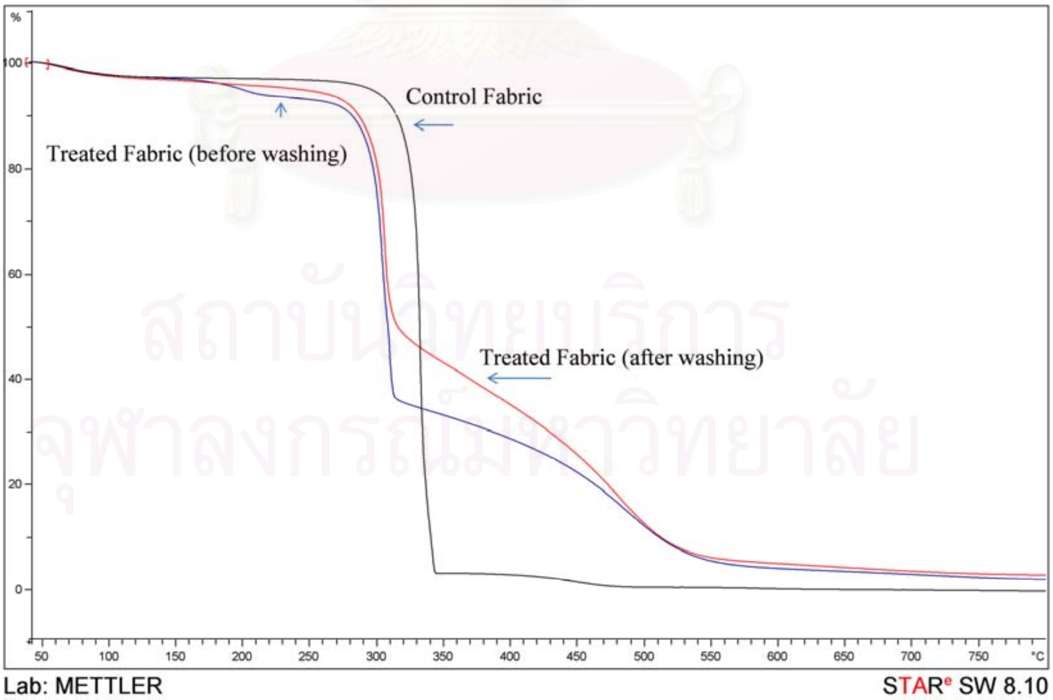

Figure 4.31 TGA thermograms of phosphorylated hyperbranched PAMAM grafted silica treated and untreated cotton fabrics.

In addition, analysis of treated and untreated cotton fabric was performed by TGA analysis, with representative thermograms shown in Figure 4.31. The untreated fabric starts to decompose at about 300^{o}C and rapidly increases from 330^{o}C reaching 100 % weight loss at 350^{o}C, as reported earlier [77]. Degradation of the treated fabric begins at the relatively lower temperature of 260^{o}C and progresses rapidly from 300^{o}C, leaving ca 35% residual weight (at 320^{o}C). Thereafter, a slow decomposition to about 2-3 % residual weight by ~600^{o}C due to the retardant effect of phosphonate silica was observed. The pyrolysis of the flame retardant treated cotton fabric typically starts at a relatively lower decomposition temperature because of the catalytic dehydration of cellulose by the flame retardant, leading to char formation on the fabric surface, a well established flame retardancy mechanism of phosphorus containing compounds. In this scenario, the decline of degradation temperature is due to the reaction of the phosphonic acid with the C_6 hydroxyl of the cellulose anhydroglucose unit, blocking the formation of levoglucosan (source of fuel) and so promoting char rather than flame formation. As a result, the percentage weight loss for treated fabric measured at 350^{o}C (the temperature of 100 % weight loss of untreated fabric) is reduced to 70 %, supporting the flame retardant effect of phosphorylated hyperbranched PAMAM grafted silica. Moreover, PAMAM contains nitrogen atoms which act synergistically with phosphorus [78] enhancing the electrophilicity of phosphorous and, through making a stronger Lewis acid, promoting the phosphorylation reaction with C-6 hydroxyl group of anhydroglucose unit. TGA thermogram of treated fabric after washing also presented in Figure 4.31 shows the decomposition temperature at 280^{o}C which is higher than those of unwashed fabric but lower than that of control fabric. This result indicates that the phosphoester linkages between the phosphorylated PAMAM grafted silica and C-6 hydroxyl groups exhibits wash-off resistance. From this finding, it is reasonable to say that an immobilization of the water soluble compound (phosphodendrimers to insoluble nanoparticles) could help improve its durability to washing.

CHAPTER V

CONCLUSIONS

The synthesis of PAMAM dendrimers was carried out by repeating two processes; Michael addition to produce ester terminated products and Amidation of the ester terminated with large excess of ethylenediamine to produce amine terminated hyperbranched PAMAM polymers. The FTIR, ^{1}H and ^{13}C-NMR analysis can confirm the synthesized products.

The grafting of hyperbranched PAMAM polymer onto amino group functionalized silica was successfully achieved by performing three rounds of paired reactions comprised of a Michael addition of the silica amino group to methyl acrylate and the amidation of the resulting terminal methyl ester group with ethylenediamine. The percent grafting, relative to the initial silica weight and calculated from TGA results, were 74%, 342% and 1332% for the three reaction cycles, respectively, with corresponding amino group contents of 14.6, 23.3, and 60.2 mmol/g silica, respectively. However, the attained amino group contents were much lower than the expected values relative to the amount of grafting, perhaps due to the effect of steric hindrance in later cycles as hyperbranched PAMAM are formed, and the intra and inter group crosslinking. Regardless, grafted hyperbranched PAMAM enhanced particle dispersion and reduced particle agglomeration. Thus, the agglomerate particle size before grafting averaged ~70 microns and after grafting the particle size significantly decreased to a range of 50 – 500 nm (average ~ 150 nm) with major composition of the two discrete populations.

The phosphorylation of the PAMAM dendrimers and hyperbranched PAMAM grafted silica terminal amino groups were also successfully achieved by the Mannich type reaction. The phosphorylated products containing the phosphonic acids exhibited flame retardancy when applied onto flammable cotton fabric. After washing test, the phosphorylated hyperbranched PAMAM grafted silica showed more good retention of fire retardancy than phosphorylated PAMAM dendrimers, indicating its wash-off resistancy performance. In case of phosphorylated PAMAM dendrimers, the finished fabric after washing showed the relatively poor wash fastness although the amount of finishing agent was up to 30% w/v. In addition, the bursting strength was reduced to almost 50 % when compared to the unfinished fabric. This may be due to the effect of more phosphonic acid groups content of phosphorylated PAMAM dendrimers than phosphorylated hyperbranched PAMAM grafted silica. The higher acidicity accelerates the thermal degradation of cotton fabric during fixation of phosphorylated PAMAM dendrimers.

.

REFERENCES

[1] Tomalia, D. A. Birth of a new macromolecular architecture: dendrimers as quantized building blocks for nanoscale synthetic polymer chemistry. Progress in Polymer Science 23 (2005): 1517-1526.

[2] Lee, C. C.; Mackay, J. A.; Frechet, J. M. J.; and Szoka, F. C. Designing dendrimers for biological applications. Nature Biotechnology 23 (2005): 1517-1526.

[3] Tomalia, D. A.; Baker, H.; Dewald, J.; Hall, M.; Kallos, G.; and Martin, S. A new class of polymers: starburst-dendritic macromolecules. Polymer Journal 17 (1985): 117-132.

[4] Aulenta, F.; Hayes, W.; and Rannard, S. Dendrimers: a new class of nanoscopic containers and delivery devices. European Polymer Journal 39 (2003): 1741-1771.

[5] Smith, D. K.; Hirst, A. R.; Love, C. S.; Hardy, J. G.; Brignell, S. V.; and Huang, B.Q. Self-assembly using dendritic building blocks – towards controllable nanomaterials. Progress in Polymer Science 30 (2005): 220-293.

[6] Pan, B.; Gao, F.; Ao, L.; Tian, H.; He, R.; and Cui, D. Controlled self-assembly of thio-terminated poly(amidoamine) dendrimer and gold nanoparticles. Colloids and Surfaces A: Physiochemical and Engineering Aspect 259 (2005): 89-94.

[7] Gong, A. J.; Chen, Y. M.; Zhang, X.; Liu, H. W.; Chen, C. F.; and Xi, F. Synthesis and characterization of dendritic poly(amidoamine)-silica gel hybrids. Journal of Applied Polymer Science 78 (2000): 2186-2190.

[8] Demadis, K. D.; and Neofotiston, E. Synergistic effects of combinations of cationic polyaminoamide dendrimers/anionic polyelectrolytes on amorphous silica formation: a bioinspired approach. Chemistry of Materials 19 (2007): 581-587.

[9] Shi, X.; Lesniak, W.; Islam, M. T.; MuÑiz, M. C.; Balogh, L. P.; and Baker, J.R. Comprehensive characterization of surface-functionalized poly(amidoamine) dendrimers with acetamide, hydroxyl, and carboxyl groups. Colloids and Surfaces A: Physiochemical and Engineering Aspect 272 (2006): 139-150.

[10] Ahmed, S. M.; Budd, D. M.; McKeown, N. B.; Evans, K. P.; Beaumont, G. L.; Donaldson, C.; and Brennan, C. M. Preparation and characterization of a chromophore-bearing dendrimer. Polymer 42 (2001): 889-896.

[11] Majoros, I. J.; Keszler, B.; Woehler, S.; Bull, T.; and Baker Jr, J. R. Acetylation of poly(amidoamine) dendrimers. Macromolecules 36 (2003): 5526-5529.

[12] Heldt, J. M.; Durand, N. F.; Salmain, M.; Vessiè, A.; and Jaouen, G. Preparation and characterization of poly(amidoamine) dendrimers functionalized with a rhenium carbonyl complex and PEG as new IR probes for carbonyl metallo imminoassay. Journal of Organometallic Chemistry 689 (2004): 4775-4782.

[13] Yoshimaru, T.; Abe, S.; and Esumi, K. Characterization of quaternized poly(amidoamine) dendrimers of generation 1 with multiple octyl chains. Colloids and Surfaces A: Physiochemical and Engineering Aspect 251 (2004): 141-144.

[14] Li, H. Y.; Chen, H. Z.; Xu, W. J.; Yuan, F.; Wang, J. R.; and Wang, M. Polymer-encapsulated hydrophilic carbon black nanoparticles free from aggregation. Colloids and Surfaces A: Physiochemical and Engineering Aspect 254 (2005): 173-178.

[15] Bergemann, K.; Fanghänel, E.; Knackfuß, B.; Lüthge, T.; and Schukat, G. Modification of carbon black properties by reaction with maleic acid derivatives. Carbon 42 (2004): 2338-2340.

[16] Park, S. J.; Seo, M. K.; and Nah, C. Influence of surface characteristics of carbon blacks on cure and mechanical behaviors of rubber matrix compoundings. Journal of Colloid and Interface Scuence 291 (2005): 229-235.

[17] Qu, R.; Niu, Y.; Sun, C.; Ji, C.; Wang, C.; and Cheng, G. Synthesis, characterization, and properties for metal ions of silica-gel functionalized by ester- and amino-terminated dendrimer-like polyamidoamine polymer. Microporous and Mesoporous Materials 97 (2006): 58-65.

[18] Tsubokawa, N.; Ichioka, H.; Satoh, T.; Hayashi, S.; and Fujiki, K. Grafting of 'dendrimer-like' highly branched polymer onto untrafine silica surface. Reactive & Functional Polymers 37 (1998): 75-82.

[19] Wu, X. Z.; Liu, P.; Pu, Q. S.; Sun, Q. Y.; and Su, Z. X. Preparation of dendrimer-like polyamidoamine immobilized silica gel and its application to online preconcentration and separation palladium prior to FAAS determination. Talanta 62 (2004): 918-923.

[20] Taniguchi, Y.; Shirai, K.; Saitoh, H.; Yamauchi, T.; and Tsubokawa, N. Postgrafting of vinyl polymers onto hyperbranched poly(amidoamine)-grafted nano-sized silica surface. Polymer 46 (2005): 2541-2543.

[21] Jiang, Y.; Gao, Q.; Yu, H.; Chen, Y.; and Deng, F. Intensively competitive adsorption for heavy metal ions by PAMAM-SBA-15 and EDTA-PAMAM-SBA-15 inorganic-organuc hybrid materials. Microporous and Mesoporous Materials 103 (2007): 316-324.

[22] Perignon, N.; Marty, J. D.; Mingotaud, A. F.; Dumont, M.; Rico-Lattes, I.; and Mingotaud, C. Hyperbranched Polymers Analogous to PAMAM Dendrimers for the Formation and Stabilization of Gold Nanoparticles. Macromolecules 40 (2007): 3034-3041.

[23] Horrocks, A. R. Developments in flame retardants for heat and fire resistant textiles – the role of char formation and intumescence. Polymer Degradation and Stability 54 (1996): 143-154.

[24] Charuchinda, S.; Srikulkit, K.; and Mowattana, T. Co-application of sodium polyphosphate and chitosan to improve flame retardancy of cotton fabric. Journal of Scientific Research Chulalongkorn University 30 (2005): 98-107.

[25] Giraud, S.; Bourbigot, S.; Rochery, M.; Vroman, I.; Tighzert, L.; and Delobel, R. Microencapsulation of phosphate: application to flame retarded coated cotton. Polymer Degradation and Stability 77 (2002): 285-297.

[26] Giraud, S.; Bourbigot, S.; Rochery, M.; Vroman, I.; Tighzert, L.; and Delobel, R. Flame retarded polyurea with microencapsulated ammonium phosphate for textile coating. Polymer Degradation and Stability 88 (2005): 106-113.

[27] Frécet, J. M. J.; and Tomalia, D. A. Dendrimers and Other Dendritic Polymers. New York: John Wiley & Sons Inc, 2001.

[28] Kim, Y. H.; and Webster O. W. Water-soluble hyperbranched polyphenylene: “a unimolecular micelle”. Journal of the American Chemical Society 112 (1990): 4592-4593.

[29] Miravet, J. F.; and Frécet, J. M. J. New hyperbranched poly(siloxysilane): variation of the branching pattern and end-functionalization. Macromolecules 31 (1998): 3461-3468.

[30] Teertstra, S. J.; and Gauthier, M. Dendrigraft polymers: macromolecular engineering on a mesoscopic scale. Progress in Polymer Science 29 (2004): 277-327.

[31] Tomalia, D. A. Comb-burst dendrimer topology - new macromolecular architecture derived from dendritic grafting. Macromolecules 24 (1991): 1435-1438.

[32] Gauthier, M.; and Möller, M. Uniform highly branched polymers by anionic grafting: arborescent graft polymers. Macromolecules 24 (1991): 4548-4553.

[33] Frauenrath, H. Dendronized polymers – building a new bridge from molecules to nanoscopic objects. Progress in Polymer Science 30 (2005): 325-384.

[34] Matthews, O. A.; Shipway, A. N.; and Stoddart, J. F. Dendrimers - branching out from curiosities into new technologies. Progress in Polymer Science 23 (1998): 1-56.

[35] Esfand, R.; and Tomalia, D. A. Laboratory synthesis of poly(amidoamine) (PAMAM) dendrimers. In: Fréchet, J. M. J.; and Tomalia, D. A. editor. Dendrimers and other dendritic polymers. Chichester: Wiley; 2001. 587-604.

[36] Hermanson, G. T. Bioconjugate techniques. 2nd ed. Elsevier Inc, 2008.

[37] Tomalia, D. A. The dendritic state. Materials Today March (2005): 34-46.

[38] Sayed-Sweet, Y.; Hedstrand, D. M.; Spinder, R.; and Tomalia, D. A. Hydrophobically modified poly(amidoamine) (PAMAM) dendrimers: their properties at the air-water interface and use as nanoscopic container molecules. Journal of Materials Chemistry 7 (1997): 1199-1205.

[39] Jikei, M.; and Kakimoto, M. Hyperbranched polymers: a promosing new class of materials. Progress in Polymer Science 26 (2001): 1233-1285.

[40] Yates, C. R.; and Hayes, W. Synthesis and applications of hyperbranched polymers. European Polymer Journal 40 (2004): 1257-1281.

[41] Hobson, L. J.; and Feast, W. J. Poly(amidoamine) hyperbranched systems: synthesis, structure and characterization. Polymer 40 (1999): 1279-1297.

[42] Twyman, L. J.; King, A. S. H.; Burnett, J.; and Martin, I. K. Synthesis of aromatic hyperbranched PAMAM polymers. Tetrahedron Letters 45 (2004): 433-435.

[43] Twyman, L.; and Martin, I. Hyperbranched polyamidoamine. Patent WO 2004/011527 A1.

[44] Martello, F.; Engbersen J. F. J.; and Ferruti, P. Hyperbranched poly(amidoamine)s containing disulfide linkages in the main chain for DNA transfection. Abstracts/Journal of Controlled Release 132 (2008): e1-e18.

[45] Cao, L.; Yang, W.; Wang, C.; and Fu, S. Synthesis and striking fluorescence properties of hyperbranched poly(amidoamine). Journal of Macromolecular Science Part A: Pure and Applied Chemistry 44 (2007): 417-424.

[46] Sun, Y.; Liu, Y.; Guizhe, Z.; and Zhang, Q. Effect of hyperbranched poly(amidoamine)s generation number on synthesis of Ag nanoparticles. Journal of Polymer Research 15 (2008): 269-273.

[47] Dodiuk-Kenig, H.; Buchman, A.; and Kenig, S. Novel adhesion promoters based on hyper-branched polymers. Composite Interfaces 11 (2004): 453-469.

[48] Kaneko, Y.; Imai, Y.; Shairai, K.; Yamauchi, T.; and Tsubokawa, N. Preparation and properties of hyperbranched poly(amidoamine) grafted onto a colloidal silica surface. Colloids and Surfaces A: Physiochemical and Engineering Aspect 289 (2006): 212-218.

[49] Yoshikawa, S.; Satoh, T.; and Tsubokawa, N. Post-grafting of polymer with controlled molecular weight onto silica surface by termination of living polymer cation with terminal amino groups of dendrimers-grafted ultrafine silica. Colloids and Surfaces A: Physiochemical and Engineering Aspect 153 (1999): 395-399.

[50] Qu, R.; Niu, Y.; Liu, J.; Sun, C.; Zhang, Y.; Chen, H.; and Ji, C. Adsorption and desorption behaviors of Pd(II) on silica-gel functionalized with ester- and amino-terminated dendrimer-like polyamidoamine polymers. Reactive & Functional Polymers 68 (2008): 1272-1280.

[51] Qu, R.; Sun, C.; Ji, C.; Wang, C.; Chen, H.; Niu, Y.; Liang, C.; and Song, Q. Preparation and metal-binding behaviour of chitosan functionalized by ester- and amino-terminated hyperbranched polyamidoamine polymers. Carbohydrate Research 343 (2008): 267-273.

[52] Tsubokawa, N.; and Takayama, T. Surface modification of chitosan powder by grafting of ‘dendrimer-like’ hyperbranched polymer onto the surface. Reactive & Functional Polymers 43 (2000): 341-350.

[53] Yoza, B.; Arakaki, A.; Maruyama, K.; Takeyama, H.; and Matsunaga, T. Fully automated DNA extraction from blood using magnetic particles modified with a hyperbranched polyamidoamine dendrimer. Journal of Bioscience and Bioengineering 95 (2003): 21-26.

[54] Yoza, B.; Arakaki, A.; and Matsunaga, T. DNA extraction using bacterial magnetic particles modified with hyperbranched polyamidoamine dendrimers. Journal of Biotechnology 101 (2003): 219-228.

[55] Seiler, M. Hyperbranched polymers: Phase behavior and new applications in the field of chemical engineering. Fluid Phase Equilibria 241 (2006): 155-174.

[56] Miklis, P.; Çağin, T.; and Goddard III, W. A. Dynamics of bengal rose encapsulated in the Meijer dendrimer box. Journal of the American Chemical Society 119 (1997): 7458-7462.

[57] Jansen, J. F. G. A.; and Meijer, E. W. The dendritic box: shape-selective liberation of encapsulated guests. Journal of the American Chemical Society 117 (1995): 4417-4418.

[58] Arunkumar, E.; Forbes, C. C.; and Smith, B. D. Improving the properties of organic dyes by molecular encapsulation. European Journal of Organic Chemistry (2005): 4051-4059.

[59] Quadir , M. A.; Radowski, M. R.; Kratz, F.; Licha, K.; Hayff, P.; and Haag, R. Dendritic multishell architectures for drug and dye transport. Journal of Controlled Release 132 (2008): 289-294.

[60] Baars, M. W. P. L.; Froehling, P. E.; and Meijer, E. W. Liquid-liquid extractions using poly(propylene imine) dendrimers with an apolar periphery. Chemical Communications (1997): 1959-1960.

[61] Froehling, P. E. Dendrimers and dyes – a review. Dyes and Pigments 48 (2001): 187-195.

[62] Yiyon, C.; and Jiepin, Y. Effect of polyamidoamine dendrimers in decolorizing triarylmethane dye effluent. Coloration Technology 121 (2005): 72-75.

[63] Stephan, H.; Spies, H.; Johannsen, B.; Kauffmann, C.; and Vögtle. pH-Controlled inclusion and release of oxyanions by dendrimers bearing methyl orange moieties. Organic 2 Letters (2000): 2343-2346.

[64] Burkinshaw, S. M.; Froehling, P. E.; and Mignanelli, M. The effect of hyperbranched polymers on the dyeing of polypropylene fibres. Dyes and Pigments 53 (2002): 229-235.

[65] Zhang, F.; Chen, Y.; Lin, H.; and Lu, Y. Synthesis of an amino-terminated hyperbranched polymer and its application in reactive dyeing on cotton as a salt-free dyeing auxiliary. Coloration Technology 123 (2007): 351-357.

[66] Burkinshaw, S. M.; Mignanelli, M.; Froehling, P. E.; and Bide, M. J. The use of dendrimers to modify the dyeing behaviour of reactive dyes on cotton. Dyes and Pigments 47 (2000): 259-267.

[67] ASTM International. D3786-01 Standard test method for hydraulic bursting strength of textile fabrics – Diaphragm bursting strength tester method.

[68] Shirley. Instruction Manual for the SDL 229B Bursting Strength Tester P1000. (Unpublished manuscript)

[69] British Standard. BS EN ISO 6940:1995 Textile fabrics- Burning behaviour- Determination of ease of ignition of vertically oriented specimens.

[70] Simon, A.; Cohen-Bouhacina, T.; Porté, M. C.; Aimé, J. P.; and Baquey, C. Study of two grafting methods for ontaining a 3-aminopropyltriethoxysilane monolayer on silica surface. Journal of Colloid and Interface Science 251 (2002): 278-283.

[71] Demadis, K. D.; and Kataracha, S. D. Metal-phosphonate chemistry: synthesis, crystal structure of calcium-amino-tris-(methylene phosphonate) and inhibition of $CaCO_3$ crystal growth. Phosphorus, Sulphur, and Silicon 179 (2004): 627-648.

[72] Heras, A.; Rodriguez, N. M.; Ramos, V. M.; and Agulló, E. *N*-methylene phosphonic chitosan: a novel soluble derivative. Carbohydrate Polymers 44 (2001): 1-8.

[73] Chaplais, G.; Bideau, J. L.; Leclercq, D.; and Vioux, A. Polarized-dependent IR ATR study for the structural characterization of solid-state phosphonates: case of aluminum (4-carboxyphenyl) methylphosphonate. Chemistry of Materials 15 (2003): 1950-1956.

[74] Danilich, M. J.; Burton, D. J.; and Marchant, R. R. Infrared study of perfluorovinylphosphonic acid, perfluoroallyphosphonic acid, and pentafluoroallyldiethylphosphonate. Vibrational Soectroscopy 9 (1995): 229-234.

[75] Binsu, V. V.; Nagarale, R. K.; and Shahi, V. K. Phosphonic acid functionalized aminopropyl triethoxysilane-PVA composite material: organic-inorganic hybrid proton-exchange membranes in aqueous media. Journal of Materials Chemistry 15 (2005): 4823-4831.

[76] Mucalo, M. R.; Kato, K.; and Yokogawa, Y. Phosphorylated, cellulose-based substrates as potential adsorbents for bone morphogenetic proteins in biomedical applications: A protein adsorption screening study using cytochrome C as a bone morphogenetic protein mimic. Colloids and Surfaces B: Biointerfaces 71 (2009): 52-58.

[77] Zhu, P.; Sui, S.; Wang, B.; Sun, K.; and Sun, G. A study of pyrolysis and pyrolysis products of flame-retardant cotton fabrics by DSC, TGA, and PY-GC-MS. Journal of Analytical and Applied Pyrolysis 71 (2004): 645-655.

[78] Gaan, S.; and Sun, G. Effect of phosphorus and nitrogen on flame retardant cellulose: A study of phosphorus compounds. Journal of Analytical and Applied Pyrolysis 78 (2007): 371-377.

APPENDIX

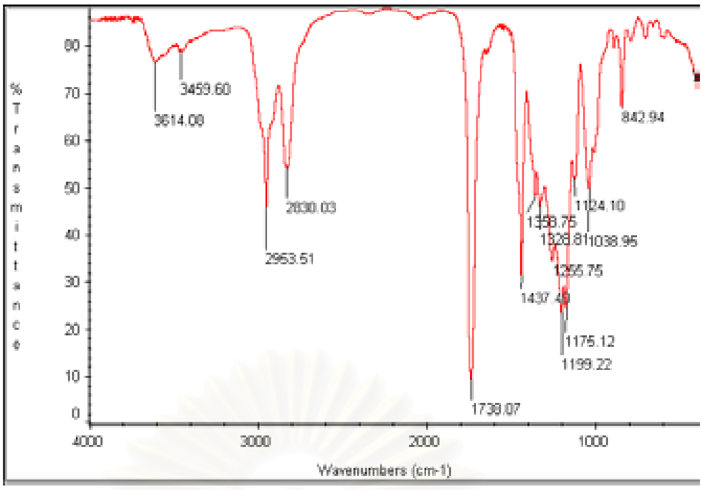

Figure A-1 FTIR spectrum of G-0.5 PAMAM dendrimer

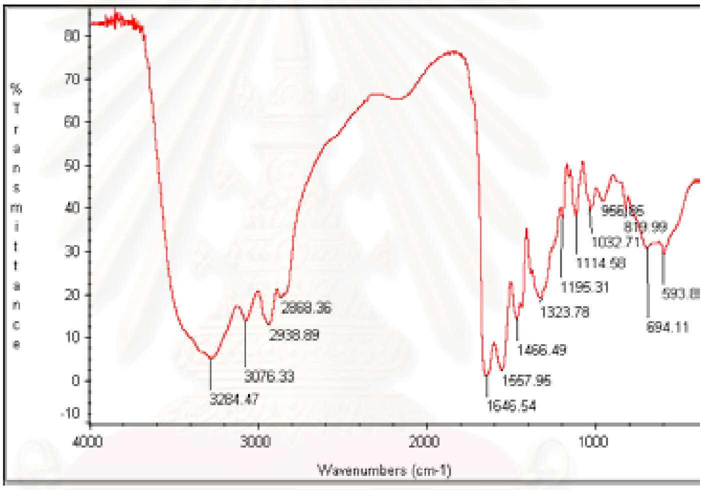

Figure A-2 FTIR spectrum of G0.0 PAMAM dendrimer

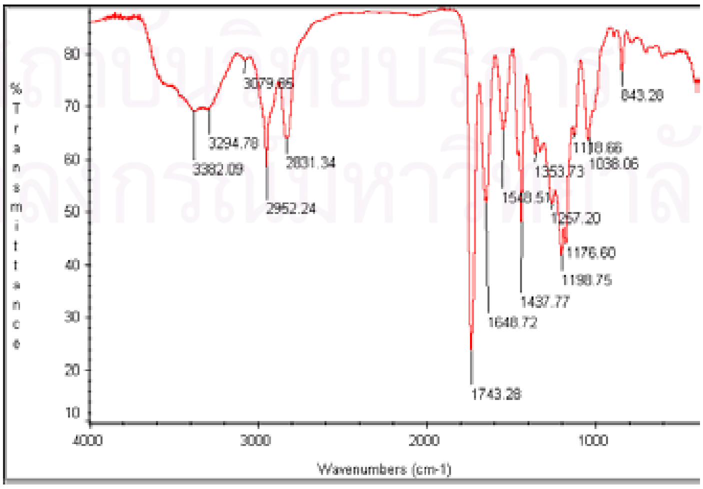

Figure A-3 FTIR spectrum of G0.5 PAMAM dendrimer

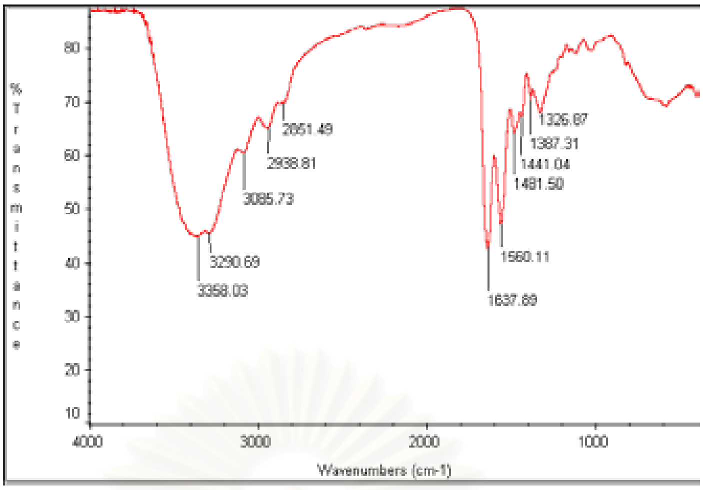

Figure A-4 FTIR spectrum of G1.0 PAMAM dendrimer

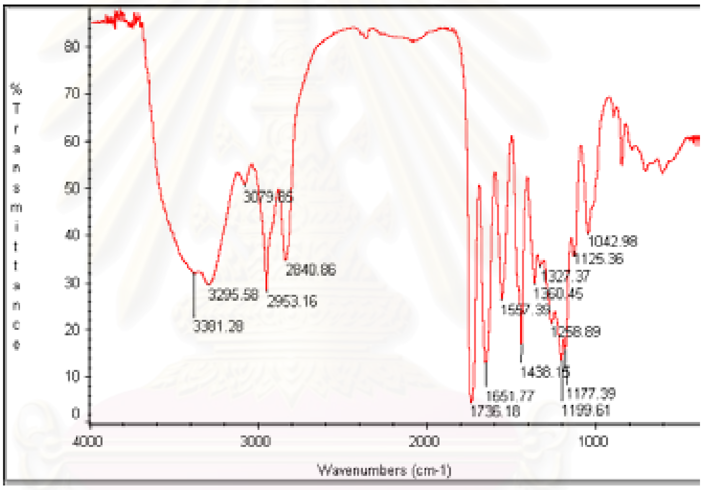

Figure A-5 FTIR spectrum of G1.5 PAMAM dendrimer

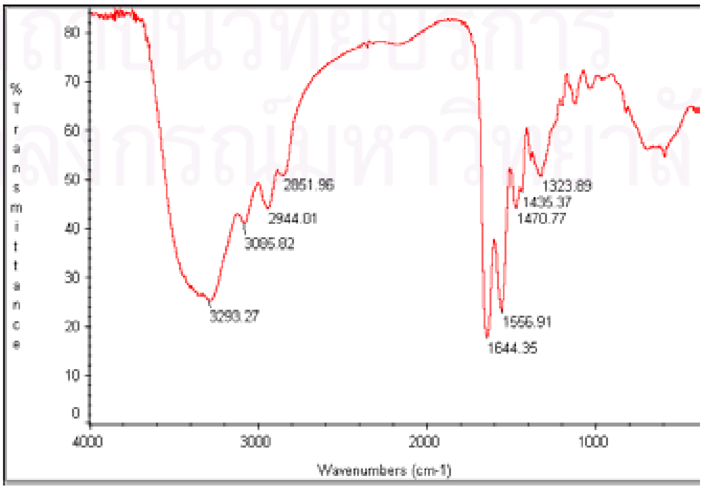

Figure A-6 FTIR spectrum of G2.0 PAMAM dendrimer

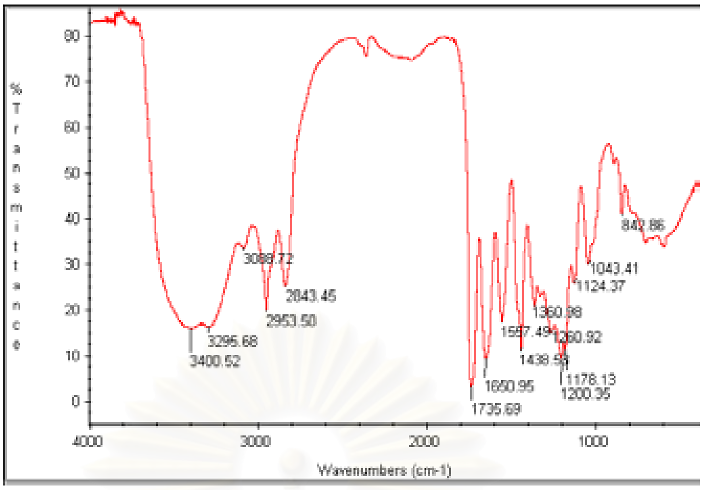

Figure A-7 FTIR spectrum of G2.5 PAMAM dendrimer

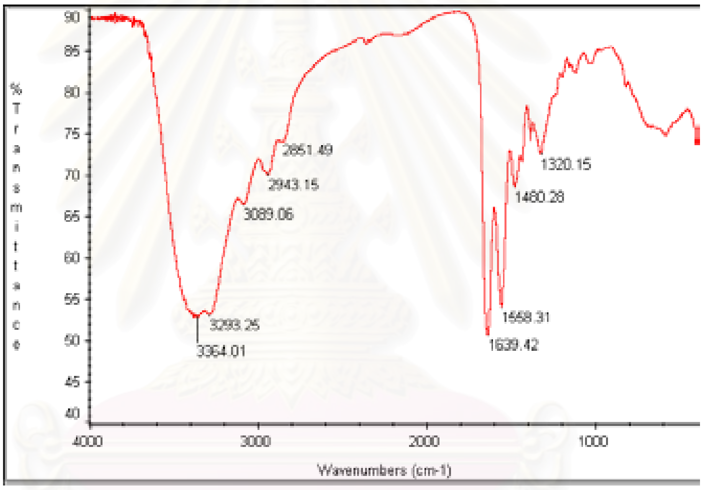

Figure A-8 FTIR spectrum of G3.0 PAMAM dendrimer

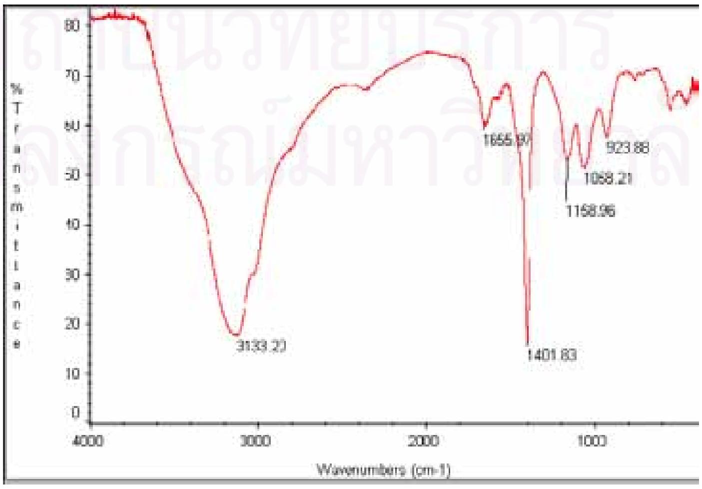

Figure A-9 FTIR spectrum of phosphorylated G3.0 PAMAM dendrimer

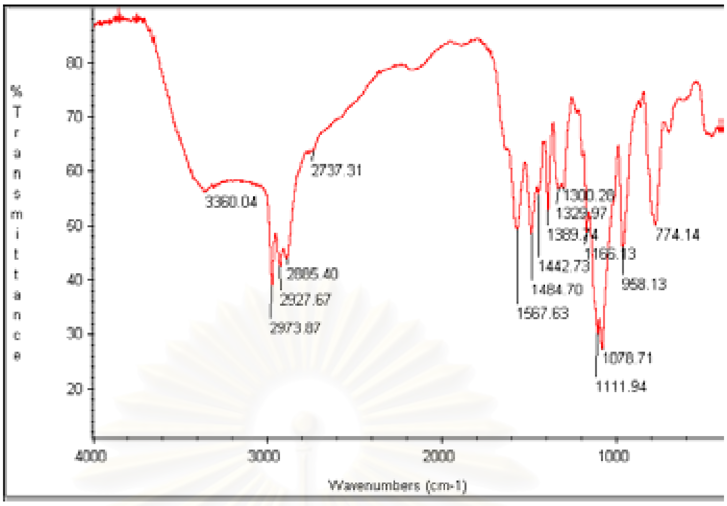

Figure A-10 FTIR spectrum of 3-Aminopropyltriethoxysilane

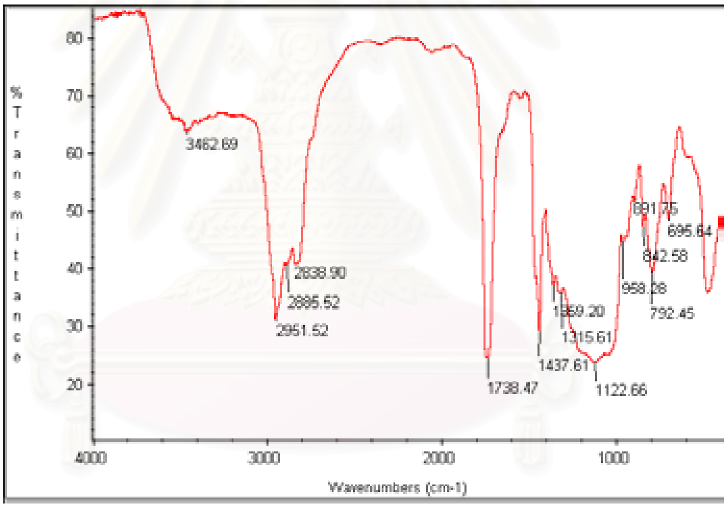

Figure A-11 FTIR spectrum of G0.5 hyperbranched PAMAM grafted silica

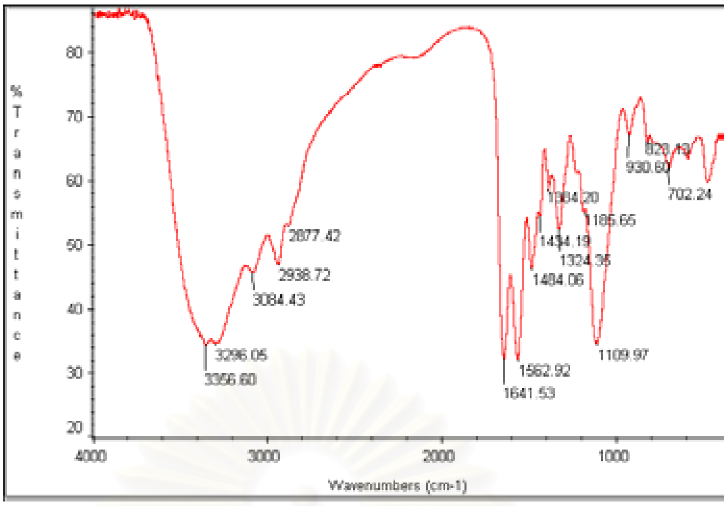

Figure A-12 FTIR spectrum of G1.0 hyperbranched PAMAM grafted silica

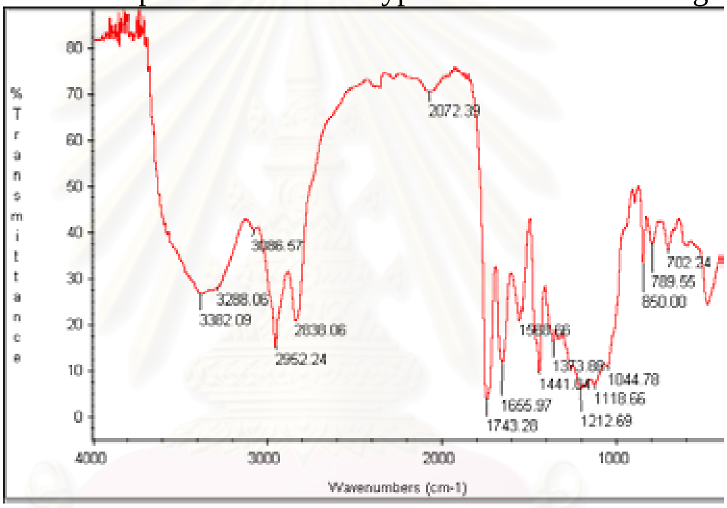

Figure A-13 FTIR spectrum of G1.5 hyperbranched PAMAM grafted silica

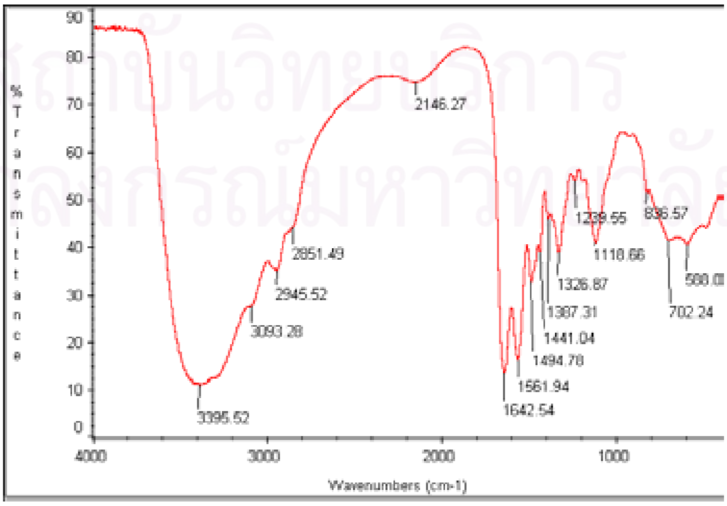

Figure A-14 FTIR spectrum of G2.0 hyperbranched PAMAM grafted silica

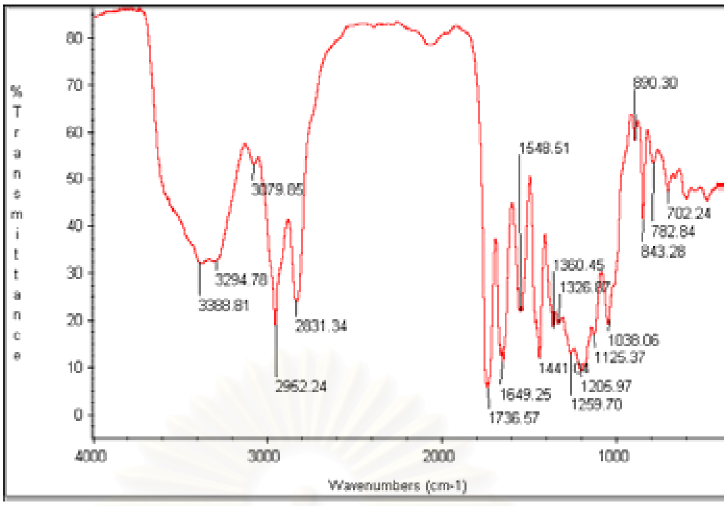

Figure A-15 FTIR spectrum of G2.5 hyperbranched PAMAM grafted silica

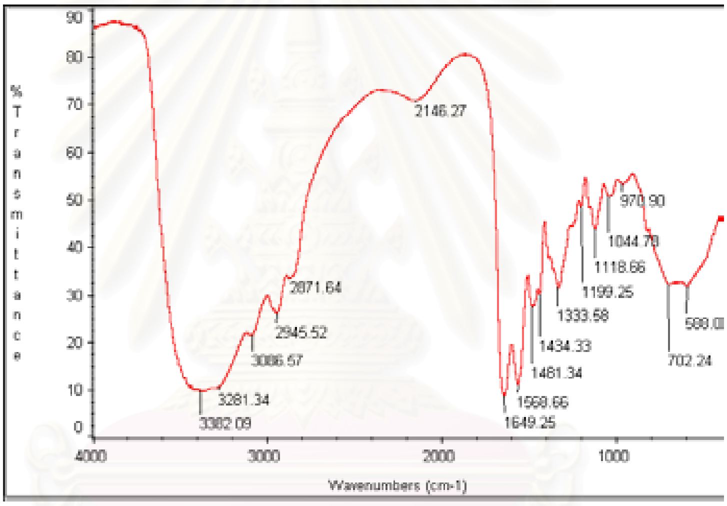

Figure A-16 FTIR spectrum of G3.0 hyperbranched PAMAM grafted silica

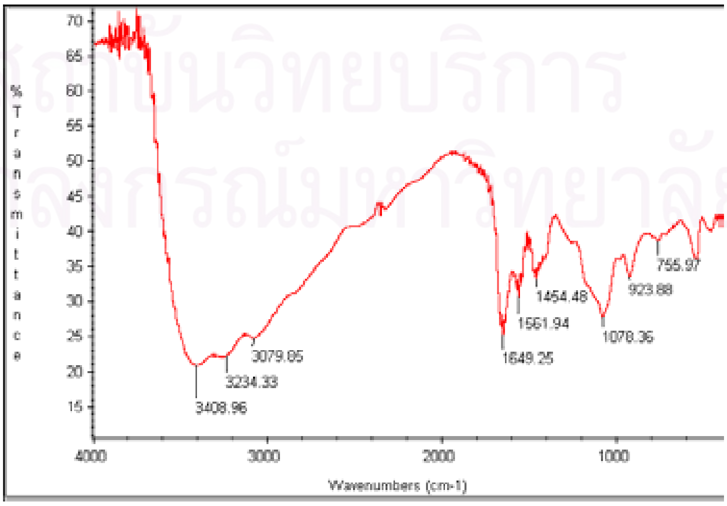

Figure A-17 FTIR spectrum of phosphorylated G3.0 hyperbranched PAMAM grafted silica

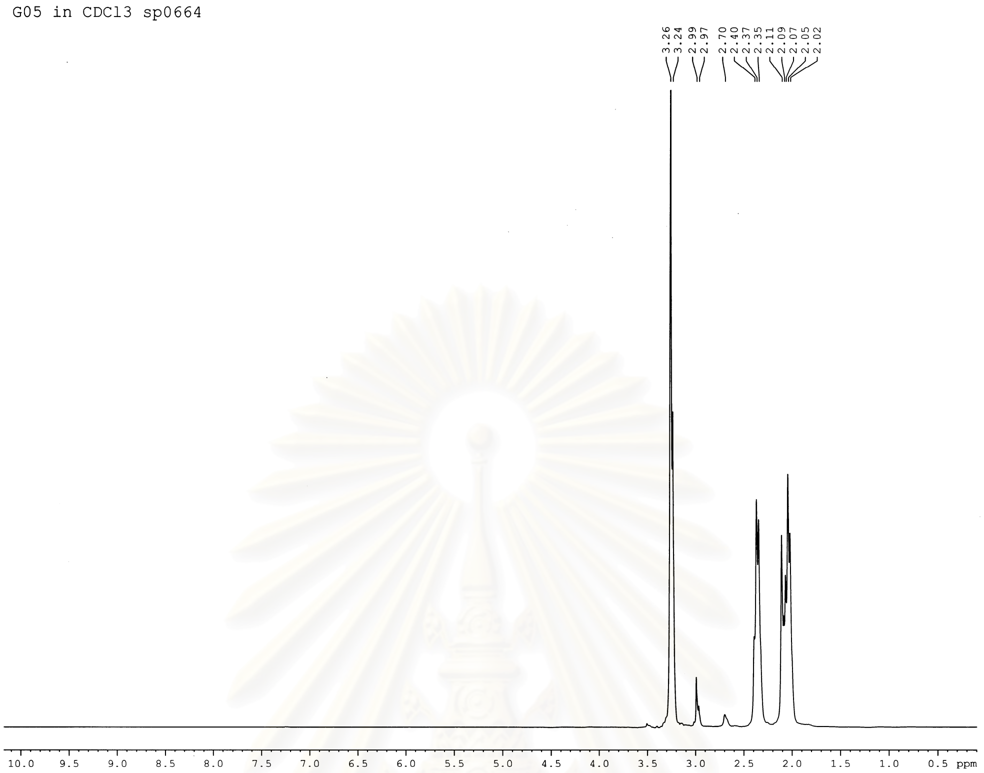

Figure A-18 ^{1}H NMR spectrum of G-0.5 PAMAM dendrimers

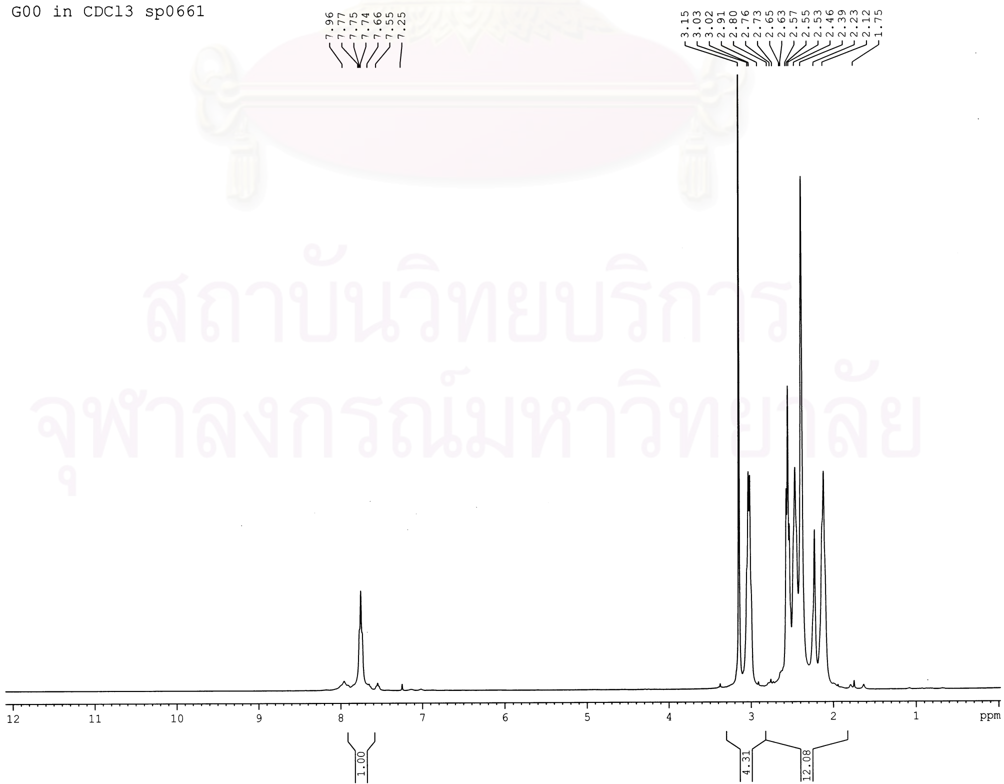

Figure A-19 ^{1}H NMR spectrum of G0.0 PAMAM dendrimers

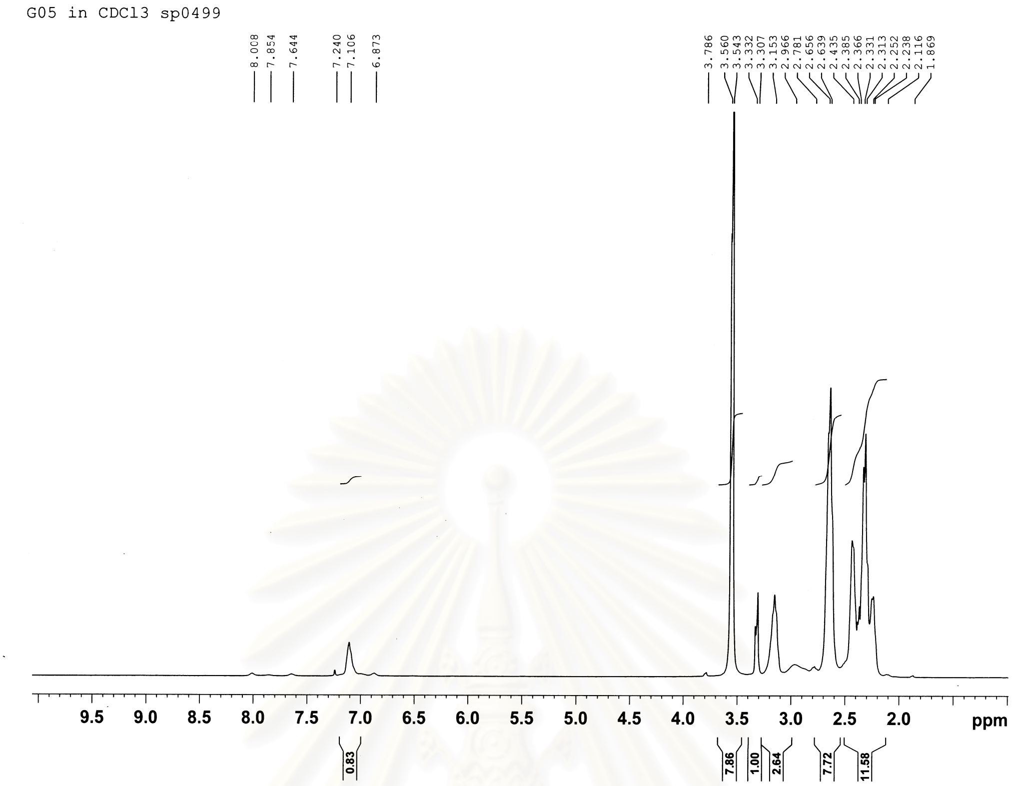

Figure A-20 ^{1}H NMR spectrum of G0.5 PAMAM dendrimers

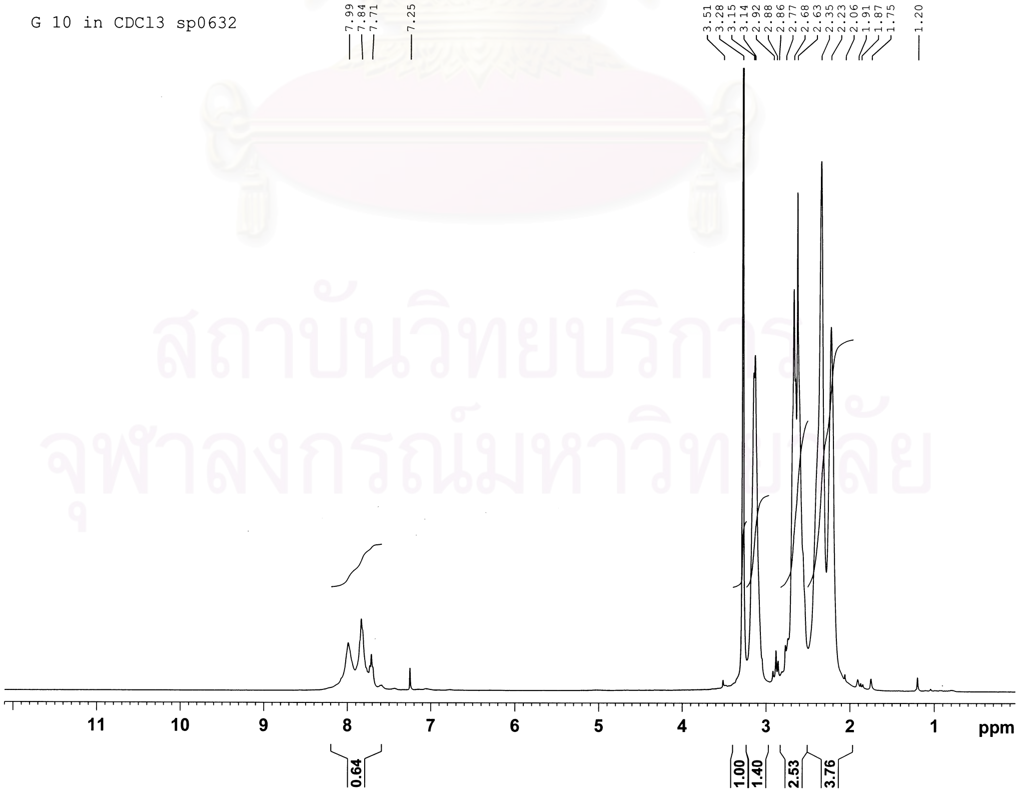

Figure A-21 ^{1}H NMR spectrum of G1.0 PAMAM dendrimers

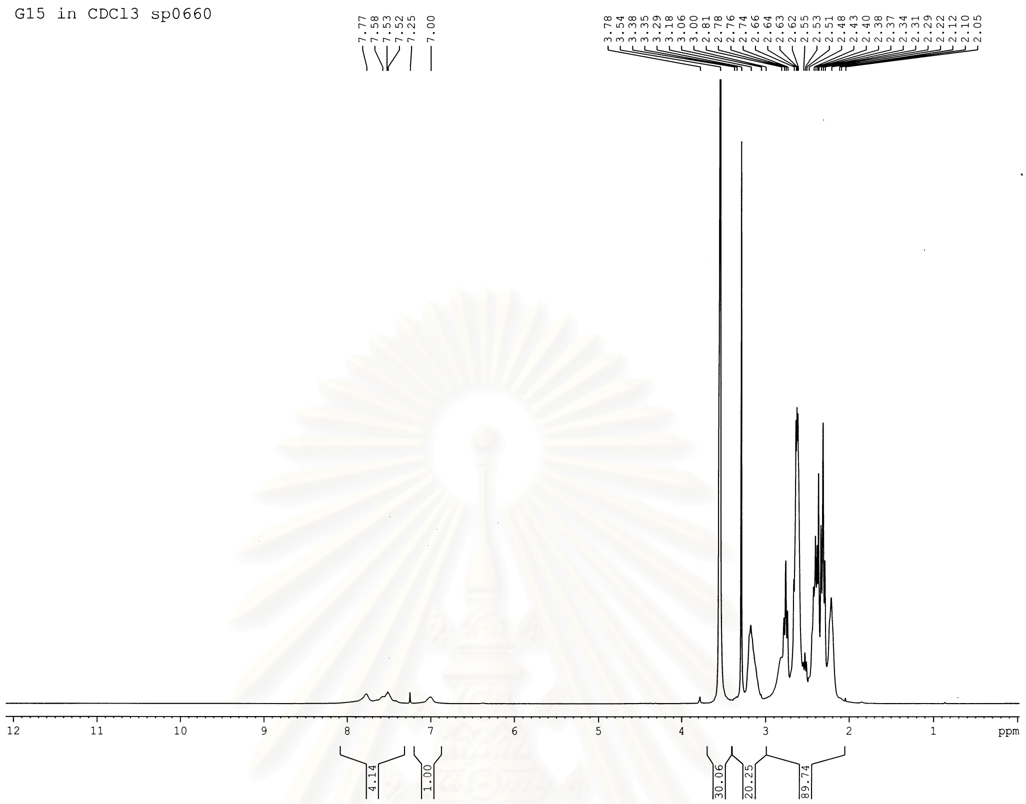

Figure A-22 ^{1}H NMR spectrum of G1.5 PAMAM dendrimers

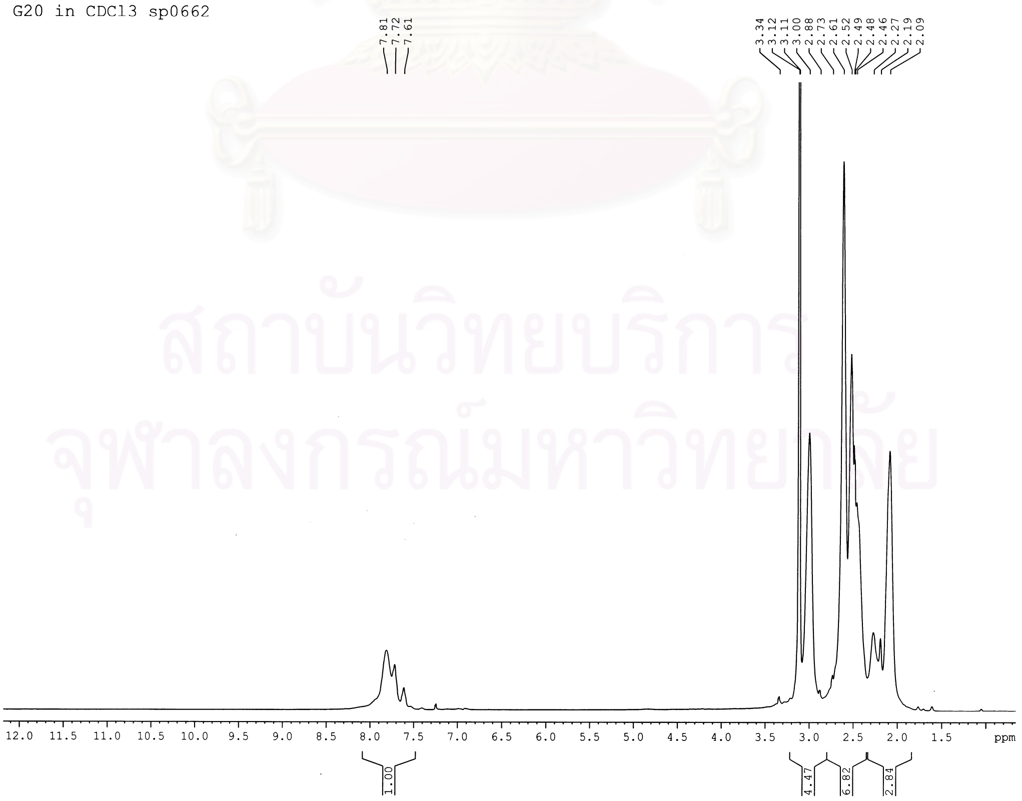

Figure A-23 ^{1}H NMR spectrum of G2.0 PAMAM dendrimers

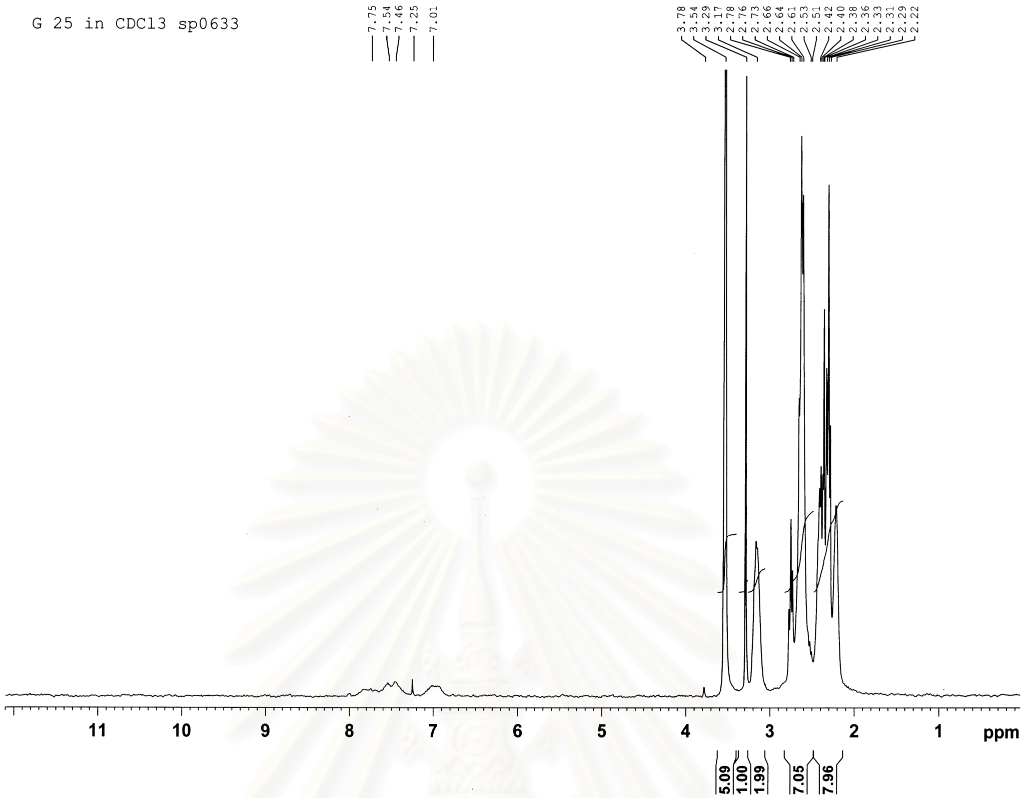

Figure A-24 ^{1}H NMR spectrum of G2.5 PAMAM dendrimers

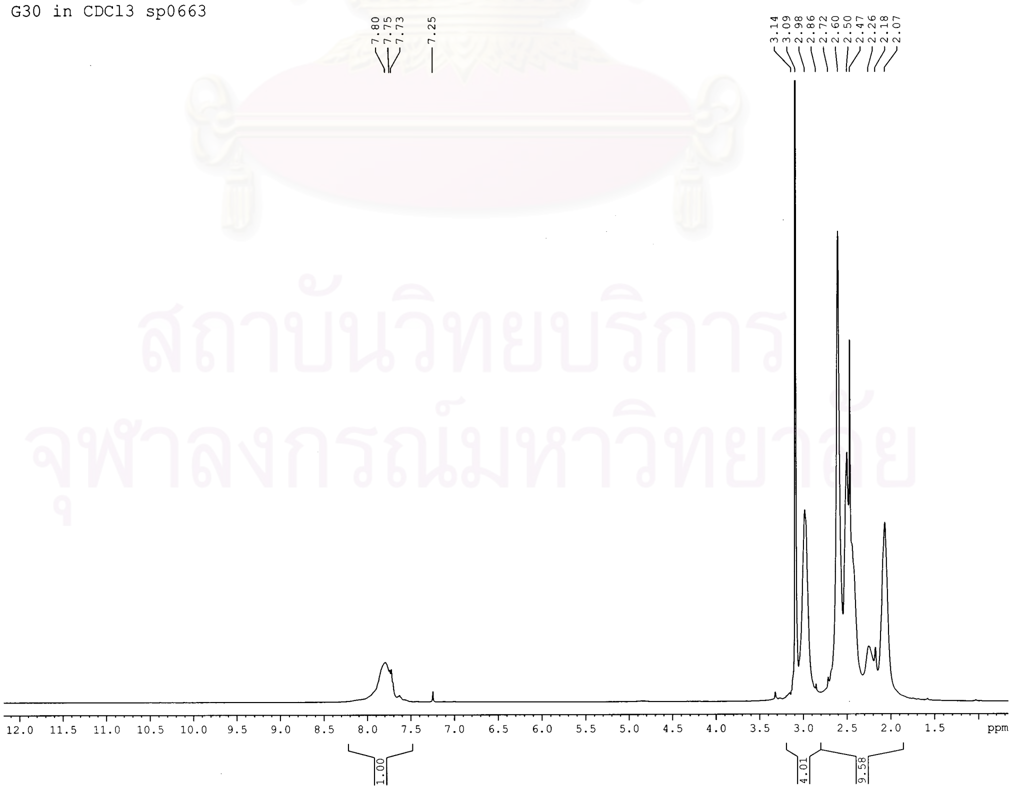

Figure A-25 ^{1}H NMR spectrum of G3.0 PAMAM dendrimers

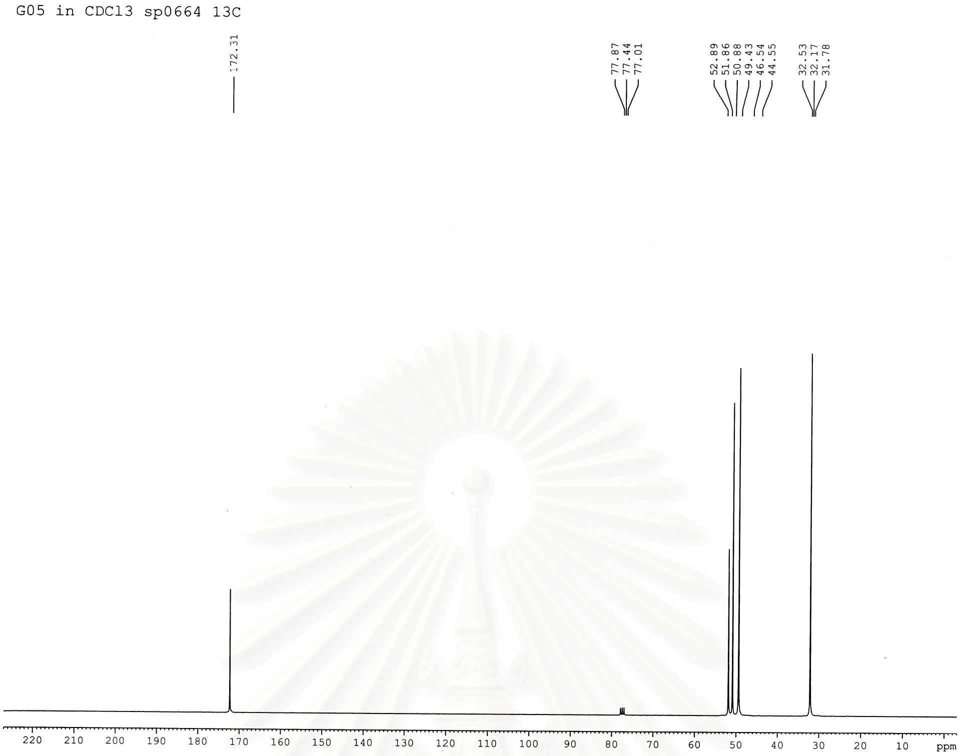

Figure A-26 ^{13}C NMR spectrum of G-0.5 PAMAM dendrimers

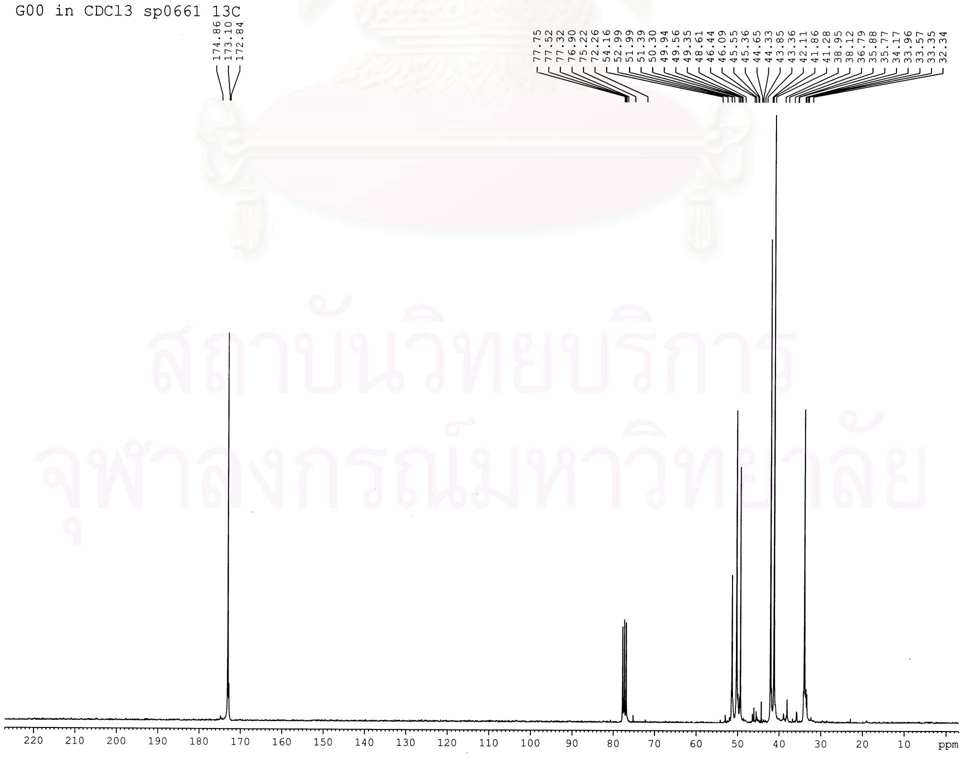

Figure A-27 ^{13}C NMR spectrum of G0.0 PAMAM dendrimers

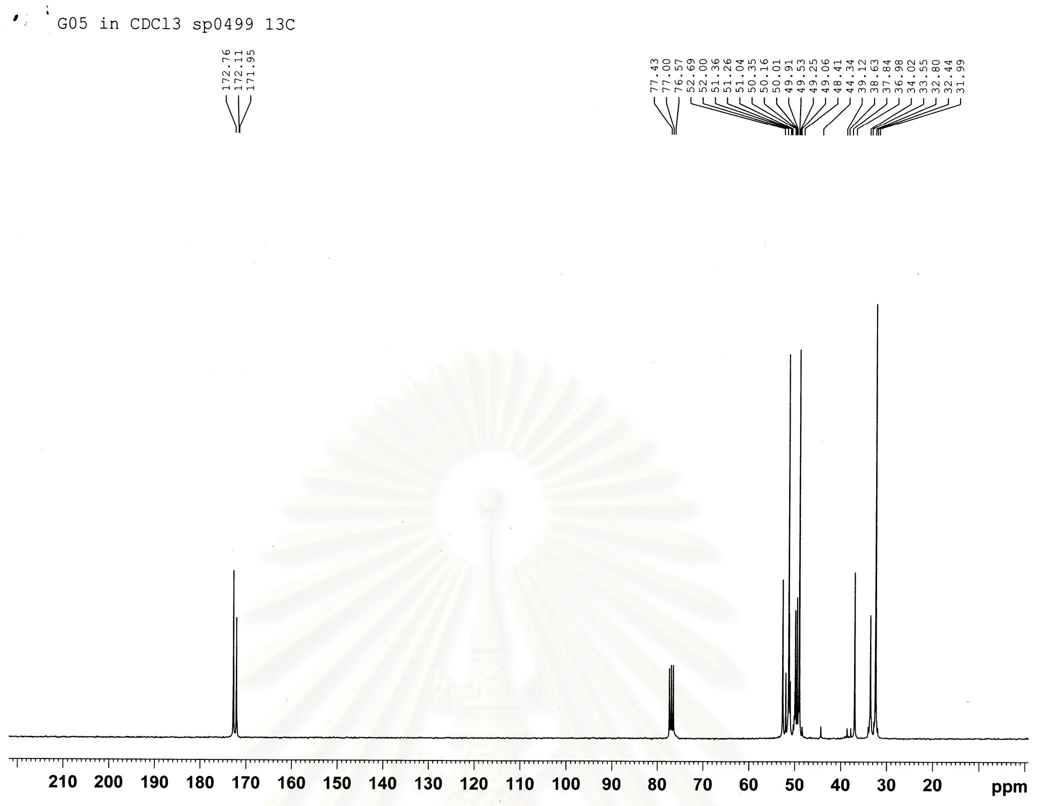

Figure A-28 ^{13}C NMR spectrum of G0.5 PAMAM dendrimers

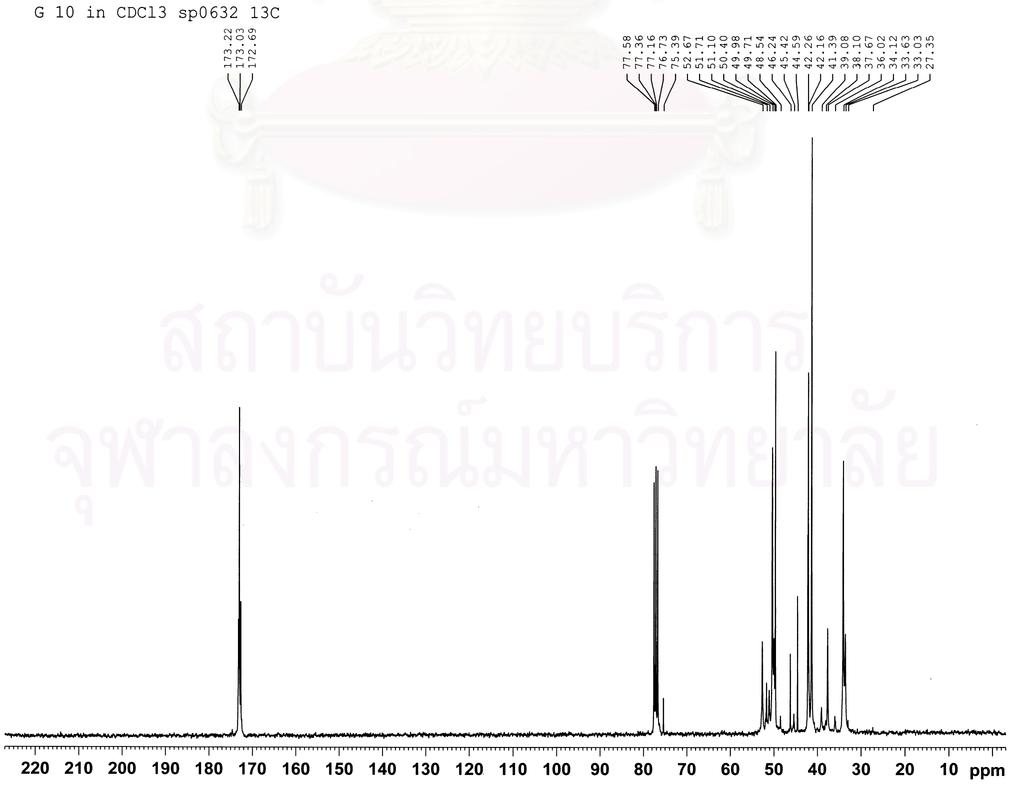

Figure A-29 ^{13}C NMR spectrum of G1.0 PAMAM dendrimers

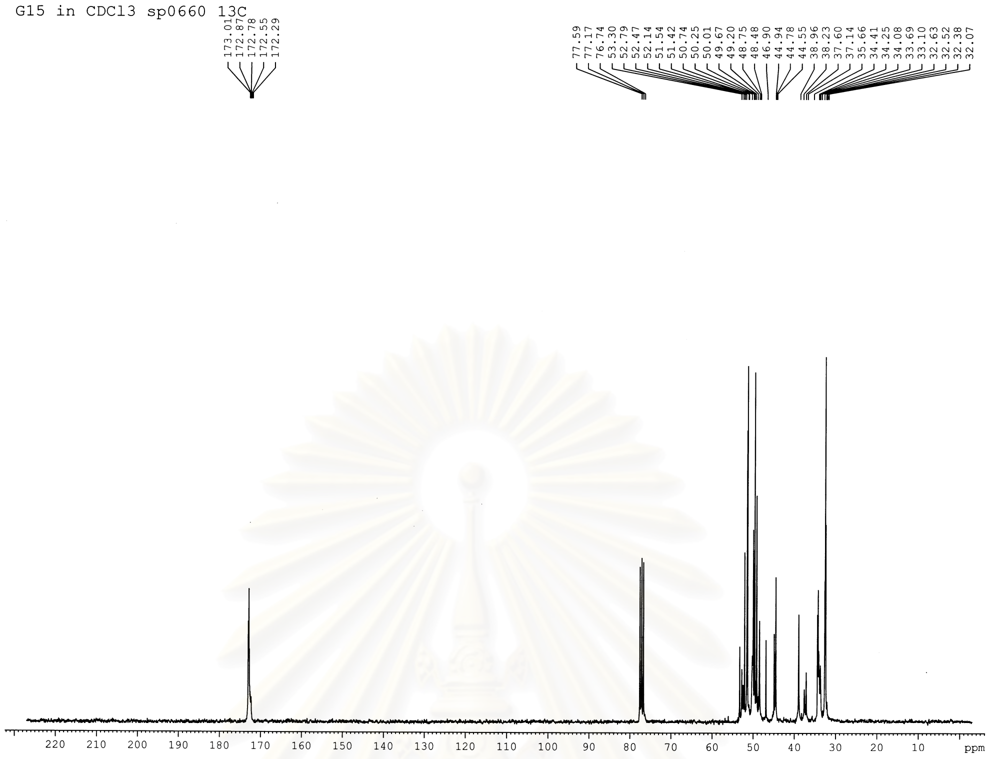

Figure A-30 ^{13}C NMR spectrum of G1.5 PAMAM dendrimers

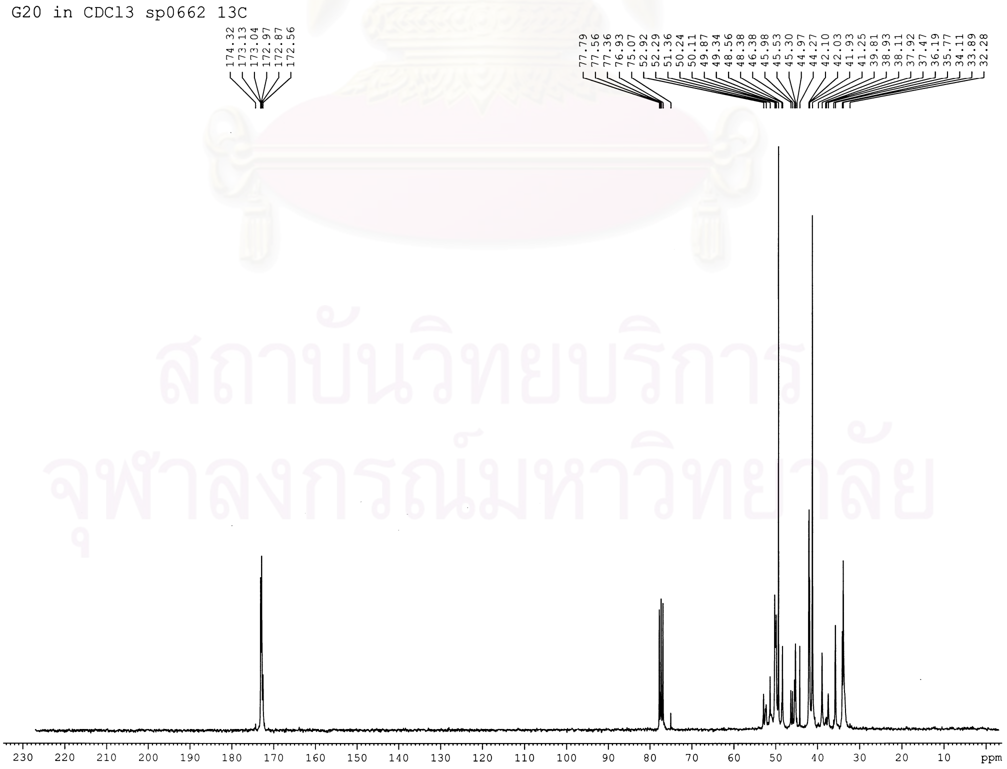

Figure A-31 ^{13}C NMR spectrum of G2.0 PAMAM dendrimers

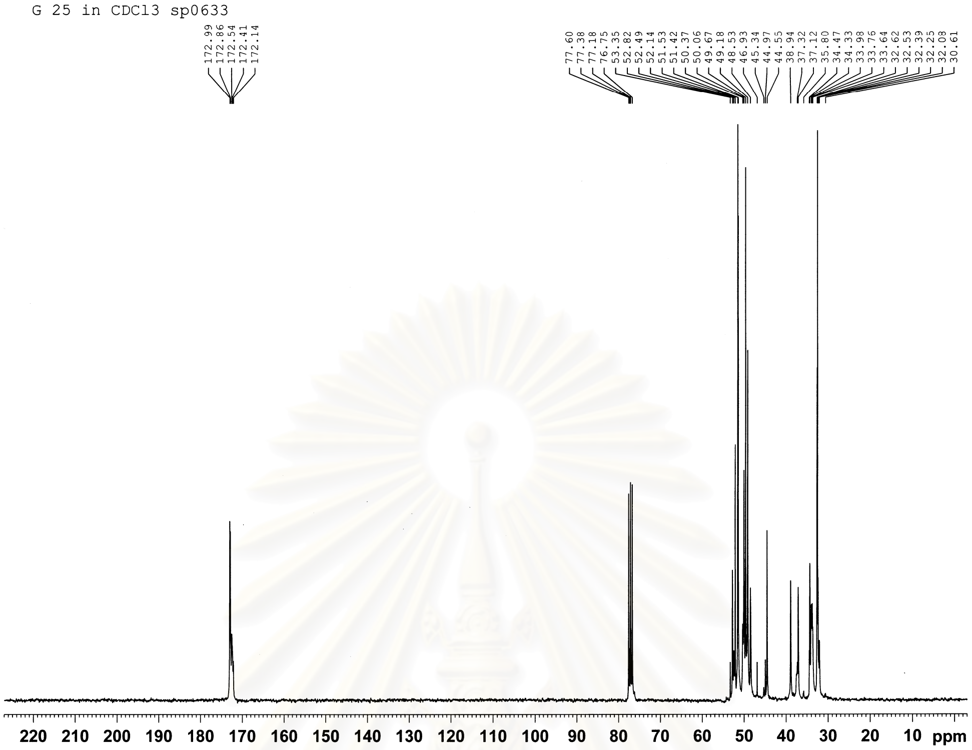

Figure A-32 ^{13}C NMR spectrum of G2.5 PAMAM dendrimers

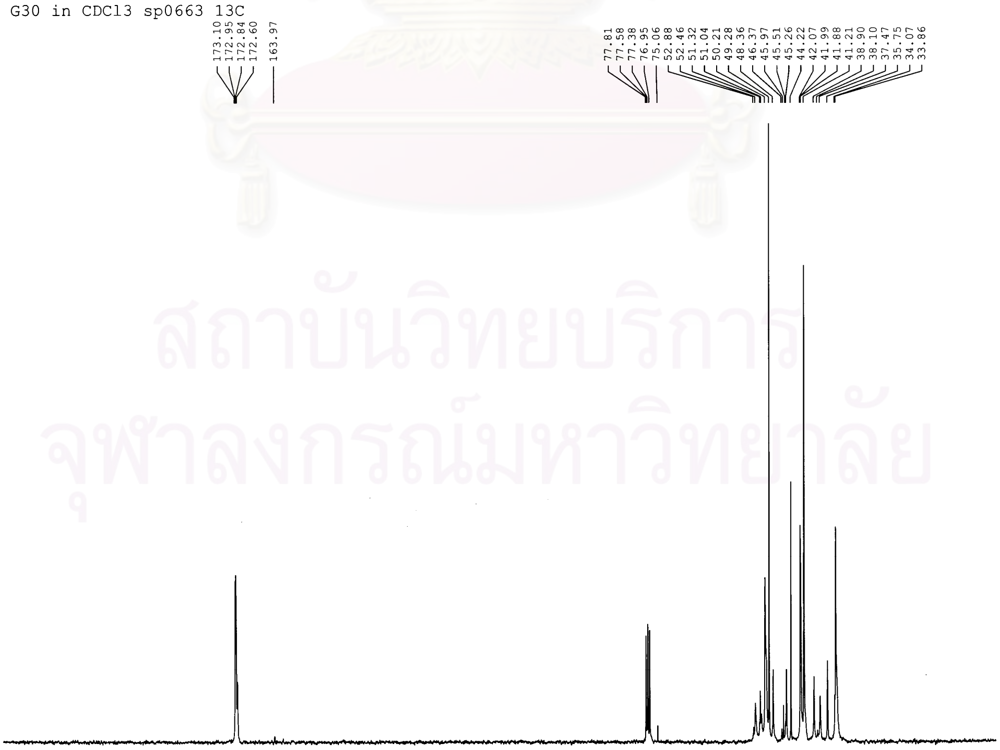

Figure A-33 ^{13}C NMR spectrum of G3.0 PAMAM dendrimers

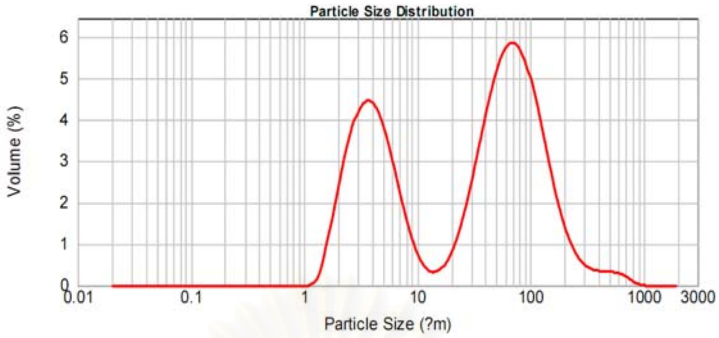

gsiog10

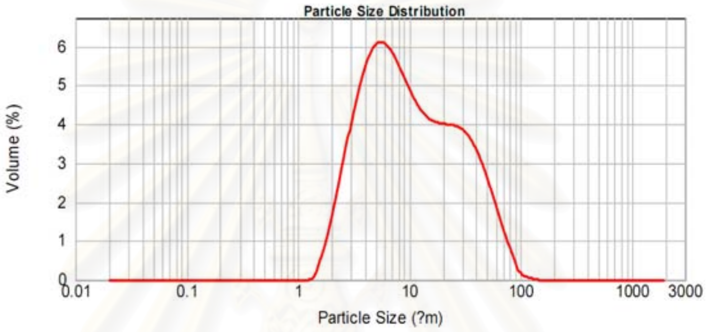

gsiog20

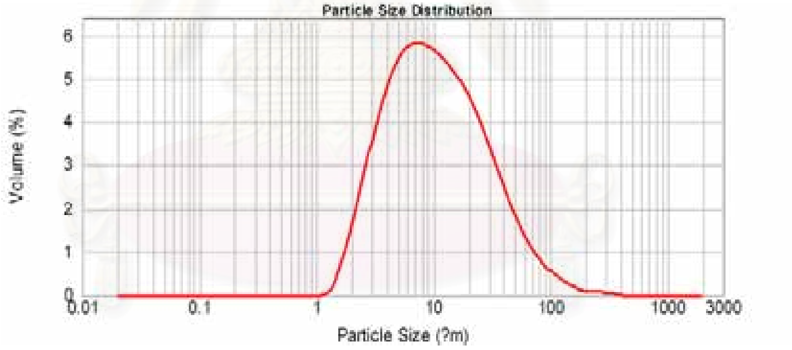

gsiog30

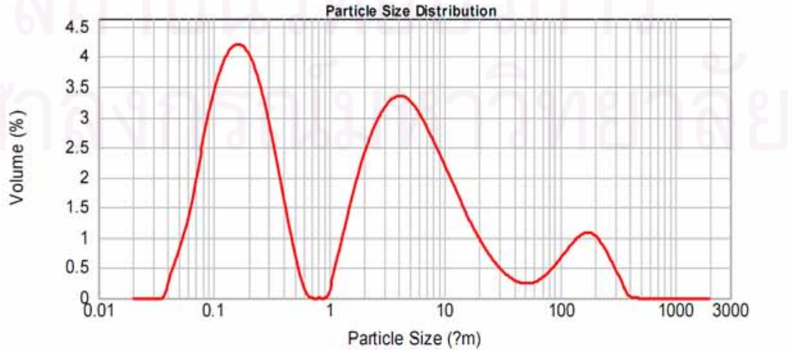

pgsio30

Figure A-34 Particle size distribution of hyperbranched PAMAM grafted silica generation 1.0, 2.0, 3.0 and phosphorylated hyperbranched PAMAM grafted silica generation 3.0.

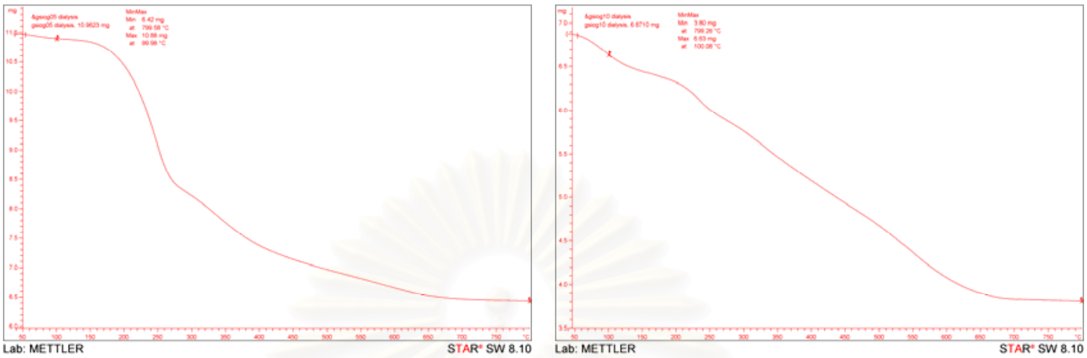

gsiog05 gsiog10

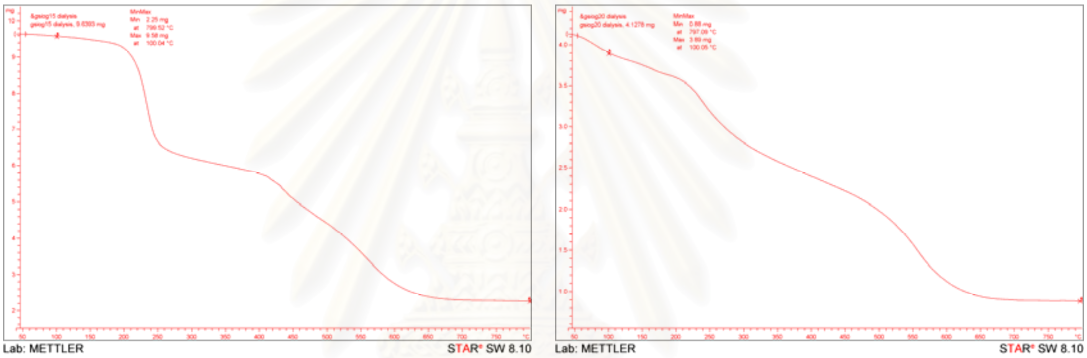

gsiog15 gsiog20

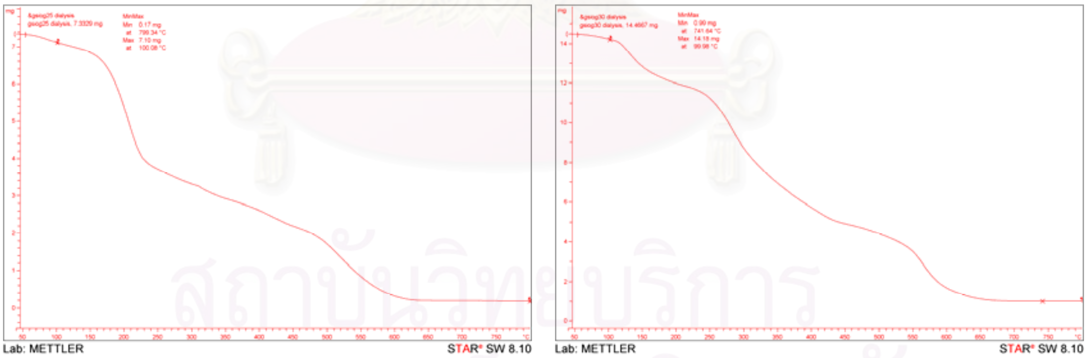

gsiog25 gsiog30

Figure A-35 TGA thermograms of G0.5 – G3.0 hyperbranched PAMAM grafted silicas.

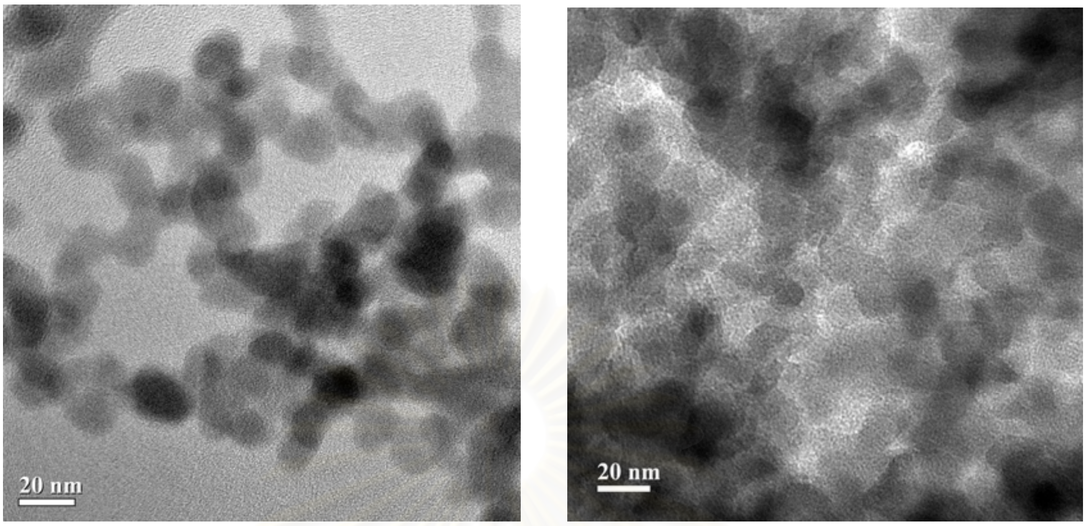

Virgin silica gsiog05

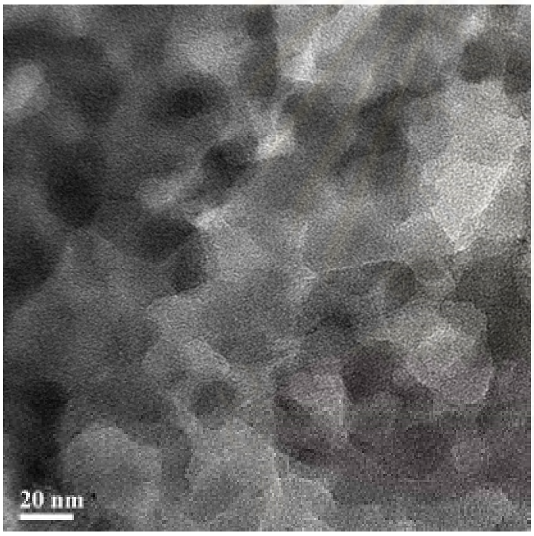

gsiog10

Figure A-36 TEM images of virgin silica, G0.5 hyperbranched PAMAM grafted silica and G1.0 hyperbranched PAMAM grafted silica

BIOGRAPHY

Mr. Phairat Punyacharoennon was born in Nonthaburi, Thailand, on April 27th, 1972. He received a Bachelor of Engineering with a major in Textile Chemistry Engineering from Rajamangala Institute of Technology, Thailand, in 1997. And he graduated a Master of Science with a major in Polymer Science from Mahidol University, Thailand, in 2001. He started as a graduate student in the field of Materials Science, Department of Materials Science, Chulalongkorn University in 2004 and completed the program in 2009.